JOURNAL OF APPLIED PHYSICS

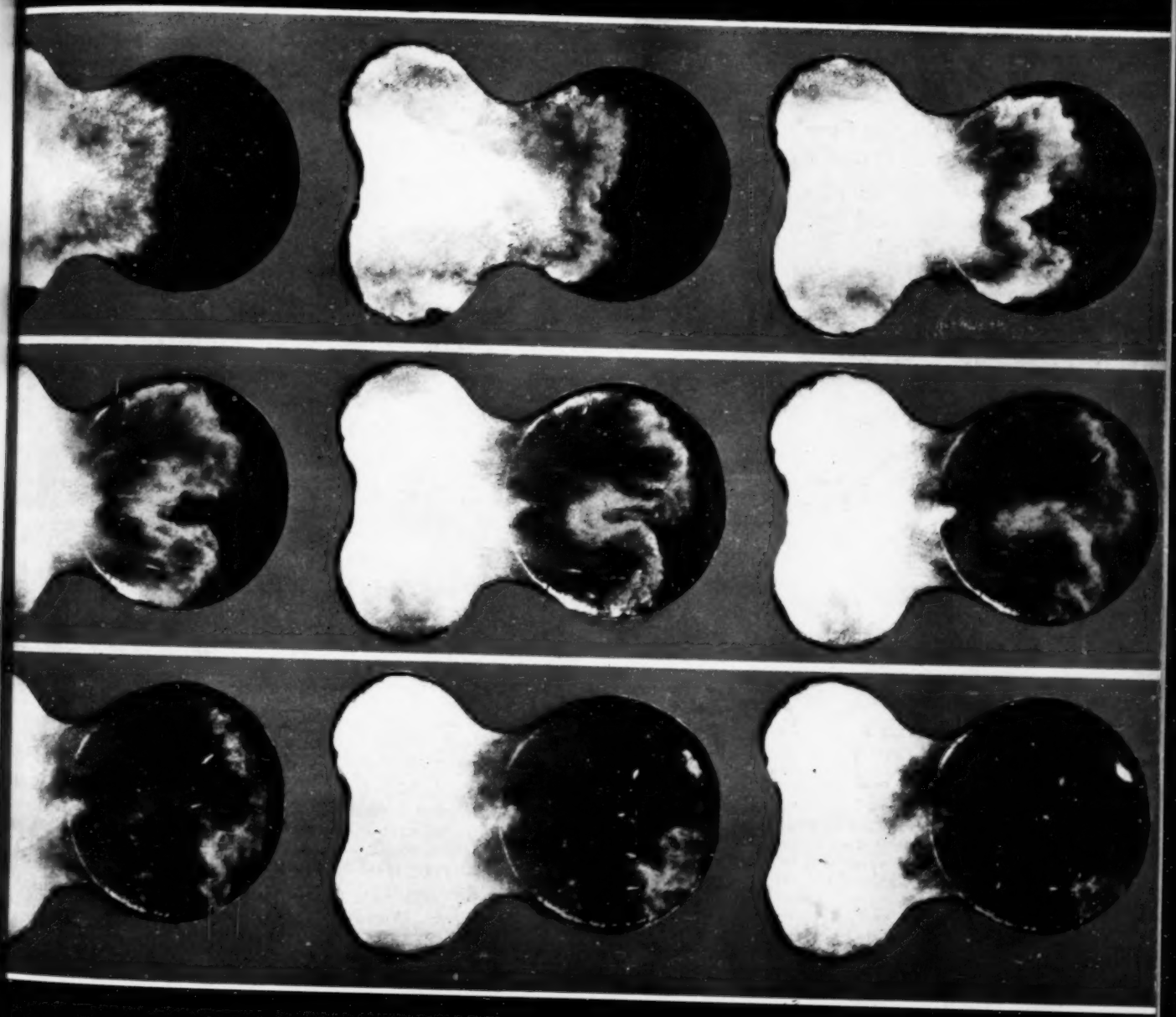

JOURNAL OF APPLIED

PHYSICS

(Formerly PHYSICS)

JUNE, 1938 Vol. 9, No. 6

In This Issue

Page

Applications of Physics in the Automotive Industry THE EDITOR 349

Physics and the Automotive Industry F. K. RICHTMYER 350

Resumés of Recent Research 352

Contribution of the Physicist to Highway Illumination CLIFTON G. FOUND 354

Studying Engine Combustion by Physical Methods LLOYD WITHROW AND GERALD M. RASSWEILER 362

Mobility Method of Computing the Vibration of Linear Mechanical and Acoustical Systems: Mechanical-Electrical Analogies F. A. FIRESTONE 373

Contributed Original Research

Studies in Lubrication. I. The Theory of the Thick Film Lubrication of a Complete Journal Bearing of Finite Length M. MUSKAT AND F. MORGAN 393

Film Lubrication of Finite Curved Surfaces SELBY M. SKINNER 409

Dynamic Characteristics of Glow Discharge Tubes HERBERT J. REICH AND WALLACE A. DEPP 421

In Every Issue

Here and There 388

Among Our Authors 390

Some of the New Books 392

Current Literature of Physics viii

Advertising Index xviii

BOARD OF EDITORS

ELMER HUTCHISSON, *Editor*

Associate Editors

R. M. BOZORTH
D. W. BRONK
W. P. DAVEY
O. S. DUFFENDACK
SAUL DUSHMAN
A. STUART HUNTER
C. H. KUNSMAN
J. T. LITTLETON
L. L. NETTLETON
W. B. NOTTINGHAM
A. R. OLPIN
JOHN T. TATE

Publication of the American Institute of Physics

ADMINISTRATIVE STAFF

HENRY A. BARTON, *Director*

MADELINE M. MITCHELL, *Publications Manager*

WILLIAM C. COPP, *Advertising Manager*

GOVERNING BOARD

JOHN T. TATE, *Chairman*
KARL T. COMPTON
E. C. CRITTENDEN
WHEELER P. DAVEY
HOMER L. DODGE
HARVEY FLETCHER
ARTHUR C. HARDY
VERN O. KNUDSEN
MELVIN MOONEY
FREDERIC PALMER, JR.
R. L. PEEK, JR.
GEORGE B. PEGRAM
W. B. RAYTON
F. K. RICHTMYER
WALLACE WATERFALL

THE JOURNAL OF APPLIED PHYSICS, published monthly at Prince and Lemon Sts., Lancaster, Pa., is devoted to physics in its role as the science basic to other natural sciences and to the arts and industries. Previous to 1937 this publication was known as PHYSICS. It aims to be of service not only in physical laboratories, but also in the laboratories of industrial, chemical, geological, geophysical, meteorological, radio, and similar concerns. THE JOURNAL OF APPLIED PHYSICS publishes editorials, news of physicists and reviews, as well as technical papers of applied physics.

SUBSCRIPTION PRICE

	U. S., POSS. AND CANADA	FOREIGN
To members of scientific societies	$5.00	$5.70
To all others	7.00	7.70

Manuscripts should be submitted to Elmer Hutchisson, Editor, University of Pittsburgh, Pittsburgh, Pennsylvania.

Changes of address, proofs, and complaints of failure to receive the JOURNAL OF APPLIED PHYSICS should be addressed to the Publications Manager. New copies can be sent free only if notice of nondelivery is received within three months of date of issue.

Subscriptions and orders for back numbers should be addressed to Prince and Lemon Streets, Lancaster, Pa. or to the American Institute of Physics, 175 Fifth Avenue, New York, N. Y.

Advertising rates supplied on request. Orders, advertising copy and cuts should be sent to the American Institute of Physics.

Entered as second class matter at the Post Office at Lancaster, Pennsylvania, under the Act of March 3, 1897. Accepted for mailing at the special rate of postage provided for in the Act of February 28, 1925, authorized May 2, 1932.

Copyright 1938, by the American Institute of Physics.

Journal of Applied

Physics

Volume 9 June, 1938 Number 6

Applications of Physics in the Automotive Industry

A SYMPOSIUM on Physics in the Automotive Industry was held under the auspices of the American Institute of Physics on March 14 and 15 at the University of Michigan in Ann Arbor. An excellent program was arranged under the chairmanship of Professor Duffendack by a committee of the department of physics of the University of Michigan.

Dean F. K. Richtmyer opened the symposium with a few introductory remarks on "What Physics Can Do for the Automotive Industry." Mr. Carl Breer discussed the need of the automotive industry for fundamental scientific research and Mr. J. S. Thomas the training of physicists. Many papers on the more technical aspects of automotive research—such as the lubrication of journal bearings, the design of electric discharge lamps for highway illuminants, the methods of studying engine combustion, and the study of the vibration of mechanical systems—were given. Among the more general topics discussed were the modern theory of solids, the physics of rubber, noise measurement, and the application of photoelastic analysis to design problems.

A dinner was held on the evening of the first day and a very stimulating address was given by Mr. Charles F. Kettering on "Scientific Training and Its Relation to Industrial Problems."

An outstanding feature of the meeting was an inspection tour of the research laboratories of the physics department of the University of Michigan. The tour of the East Physics Building included a visit to the cyclotron, to the million-volt generator, the automatic recording spectrometer, the instrument for spectrochemical analysis, experiments in the field of ultra-high frequency, research in acoustics, and the 12-inch Wilson cloud chamber which was in operation.

It was generally agreed that this symposium was a very successful one, and it is hoped that it will bring about more applications of physics in the automotive industry and a greater understanding on the part of the academic physicist of the problems which occur in industry.—THE EDITOR.

For July

Scientific Training and Its Relation to Industrial Problems, by CHARLES F. KETTERING

Needs of the Automotive Industry for Fundamental Scientific Research, by CARL BREER

Physics of Rubber as Related to the Automobile, by W. F. BUSSE

Photoelastic Analysis Practically Applied to Design Problems, by O. J. HORGER

Some Physical Problems in Noise Measurement, by PAUL HUBER

Beginning with the July issue, the publication date of the Journal of Applied Physics *will be advanced to a few days before the first of the month listed on the cover.*

Physics and the Automotive Industry*

BY F. K. RICHTMYER

Cornell University, Ithaca, New York

THE purpose of research in the pure science of physics is to extend our knowledge of the properties of matter and energy and of the interrelations between these two great entities of nature. It is the purpose of research in applied physics to see how the laws of physics discovered in pure science laboratories can be applied to other sciences and to engineering. Since engineering itself deals with matter in its various forms—such as *I* beams, airplane propellers, coal, gasoline and the like—and with energy and its transmission, it follows that pure physics is one of the basic elements in all engineering.

This relationship is perfectly obvious when one considers the history of the development of physics and engineering. A single illustration suffices. Nearly 120 years ago, the Danish experimenter Oersted made an accidental discovery during one of his lectures to a class in physics. He found that a wire carrying an electric current would cause a nearby magnetic needle to deflect. For the first time man observed a relation between electricity and magnetism; an electric current could produce a magnetic field. Twelve years later, as a result of intensive research, at an institution which had only academic objectives, Michael Faraday demonstrated the converse effect, namely the production of an electric current by use of a magnetic field. Everybody today understands that these two discoveries form the basis of our vast electrical industry. It should be pointed out, however, that it was not sufficient from the standpoint of either physics or of subsequent engineering, for Oersted merely to have *observed* the production of a magnetic field by an electric current; or for Faraday to have observed the converse effect. In each case, before the observed phenomenon could be put to use, quantitative relations had to be discovered. It is this latter type of research in pure physics which constitutes the bulk of all research in academic laboratories. Great discoveries are few and far between. The establishment of quantitative relations, which alone can satisfy both the engineer and the physicist, take almost the entire energies of our research laboratories.

In short, discoveries, most of them accidental, in the laboratories of physics during the past hundred years, together with the vast amount of quantitative work which have followed these discoveries, form the basis of modern engineering. Out of physics has grown in turn mechanical engineering—certainly in its later developments—and electrical engineering, radio engineering, aeronautical engineering, illuminating engineering and more recently, geophysical engineering.

It is easy to see these intimate relationships between physics and engineering as one looks backward. It is not so easy, particularly for the industrialist, to appreciate the importance of future contributions which physics will make to industry. Even to believe in the probability of these contributions requires a faith in the future based on the experience of the past, which is possessed by only the more hardy far-seeing souls. I emphasize the word "faith," for no one can predict precisely the way in which even the current concepts of modern physics, let alone concepts, phenomena and laws to be developed in the future, can be applied to the automobile industry. Research alone can indicate the nature and importance of these applications. If one could predict the extent of these applications, there would be no problem of research, for it is the very essence of research to find the unknown whether such unknown be a new physical fact or the application of a physical fact to industrial processes. The piezoelectric effect, discovered more or less by accident a half-century ago, was an interesting physical phenomenon. No one had any thoughts of its utilitarian values, until the development of radio made a need for

* Introductory address presented at the Symposium on Physics in the Automotive Industry at Ann Arbor, Michigan, March 14 and 15, 1938.

high frequency oscillations of great constancy. It might be said that at present the piezoelectric effect is the *sine qua non* of modern radio-engineering. One could multiply examples of this kind by the dozen.

Among the many fields of present-day physics which promise significant contributions to the automotive industry in the near future, is the physics of the "solid state." Automotive engineering is concerned, among other things, with the properties of the great variety of materials which go into the making of automobiles. Save as to fuel and oil, these materials are for the most part what the physicist calls "solids." Solids are spoken of as matter in the "solid state." A vast amount of research in academic laboratories of physics, in the great industrial laboratories and in the engineering laboratories has been carried out to determine the properties of solids. While there is some law and order to this vast amount of information, we have to admit that a very great deal of it is empirical.

Rather recently however, as a result of developments in the field of both experimental and theoretical physics, new lines of attack on studying the fundamental properties of solids have been developed. Investigations in this field are just being started. I think we can say that our knowledge of solids is now about where our knowledge of atoms and of atomic spectra was about twenty-five years ago when the development of the Rutherford-Bohr theory of atomic structure provided new concepts and new techniques for studying the atom. In this study of the atom and atomic spectra tremendous strides have been made in the last twenty years. I need not point out the industrial value, let alone scientific value, of these results.

Similarly, I feel sure that in the next ten or twenty years our basic knowledge of the properties of matter in the solid state is going to be far beyond anything which any one at this moment can visualize. I am equally sure that the results of these researches will have a bearing upon the future development of engineering in general and of the automotive industry in particular, which will be almost as significant as the quantitative work which followed Oersted and Faraday, was to electrical engineering.

In the above, I have discussed research in pure science. The importance of such research is indicated by the recent remark of an internationally known engineer, who is an executive in one of our largest industrial concerns. He made a plea for research in pure science, saying that his industry was "scraping the bottom of the barrel" for new basic principles upon which to make engineering advances.

It is, however, obvious that between the research man in the laboratory of pure physics and the engineer who is concerned with "making and doing things" there is that vast field of applied science. Only recently—as the history of the development of society goes—have applied science laboratories become recognized as an established link between the pure scientist and the engineer. The success of these laboratories is so well known as to require no further comment. Until the advent of these large industrial laboratories, the utilization by industry of the fundamental discoveries and laws of physics was left largely to chance. Even now, these fundamental discoveries themselves are left largely to the chance interests and enthusiasm of physicists in academic institutions. We all realize that what we call "chance" must play an indispensable part in all phases of modern life. But to leave to chance the development of basic ideas in the physical sciences, is like it would be to leave to chance the securing of our food supply unaided by agriculture. It is high time that we emphasize the importance of better team work among pure scientists, applied scientists and engineers.

It is to be hoped that out of this conference there will develop a sort of philosophy based upon an abiding faith in the value of cooperation among those who are concerned with progress in its largest aspects.

"When better automobiles are built," physics will help build them.

Resumés of Recent Research

Recent advances in experimental and theoretical physics are described in nontechnical language in these columns. It is intended that sufficient background be given to introduce the reader to the subject.

Recent Experiments on the Variation of Electron Mass with Velocity

It will be remembered that the original classical experiments, to determine the velocity variation of the ratio e/m for electrons, were performed by Bucherer and Neumann. Their method consisted first in the selection of a particular velocity by means of a shallow condenser placed in a crossed magnetic field, and finally the momentum was measured photographically in terms of the deflection in the simple magnetic field. Recently the question arose whether beta-particles coming *directly* from radioactive nuclei might not be heavier than normal. To answer this question C. T. Zahn and A. H. Spees,[1] at the University of Michigan, have developed a new method which is essentially a reversal of the Bucherer experiment.

In their modified method, after first selecting a momentum by means of the simple magnetic field, the rays are directed into the condenser space. Then the velocity is measured by determining the value of the electric field which allows the electrons to pass freely through the condenser. The rays are detected by means of a Geiger counter in a fixed position, and inaccuracies and inconveniences of the photographic method are thereby dispensed with. Amongst other advantages, however, the most important consists in the fact that grave uncertainties due to reflection of electrons from the condenser plates are practically eliminated.

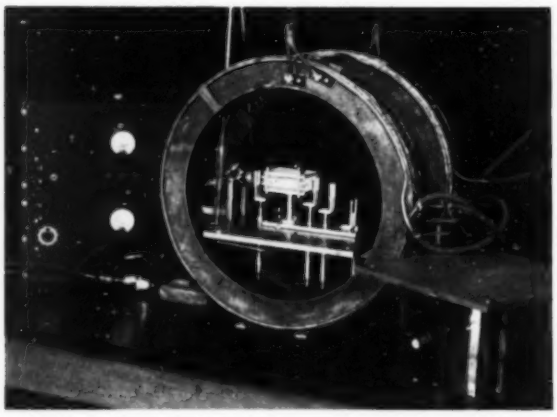

Apparatus used to determine the ratio e/m for beta particles from radium E.

By a mathematical investigation of the "electron optics" for the "rays" passing through the condenser they have shown that the resolution characteristics of the new apparatus are superior to those of the Bucherer-Neumann arrangement. In fact, their analysis of the classical experiments has revealed that Neumann's supposed velocity filter, even for the case of negligible reflection, must have been completely "broken down" on the high velocity side, for $\beta > 0.7$—and that, even for the lower velocities observed, the resolution width was approximately as great as the whole relativistic mass effect! Moreover, the analysis has shown why one was nevertheless able to obtain apparent lines with the classical method,—but has indicated that these lines may be seriously displaced, in consideration of the small difference between the relativity and the Abraham electrons.

It would therefore seem that a satisfactory direct experimental verification of the relativistic mass formula is still lacking, and that from this point of view the question is still open, particularly for the higher velocities. The above-mentioned improved method, however, offers the possibility for satisfactory experiments of this kind. (Although no special aim has as yet been

[1] The present note is a brief resumé of the following series of articles and letters in the Physical Review: C. T. Zahn and A. H. Spees, **52**, 524 (1937); **53**, 357 (1938); **53**, 365 (1938); **53**, 431 (1938); **53**, 511 (1938).

made at great accuracy, actual experiments by this method, for beta-particles from radium E at the single velocity $\beta \sim 0.75$, do give agreement with the theory of relativity, to within the limits of experimental error.) There is also promised the possibility of extending the range of observation to energies at least of the order of ten times those observed by Bucherer and Neumann.

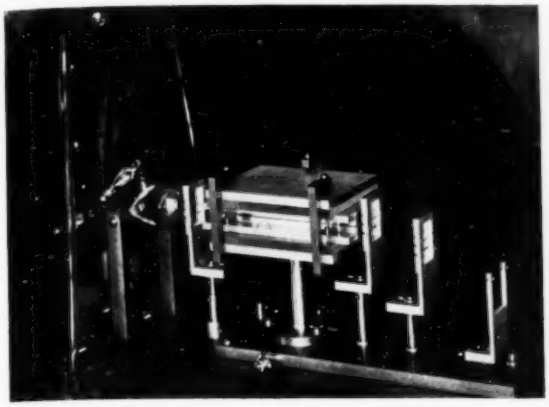

Detail of apparatus used by Messrs. Zahn and Spees to determine e/m.

Ideas Concerning Field and Motion

In Newtonian mechanics the equation of motion is assumed: the force is proportional to the acceleration. But if we regard not matter but *field* as something fundamental then the equation of motion must follow from the field theory. In a paper published recently by Einstein, Infeld and Hoffmann* it was shown that the equations of motion are contained in the gravitational equations and can be deduced from them by an approximation method which, in principle, enables these equations to be calculated with an arbitrary degree of accuracy. Professor Robertson solved these equations and obtained interesting results concerning the motion of double stars (Ann. Math. (1938)). The paper, "Electrodynamic and Gravitational Equations" by L. Infeld is closely connected with this problem. In this paper it was shown that gravitational radiation does not play any essential part in the motion of double stars.

* "The Gravitational Equations and the Problem of Motion," Ann. Math. (1938).

Studies of the Magnetic Structure of Cobalt

Fine magnetic powders deposited from suspension in liquid onto smooth ferromagnetic crystals form in certain cases regular patterns related to the crystal symmetry (Bitter patterns). The study of these patterns and their behavior when the specimen is magnetized furnishes new information concerning the nature of the magnetic domains which have long been postulated in ferromagnetic theory. In the experiments reported* colloidal gamma-ferric-oxide was used to form patterns on basal and prism planes of cobalt crystals. Photomicrographs are shown of typical patterns formed with and without a small magnetic field applied normal to the specimen's surface.

A simple interpretation of the patterns indicates that the spontaneous magnetization in a demagnetized specimen is divided into many thread-like domains which extend completely through the crystal parallel to the hexagonal axis, the one direction of easy magnetization in cobalt. The magnetization in half of these domains is opposite to that in the other half. For a grain several millimeters in diameter the domains have an average width of about 60μ. The scale of the structure is less in smaller grains. In section the domains seem to be polygonal, exhibiting, however, considerable irregularity. The basal patterns (which give this information) possess a fine structure apparently associated with smaller dendrite-like domains of reversed magnetization extending short distances into the ends of the threads. Thread-like domains of like magnetization in many cases occur in rows forming irregular layers of considerable extent.

The original article contains a partial review of previous attempts to treat magnetic structures theoretically. It is suggested that the actual demagnetization process, with its accompanying energy losses, may cause the attained magnetic structure to deviate considerably from the one which would minimize the reversible energies involved in demagnetization.

* Phys. Rev. **53**, 757 (1938).

Contribution of the Physicist to Highway Illumination*

BY CLIFTON G. FOUND

Research Laboratory, General Electric Company, Schenectady, New York

Introduction

WHEN I was invited to present this paper I understood that the purpose of this symposium was to demonstrate what the physicist had contributed to the automotive industry, and, that my specific duty was to inform you what the physicist had contributed in the field of highway lighting. Of course, I might review the contributions of the physicist in the development of the incandescent lamp to its present state of high efficiency. I might discuss how he developed ductile tungsten wire, how he found methods of exhausting lamps to increase their life, how, after exhausting them, he put gas back to increase their efficiency, or I might describe the technique he employed to determine the physical properties of tungsten to such a high degree of accuracy that the operating characteristics of a lamp can be accurately predicted before the lamp is constructed. However, I thought that it would be more appropriate if I discussed the processes involved in the operation of the newer electric discharge lamps and show how a knowledge of these fundamentals is utilized in the design of a lamp. For particular discussion I chose the sodium vapor lamp, since its operation involves principles which are common to all low pressure discharge lamps, and, moreover, this lamp is now being used extensively to illuminate the highways.

Construction of Sodium Lamp

The structure of the 10,000 lumen sodium vapor lamp is shown in Fig. 1. It operates on a.c. and consists of an evacuated envelope in each end of which is an electrode which serves alternately as cathode and anode. The filament is coated with barium oxide, which, when heated, emits electrons; the cylinder surrounding the filament serves as anode on the half-cycle during which the electrode is positive. The glass container is filled with neon at a pressure of about 3 mm of mercury and, in addition, there is a small amount of sodium. When the lamp is first started, it operates as a neon discharge, but, since it is surrounded by an insulating vacuum flask, the heat from the neon discharge raises the temperature of the lamp, causing the evaporation of sodium, which is then excited and gives rise to the golden yellow light with which most of us are familiar.

Although sodium lamps were made in the laboratory many years ago, one of the difficulties which deterred commercial development was the action of the sodium on the glass. Sodium is an alkali metal which is very active chemically and, at high temperatures, reacts vigorously with ordinary glass. This difficulty was finally overcome by the development of a sodium resistant glass. However, this glass could not be worked satisfactorily, but success was attained by powdering the glass and applying it, as a glaze, on the inside of ordinary glass. This technique has been so successful that practically no lamps have been lost through failure of the sodium resistant coating.

Mechanism of Light Production in an Electric Discharge

In order to understand the operation of the sodium lamp, it is necessary to know the processes involved in the generation of light by an electric discharge. In contrast to the continuous spectrum of an incandescent solid, the spectrum of the radiation from a gaseous discharge is composed of a number of definite lines or bands. The origin of this line spectrum was first ex-

* Paper presented at the Symposium on Physics in the Automotive Industry at Ann Arbor, Michigan, March 14 and 15, 1938.

plained by the theory of Bohr in 1913. According to this theory an atom can absorb or emit energy only in bundles of certain definite amounts. These bundles of energy are known as quanta. The absolute values of the quanta which an atom can absorb or emit depend on the kind of gas and the configuration of the atomic system. Thus, an atom can exist in only a discrete number of

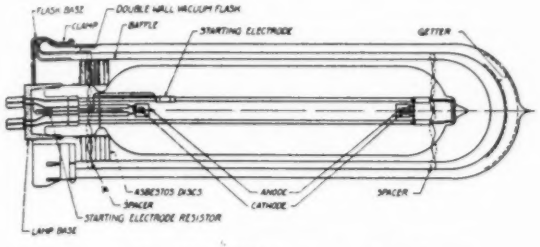

FIG. 1. Na (9) 10,000 lumen sodium lamp.

abnormal or excited states, and the particular state to which it is raised by the absorption of a quantum will depend on the magnitude of the energy absorbed. After an atom has been raised to an excited state by absorption of energy, it will return to the normal state either directly or by passing successively from one excited state to a lower. When the atom goes from a state of high energy, E_k, to a state of lower energy, E_j, the excess energy, E_k-E_j, is emitted as radiation whose wave-length in A is given by the relation $\lambda=12336/(E_k-E_j)$,* where E_k and E_j are measured in electron volts. The magnitude of the quantum is usually measured in units known as electron volts (ev), where an electron volt is the energy an electron acquires after it has been accelerated through 1 volt difference of potential. If the energy difference lies between 1.7 and 3.1 ev, the radiation will occur in the visible portion of the spectrum. A quantum with energy of 1.7 ev corresponds to red light of wave-length about 7200A, and a quantum with energy of 3.1 ev to blue light of wave-length about 4100A. When one considers that an energy change in an atomic system may amount to as much as 25 ev, it is seen that visible radiation is confined to a comparatively small range.

Before an atom can emit light it must first receive energy sufficient to raise it to a higher energy state. The values of the energy differences between the different states can be obtained from spectroscopic data, and are quite well known for most of the elements. This knowledge permits the construction of energy level diagrams of the type shown in Fig. 2 for sodium. The wave-lengths corresponding to the different transitions are marked on the diagram. Transitions between all possible combinations of energy levels are not possible, but the laws limiting the transitions are well established, and there is a vast amount of data on the energy states and emission lines of nearly all the elements. From the energy diagram it is seen that the minimum energy which a normal sodium atom can absorb is a quantum of 2.1 ev. When one of these excited atoms returns to its normal state, it will emit radiation in the visible spectrum of wave-length 5890A. Radiation of this kind, namely,

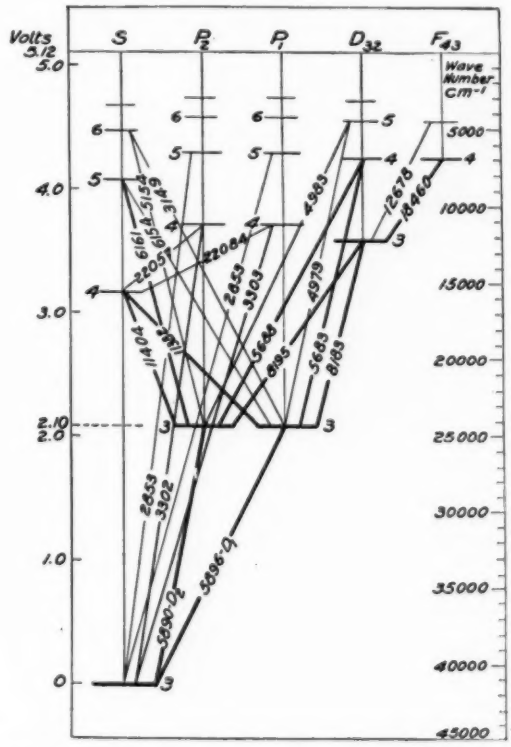

FIG. 2. Energy levels and lines in spectrum of sodium.

* The velocity of an electron or the energy of a light quantum can be expressed as equivalent electron volts which are obtained from the relations

$$Ve=\tfrac{1}{2}m_e v^2=h\nu=hc/\lambda,$$

where m_e is the mass, e the charge, v the velocity of an electron; thus 1 electron volt (ev) = velocity in cm/sec./5.935×10^7 = frequency/2.43×10^{14} = 12336/wave-length in A, where 1 angstrom (A) = 10^{-8} cm.

that produced by a transition from the first excited state to the normal, is known as resonance radiation.

It is known that the sensitivity of the eye varies with the wave-length of the light observed. In Fig. 3 the eye sensitivity for light of different

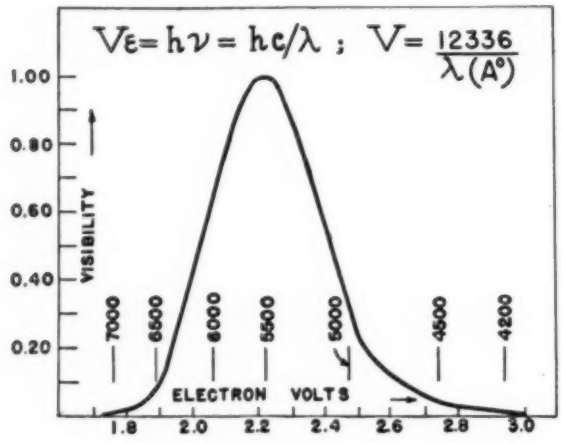

FIG. 3. Visibility curve.

wave-lengths is plotted as a function of the wave-length. It will be observed that the sensitivity of the eye for sodium light is close to the maximum which occurs at 5550A. The high sensitivity of the eye for this yellow light is one of the factors which explains the high efficiency of sodium vapor lamps.

A second characteristic which also contributes to the high efficiency of these lamps is the fact that this visible light is the resonance radiation. Sodium and lithium are the only two elements in the periodic table for which this is true, and, since the resonance radiation of lithium lies in the deep red, sodium holds the unique honor of being the only element capable of producing appreciable quantities of visible light by this simple process. When the resonance radiation is in the visible range, all the energy absorbed by a sodium atom in raising it to the resonance or first excited state can be emitted as visible light. Moreover, this energy, theoretically, can be transferred to sodium atoms in exactly the correct amount without any additional energy transfer.

In order to obtain visible light from atoms of other elements, the atom must be excited to a state higher than the first excited state. This requires much more energy than is equivalent to a quantum of visible light. As an example, consider neon, the energy diagram of which is given in Fig. 4. It will be observed that the first excited state of neon requires an energy of 16.5 ev, and in order to obtain visible radiation, it must be raised to the second series of levels, requiring 18.5 ev. The red light of neon is then obtained by atoms falling from the 18.5 state to the 16.5 state. Thus, an energy of 18.5 ev must be absorbed by a neon atom in order to obtain visible light corresponding to about 2 ev. The remainder of the energy is emitted as ultraviolet radiation.

For a process such as that in sodium all of the energy absorbed can be re-emitted as visible light, and the efficiency of converting energy into visible light would be 100 percent. This corresponds to an efficiency of light production of about 475 lumens per watt. However, this high efficiency cannot be obtained in practice as losses of other types are present.

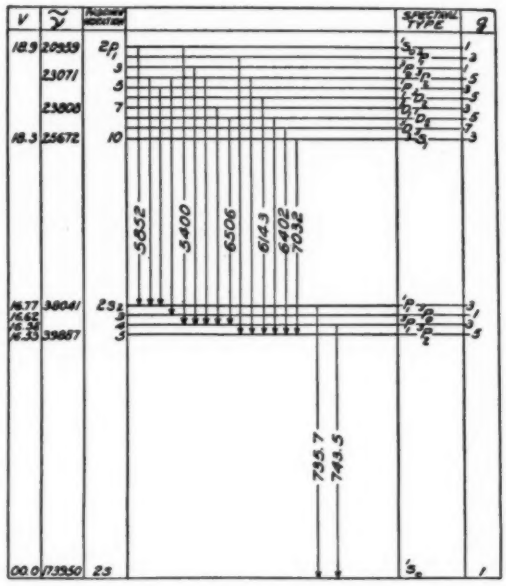

FIG. 4. Lower energy levels in spectrum of neon.

Energy Losses in Sodium Lamps

(*a*) *To vaporize sodium.* Sodium is a solid at ordinary temperatures, and, in order to be excited, it must be present in the vapor form. The vaporization of sodium requires a consumption of energy which will result in a lower efficiency than that mentioned above. Vapor lamps are

usually designed so that this energy is supplied by other necessary losses. In some cases, like sodium, a vacuum flask is used to conserve this heat. However, if one transported a sodium lamp to a location at such a high temperature that the sodium was in the vapor state, one would find that the efficiency would still be less than the theoretical limit of 475 lumens per watt, because there is no method of transferring energy to raise the sodium to the first excited state without, at the same time, consuming energy in other processes. This statement is not entirely true, but it is true for all except very small energy input. Efficiencies greater than 300 lumens per watt for a sodium lamp have been obtained at very low currents, when the tube was heated in an oven, if the energy to heat the oven was neglected.

The customary method of transfer of energy to atoms in a discharge lamp is by means of electrons. These electrons are liberated at the cathode and carry current through the discharge tube to the anode. If the tube contains gas or vapor, the electrons will collide with some of the gas atoms on their journey across the tube. If the energy of the electrons is of the proper value, some of their kinetic energy will be converted into potential energy of the atomic system, raising it to an excited state. For example, if a

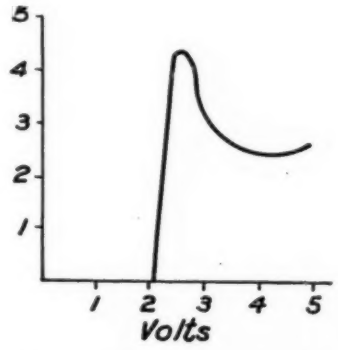

FIG. 5. Excitation function for resonance level of sodium.

swarm of electrons with energy of 2.1 ev is traveling across a tube containing sodium, and, if they collide sufficiently often with sodium atoms, all of the kinetic energy of the electrons will be transferred to the sodium atoms, raising them to the first excited or resonance state, in which they exist for a very short time, about 10^{-8} sec. They then return to the normal state emitting their absorbed energy as yellow light. In this illustration, the production of light would be very efficient, as the only energy loss would

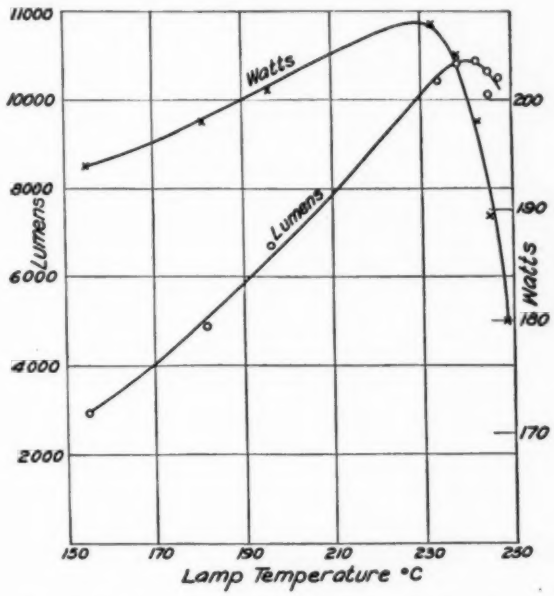

FIG. 6. Characteristics of 10,000 lumen sodium lamp.

be that necessary to liberate the electrons at the cathode, again neglecting the energy required to vaporize the sodium. The amount of light that can be generated by such a simple process as that given above is very limited, since, due to the action of space charge, that is the force of repulsion between electrons, the rate of flow of electrons would be limited to a very small value.

(*b*) *To produce positive ions.* In practice the effect of electron space charge is overcome by forming positive ions to neutralize the negative space charge of the electrons. When a sufficient number of ions is present, currents of electrons of several amperes can flow at comparatively low voltage. However, another loss has been introduced, namely that required to form the ions. Since the energy to form an ion is greater than that necessary to produce an excited atom, the electrons must now be accelerated to a much higher velocity. Now, the probability that an electron will excite a sodium atom depends on the energy of the electron as shown in Fig. 5. It will be noted that no excitation takes place until the energy of the electron reaches 2.1 ev.

As the electron energy rises above this value, the probability increases to a maximum at about 2.6 ev and decreases as the energy is still further increased. Obviously, the electron energy most effective in producing excited atoms of this sort is at 2.6 ev, but, in order to be able to produce positive ions, it is necessary to exceed this value, and, consequently, reduce the probability of excitation below the maximum. Thus, the difficulty of constructing a sodium lamp is increased by the requirement that the same group of electrons must produce both excited atoms and positive ions, and these two processes require electrons of different energies.

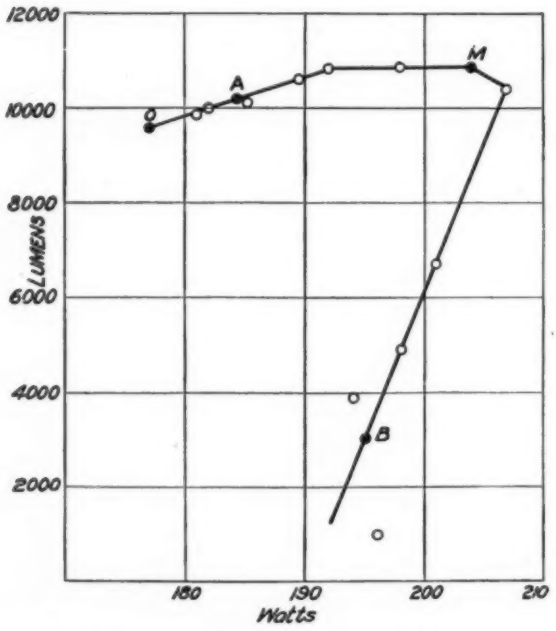

FIG. 7. Lumens-watts relation for 10,000 lumen sodium lamp.

Energy of Electrons in a Discharge

Actually, although all of the electrons originating at the same source are accelerated by the same fields, because of the difference in the amounts of energy which they have lost at collisions with gas atoms, the energy of all the electrons is no longer the same when they reach the main body of the discharge. In addition, new electrons are formed in the discharge as a result of ionization, and the energy of these will be less than that of those originating at the cathode. As a consequence of these processes, the electrons in the discharge have a random distribution of energies similar to that of molecules of a gas at an elevated temperature. The electrons with the highest energies are capable of forming positive ions, while those of lower energy produce the excited atoms. The electrons with energies between these two values may excite atoms to states other than those from which visible radiation is obtained.

Control of Electron Energy

One of the problems in designing a discharge lamp is to control the energy of the electrons so that there will be enough electrons of high energy to form the necessary ions, and, at the same time, there will be plenty of electrons with lower energy for producing excited atoms. A discharge tube is fundamentally a conductor of electricity, and the first obligation of the electrons is to produce the ions necessary to permit the current to flow. Thus, the positive ion requirement determines the average energy which the electrons must attain, and the production of light is merely a by-product of these processes of conduction. Experiments indicate that the group of electrons which is most effective in producing sodium light has a temperature of about 25,000 degrees. the average energy of a group of electrons having this temperature is 3.2 ev. In order to produce an efficient sodium lamp it is, therefore, desirable to construct a tube in which the processes of conduction demand electrons having this same temperature.

What are the factors which control the electron temperature? The two factors which determine the energy which the electrons must have are the diameter of the tube, more correctly the ratio of volume to surface area of the confining vessel, and the kind and pressure of the contained gas. The latter determines the rate of generation of ions by electrons of a given velocity, and the tube diameter determines the rate at which they disappear. Since the rate of generation must be equal to the rate of disappearance, it is seen that there must be a reciprocal relation between gas pressure and tube diameter. Roughly, this relation can be stated in the following form. The electron temperature will remain constant for a given gas as long as the

product of gas pressure and tube diameter remains constant.

It was pointed out earlier that the sodium lamp also contains neon. The purpose of the neon is to furnish the positive ions necessary for the conduction of the current. The pressure of neon is chosen so that the electrons will have the energy necessary for optimum excitation of the sodium. The neon also serves as a buffer gas which increases the probability that an electron will collide with a sodium atom before the electron reaches the anode. This is important as the number of sodium atoms present at the operating temperature is less than 1/1000 of the number of neon atoms, and if no neon were present, the energy which the electrons would require in order to form sufficient positive ions would be so great that comparatively few sodium atoms would be excited to the resonance state.

Even when conditions are chosen so that the electrons have the optimum energy for exciting sodium atoms to the first excited state, energy will be used in the following processes:

(1) To vaporize sodium,
(2) To liberate electrons at the cathode,
(3) To generate positive ions,
(4) To generate excited atoms.

The fourth of these methods of energy consumption is the only one that results in the production of visible radiation, a fraction of which is given off as visible light, since the heterogeneous group of electrons will also excite the sodium atoms to states other than those from which visible light is produced. The efficiency of light production will be this fraction divided by the sum of all the energy losses.

Scattering of Resonance Radiation

Resonance radiation is any radiation which is produced by a transition which ends on the normal state of the atomic system. Now, if a radiation is emitted which ends on the final state, that same radiation can be absorbed by a normal atom raising it to the upper state from which the radiation originated. The yellow light of sodium is this type of radiation and is strongly absorbed by normal sodium atoms. Of course, atoms excited in this manner will eventually return to the normal state, and re-emit radiation of the same wave-length as that absorbed. As a result of this property of resonance radiation, a quantum of sodium light generated in the center of a discharge tube may be absorbed and re-emitted several times before it finally leaves the tube. In other words, resonance light does not travel in a straight path from the point of generation to the observer. The light that comes from the tube is light that is emitted by the sodium atoms in closest proximity to the walls. For this reason, a sodium lamp is a light source from which the light is emitted at the walls, and optically can be treated the same as if it were a tungsten filament having the same dimensions as the bulb.

Brightness of Sodium Lamps

The brightness of a sodium lamp is limited as a direct consequence of the scattering of the resonance radiation. This limitation takes place in the following manner. Since the light quanta are absorbed and re-emitted many times before they leave the bulb, the concentration of quanta in the bulb will be much greater than it would be if the quanta passed directly out. One may ask how this will affect the light, since it comes out finally. In the previous discussion, it has been assumed that all atoms excited to the first excited state return directly to the normal state and emit visible light. This assumption is only

FIG 8. Duanesburg highway illuminated with G.E. Novalux sodium luminaires, Route 7, near Schenectady, N. Y.

true if nothing happens which will destroy the excited atom before it can radiate. There are, however, "accidents" which can happen and

prevent the excited atom from radiating. Such an "accident" is that it may collide with an electron having sufficient energy to ionize it or to raise it to a higher energy state from which no visible radiation is emitted. The probability that such an "accident" will happen is proportional to the concentration of electrons and to the concentration of excited atoms. Consequently at high concentrations of excited atoms, and at high currents, the rate at which excited atoms lose their energy, by processes other than those resulting in resonance radiation, increases and as a result the light output does not increase with further increase in pressure and current but reaches a saturation value. In addition, those "accidents" which result in the production of sodium ions cause a reduction in the average energy of the electrons and, thereby, cause an actual decrease in light output at high currents and high pressure of sodium. The maximum brightness which can be obtained varies slightly for different types of tubes, but is of the order of magnitude of 5–6 candles/cm², which is about the same as an incandescent filament at 1800°K.

FIG. 9. San Francisco-Oakland Bay bridge illuminated with more than 1000 G.E. sodium luminaires. View from Yerba Buena Island towards lights of San Francisco, California.

Operation of Sodium Lamp

The presence of this maximum in the lumen output is easily observed in the characteristics of the 10,000 lumen sodium lamp. In Fig. 6 the light output and the lamp wattage at 6.6 amp. are plotted as a function of the temperature of the lamp bulb (i.e., the vapor pressure of sodium). At room temperature the lamp operates as a neon discharge, but as the temperature is increased and sodium is vaporized, both the light and the wattage increase and reach a maximum and then decrease as the temperature is further increased. Both the lumens and the power are functions of the vapor pressure, and when the lumens are plotted as a function of the watts as in Fig. 7, each point on the resultant curve corresponds to a definite concentration of sodium atoms.

Temperature Sensitivity of Sodium Lamps

The relations given in the curve of Fig. 6 show that the light output of a sodium vapor lamp depends on the temperature of operation of the lamp, which with any given degree of heat insulation will vary with the temperature of the surroundings. Consequently, from a consideration of the lumen temperature curve alone it would appear that the light from a sodium lamp would depend on the temperature of the surroundings. However, this is not necessarily so if the proper point is chosen for normal operation. If the heat insulation for the lamp is chosen so that under normal conditions (ambient temperature of 15°C and still air) the lamp operates at the point 0, Fig. 7, a decrease in ambient temperature results in a displacement of the operating point to the right. However, since such a shift involves an increase in the wattage consumed in the lamp, the decrease in lamp temperature, and therefore the change in light output, will be much less than would occur if the wattage remained constant. By way of contrast, consider the result of a decrease in temperature when the lamp is operating at the point of maximum lumens M. Under these conditions a decrease in ambient temperature is accompanied by a decrease in wattage consumption, and the change in lamp temperature and light is magnified. For example, a lamp operating normally at M shifts to the point B when the temperature of the surroundings falls to -20°C with a 15-mile-per-hour wind, a decrease in light of about 75 percent. However, if 0 is the point of normal operation, the same change in

the surrounding conditions results in a shift to *A* with a change in light output of less than 5 percent.

Design of Sodium Lamps

Let us now consider how the fundamental processes enter into the design of sodium lamps. Since there is a maximum brightness, a definite surface area is required to produce a light of given luminous output. The operating current determines the cross section of the tube, and, as a result, the length is automatically fixed. The dimensions of the cathodes are also fixed by the value of the current. Knowing the tube diameter, one must next adjust the pressure of neon so that the energy, which the electrons must have to produce the necessary positive ions, will be that which will excite the greatest number of sodium atoms. The neon pressure and the length of the tube fix the voltage drop and therefore the wattage. Rough calculations of the pressure of neon and of the voltage drop can be made from the theory of electric conduction through gases. The present state of this theory is not sufficiently accurate for accurate calculations, but sufficient empirical data are available to make rough estimates. This completes the design of the tube, but one must still determine the heat insulation which is necessary to maintain the tube at the operating temperature at which it will be insensitive to changes in the ambient conditions. This factor must be found empirically.

Description of Na (9) Sodium Lamp

This is the lamp which is shown in Fig. 1, and a general description has been given in that place. The bulb is 7.5 cm in diameter, and the distance between electrodes is 22.5 cm. The lamp is designed to operate at 6.6 amp. and consumes about 180 watts, giving a light output of 10,000 lumens at an efficiency of 55 lumens per watt. The only auxiliary equipment necessary for operation on a constant current circuit is a time-delay relay to permit the cathodes, which operate in series with the arc, to heat up before the lamp starts. In addition, there is a small high frequency filter to prevent radio interference. The average life of the lamps is about 2000 hours, and the maintenance is approximately, the same as for large Mazda incandescent lamps.

In a typical highway installation the luminaires are mounted 20 ft. high and about 5 ft. over the edge of the pavement. They are spaced about 200 to 250 ft. apart. Such an installation is shown in Fig. 8, and gives a road illumination of approximately 0.35 lumens per square foot, which is in agreement with the recommendations of the I.E.S.

Features of Sodium Lamps

The features of sodium lamps which make them particularly desirable for highway illuminants are:

(1) *High efficiency.* For the reasons previously stated, the sodium lamp generates light very efficiently, producing two to three times as much light as can be obtained from incandescent lamps of the same wattage. This permits the use of higher levels of illumination for the same power consumption.

(2) *Low intrinsic brilliancy.* Since the brightness is only that of a tungsten filament operating at 1800°K, glare is greatly reduced and driving comfort greatly increased.

(3) *Distinctive color.* The soft golden color of sodium light is close to that part of the spectrum for which the eye is most sensitive, and is particularly adapted for illumination of dangerous stretches of road, such as intersections and curves, where caution is needed.

In closing I might state that at present there are over 6500 luminaires in service, which, if installed continuously, would illuminate 325 miles of highway. The longest single installation at the present time is 17 miles of the Duanesburg Road out of Schenectady. A view of this is shown in Fig. 8. The installation, on the San Francisco-Oakland Bay bridge, shown in Fig. 9, contains the largest number of lamps, 1081.

Studying Engine Combustion by Physical Methods*

A Review

BY LLOYD WITHROW AND GERALD M. RASSWEILER

General Motors Corporation, Detroit, Michigan

STUDYING the combustion process within the gasoline engine presents two principal difficulties; namely, the inaccessibility of the flames and the extreme rapidity of the burn. On the other hand the investigator is partially compensated by having an explosion vessel which automatically admits, fires and expels charge so that the combustion process may be observed many times every minute. Certain experiments are thus made possible which are difficult to perform with other apparatus.

Although the study of the reactions involved in the combustion process is usually considered to be a chemical problem, the use of pure chemical methods, consisting essentially of the analysis of samples of gas removed from the engine, meets with quite serious difficulties. Certain physical methods, notably photographic and spectrographic methods, have therefore been applied to this problem. These methods of attack, besides yielding considerable information about the chemical nature of the combustion process, have also made a distinct contribution to our knowledge of the thermodynamic and physical nature of the combustion phenomena in the engine. This paper presents illustrative examples of the information obtained at the General Motors Research Laboratories by applying spectrographic and photographic methods to the study of combustion within the engine. No attempt will be made to cover, even in summarized form, all the research which has been carried out by these methods.

In order to acquaint the reader immediately with the general nature of an engine explosion, some pictures of the engine flames will first be presented.

High Speed Cinematography

One of the latest methods to be applied to the study of engine combustion is the direct photography of the flames with a high speed motion picture camera. A special single-cylinder engine was first built with a transparent top replacing the usual cast iron cylinder head, as shown in Fig. 1. The pictures in Fig. 2, taken through this window, depict the progress of the flame during a single explosion. The frame number and crank angle are listed beneath each frame or

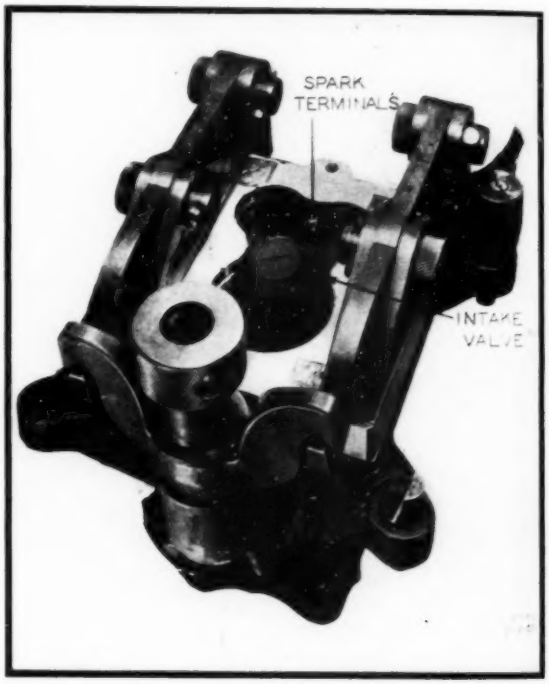

FIG. 1. Transparent head mounted on engine cylinder block.

* Paper presented at the Symposium on Physics in the Automotive Industry at Ann Arbor, Michigan, March 14 and 15, 1938.

individual flame picture. The crank angle which is expressed in degrees of rotation of the crankshaft before (−), and after (+) top dead center denotes the instant at which the exposure of each frame ended. The ignition spark is plainly visible in frame 3, the spark advance having been set for approximately 22° before top dead center. After ignition the flame accelerates rapidly with respect to the cylinder head, spreading in all directions through the charge. As the combustion proceeds, the outer boundary or envelope of the body of inflamed charge develops an irregular and continually changing shape, the shape of the envelope apparently being influenced by such factors as gas movements and combustion chamber shape. In successive explosions there is considerable variation in the form of the flame envelope and in the velocity of its propagation. These latter facts must be borne in mind when interpreting many of the results of engine combustion studies.

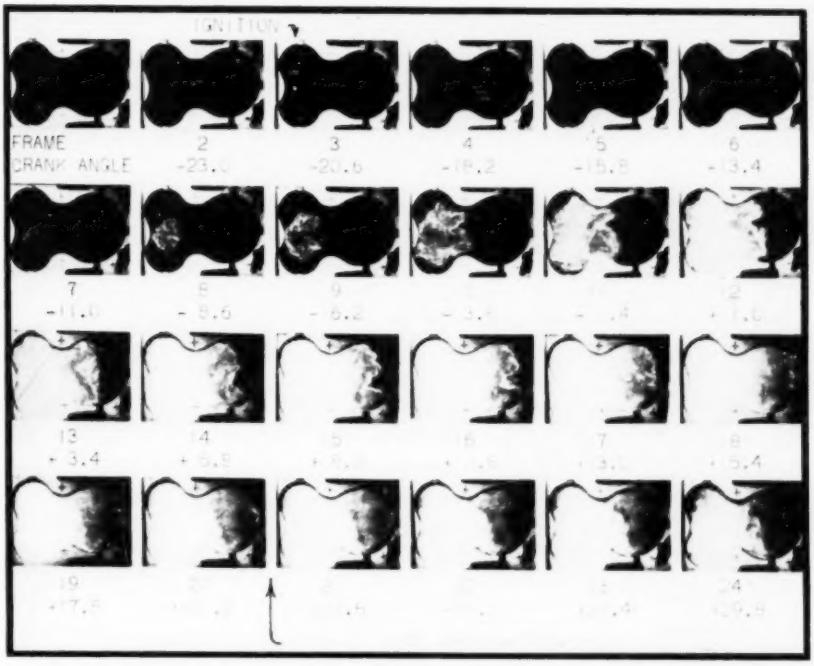

FIG. 2. Consecutive frames from a high speed moving picture of a nonknocking explosion. Picture frequency, 2250 frames per second. Duration of each exposure, 1/2550 second.

In the explosion shown in Fig. 2, the flame propagation is completed about 21 crankshaft degrees after top dead center. Thus the flame traveled the five inches across the combustion chamber in about 43 crankshaft degrees, which, at an engine speed of 900 r.p.m., represents 1/125 second. It is of considerable interest that as the engine speed increases the velocity of flame propagation likewise increases. This fact is of great practical importance because it means that even at high engine speeds the flame propagation may still be completed early in the expansion stroke.

With this brief survey of the combustion process in mind, the requirements of the camera which was designed to take the pictures in Fig. 2 may be discussed more readily. These requirements follow: (1) The object to be photographed, the flame in the engine, is self-luminous, so that any camera which depends for its action on intermittent illumination of the object by sparks, discharge tubes, or other means is not suitable. (2) To obtain 15 to 20 pictures of the flame traveling across the combustion chamber with the engine running at speeds equivalent to car speeds of from 20 to 80 miles an hour, the picture frequency range should extend from 2000 to 10,000 frames per second. For such picture speeds the tensile strength of the film does not permit intermittent film motion; thus, the film must be moved continuously. (3) To obtain sharp pictures on continuously moving film, either the time of exposure must be very short or the image to be recorded must be moved with the film during the exposure. The choice between these alternatives is determined by the light emitted by the engine flames. (4) With the available light from the flames, the duration of exposure of each picture must be comparable to the interval between pictures using a lens speed of about $f:2$; it follows that it is necessary to move the image with the film during each

exposure. (5) To avoid blurring due to flame movements, the exposure must be as short as possible; the lens system should work at full aperture throughout the exposure. (6) The

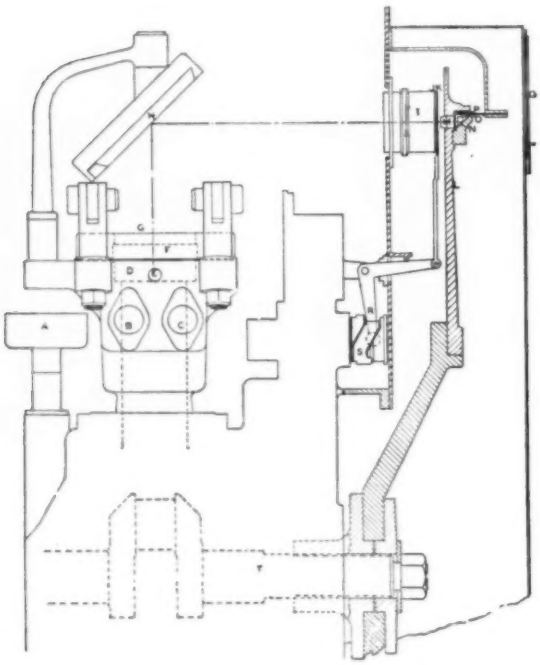

FIG. 3. High speed camera for photographing flames in the engine.

A, Ignition breaker	*K*, Shutter
B, Intake port	*L*, Rotating disk
C, Exhaust port	*M*, Moving lens
D, Combustion chamber	*N*, Moving prism
E, Spark plug hole	*O*, Focal plane shutter
F, Quartz window	*P*, Film
G, Invar window frame	*Q*, Door in light tight housing
H, Stellite mirror	*R*, Cam follower which actuates shutter
I, Stationary field lens	*S*, Shutter cam
J, Lens stop	*T*, Crank shaft

picture size should not be so small that details of flame structure are lost. (7) The angular position of the crankshaft should be accurately known for each frame.

Figure 3 shows a schematic sketch of a camera which satisfies all these requirements except for the picture frequency range. The highest picture frequency obtained to date lies between 5000 and 6000 pictures per second, the upper limit being set by the top speed at which it is practicable to run this engine. The optical parts of the camera consist of the following: the stellite mirror, *H*; the stationary master lens, *I*; thirty small lenses, *M*, mounted at intervals of 2.4 crankshaft degrees along a sector of the circumference of a large disk that is attached to the crankshaft; and, thirty reflecting prisms mounted behind corresponding lenses on the disk. Beneath the overhanging rim of the disk is a strip of 16 mm motion-picture film, which, during the recording of a set of flame pictures, remains stationary with respect to the small lenses and prisms in the rotating disk. In going through the camera, a ray of light passes through the window in the cylinder head, and is reflected by the mirror to the large stationary lens which has its focal plane in the combustion chamber. As each of the small lenses and accompanying prisms pass through the beam behind the stationary lens, an image of the flame in the combustion chamber is formed on the film. With this arrangement, the image of the combustion chamber formed by each small lens on the film moves along with the lens, prism, and film. Thus, despite the rapid continuous motion of the film, the image is held at rest with respect to the film (except for a slight relative twisting motion), long enough to permit each picture to be exposed properly with the limited amount of light available from the flames in the engine. Since the lenses are 2.4 crankshaft degrees apart, the camera can take thirty pictures of a single explosion at a rate of 5000 per second when the engine speed is 2000 r.p.m. A more detailed description of this camera has been published elsewhere.[1, 2]

As already shown, the high speed camera provides a very direct method of obtaining a good general picture of what happens when a gasoline-air mixture burns in the engine. But these pictures are being taken with a much more specific objective in mind. Thermodynamic treatments of the gasoline engine cycle do not adequately handle that portion of the cycle where combustion occurs, because of the fact that these treatments take cognizance only of the states of the system immediately before and immediately after combustion. In other words, thermodynamics pay little or no attention to the rate of chemical transformation during an engine explosion, even though this factor determines to a large degree the rate of pressure development as well as the maximum pressure attained. Thus in thermodynamic treatments of

the engine cycle, it frequently is assumed that combustion occurs instantaneously releasing all the energy of combustion when the piston is at top dead center. The fallacy of such an assumption and the desirability of taking account of the rate of reaction are generally recognized. Flame pictures such as those in Fig. 2 when correlated with the pressures developed simultaneously in the engine, offer a means of attack on this problem,[3] providing the pictures are first interpreted more fully than has been done so far in this paper. The significance of these flame pictures will therefore be discussed further by drawing upon information obtained by the application of other methods to the study of engine combustion.

The flame pictures show two regions of maximum luminosity, one along the forward edge of the flame and another behind the flame fronts in a region around the spark plug. These regions are particularly well shown by the three individual frames in Fig. 4. It is very desirable to know the nature of the processes which occur in regions *A* and *B*. The importance of this point is that if only an unknown fraction of the energy of combustion were released in the flame front, and if the gases in region *B* were not in chemical equilibrium, then it would be quite hopeless on the basis of present information to set up relationships between the fraction of charge inflamed and the pressure developed simultaneously in the engine. The study of the emission spectra of engine flames has indicated a very definite distinction between the regions represented by *A* and *B* in Fig. 4.

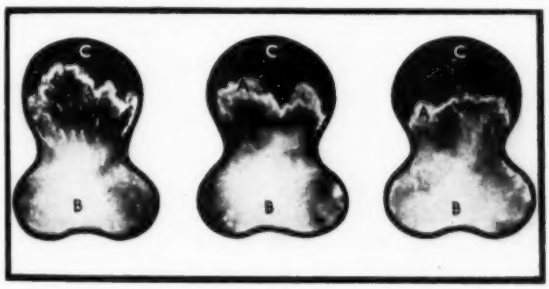

FIG. 4. Various regions distinctly differentiated on individual frames from three different explosions. *A*, Flame front; *B*, afterglow; *C*, noninflamed charge.

Emission Spectra

By mounting a spectrograph above a window in the top of the engine, and by using a stroboscopic shutter synchronized with the engine, it has been possible to photograph separately the spectra of the flame fronts and afterglows represented by regions *A* and *B* in Fig. 4.[4, 5] The differences in the spectra of the light from these two regions will now be discussed in connection with the spectra of the separate parts of the well-known Bunsen burner flame.

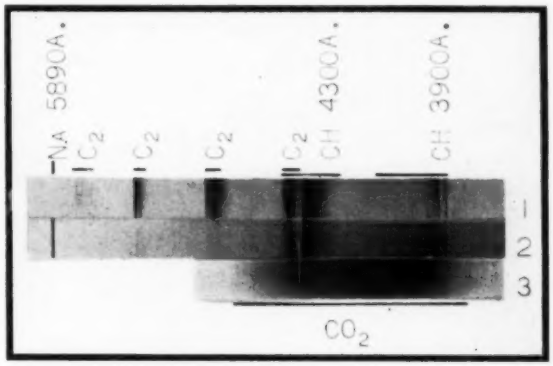

FIG. 5. Spectra of the flames of gasoline-air mixtures. 1, Inner cone of burner flame; 2, flame fronts in engine; 3, afterglow in engine.

Spectrum 1 in Fig. 5 was obtained by training the spectrograph on the inner cone of the flame of a gasoline torch operating in air. Spectrum 2 was emitted by the gases in the flame front of an engine operating on gasoline. Both of these spectra show the familiar CH and Swan C_2 bands. The third spectrum, which represents the emission from region *B* (Fig. 4), shows no trace of the CH and C_2 bands but consists of a very diffuse band system extending from about 3800A to 4500A. These diffuse bands are identical with a system observed by Weston[6] and by Kondratjew[7] in flames of CO and O_2. The latter author attributed them to carbon dioxide.

Still other bands are observed when the engine flame spectra are extended into the ultraviolet. Radiation characteristic of the OH radicals is emitted from both the flame fronts and afterglows. In addition to the OH bands, a group of very diffuse bands extending from 2800A to 3700A has been observed in the flame front spectra but not in the afterglow spectra. When

first observed on engine flame spectra, an exhaustive search through the literature failed to reveal a description of these bands. Indeed, no published reference could be found to the existence of such bands although they were identified on a spectrum photographed by Emeléus[8] while studying ether flames (see spectrum *d*, Fig. 1 of the Emeléus paper). In the meantime, however, Vaidya[9] has published the results of a careful study of the diffuse bands in spectra of the inner cones of ethylene flames. Depending on the method of producing the ethylene flame, Vaidya was able to resolve two types of bands, the so-called "*A*" and "*B*" groups. On the basis of certain similarities between the vibrational constants of the diffuse bands and those of the bands of nitric oxide, Vaidya has suggested that the *A* and *B* bands may originate in molecules of HCO which, like nitric oxide molecules, possess 15 external electrons. From Vaidya's later work[10] it appears that these bands are characteristic features of the inner cones of the flames of many hydrocarbons. A comparison of these "ethylene flame" bands with emission spectra of flame fronts in the engine when operating on either gasoline, iso-octane or benzene shows that the *A* group of diffuse bands is present in the engine flame spectra.*

Now the absence of CH, C_2 and HCO bands so typical of hydrocarbon flames, from the light emitted by the gases behind the flame fronts in the engine, indicates that the gasoline is not burning there. This deduction rests upon the similarity between the engine flame spectra and the spectra of burner flames. The sequence of reactions occurring in Bunsen burner flames has been studied carefully by Smithels and Ingle[13] who employed a unique method to study separately the processes occurring in the inner and outer cones. They used a device to separate the two cones of the ordinary Bunsen burner flame. It was then possible to remove gaseous samples from the space between the two cones of flame and to establish the presence or absence of hydrocarbons in the samples withdrawn. When air-fuel mixtures of pentane or heptane (typical constituents of gasoline) having air to fuel ratios comparable with mixtures used in the gasoline engine were burned in this apparatus, Smithels and Ingle found only carbon monoxide, hydrogen, carbon dioxide, water, and nitrogen above the inner cone. No hydrocarbons were observed. Now the similarity of the emission spectra of the inner cone of the Bunsen flame and of the engine flame fronts suggests that the chemical processes are alike. If this is true, it follows that the gasoline hydrocarbons are burning in the flame fronts in the engine.

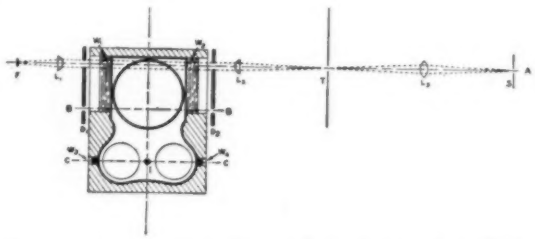

FIG. 6. Arrangement of combustion chamber windows and optical system for measuring flame temperatures and for photographing absorption spectra in the engine. *W*, Windows; *F*, source of light; *L*, lenses; *T*, stroboscopic shutter; *S*, spectrograph slit; *D*, diaphragms; *I*, spark plug location.

In a Bunsen burner, secondary air diffuses into the outer cone and there is further combustion of the carbon monoxide and hydrogen formed in the inner cone. But in the engine there is no secondary air added to the gases behind the flame front and thus there is no region in the engine exactly analogous to the outer cone of the burner. The gases between the two cones in the flame separator emit no light, but in the engine the gases behind the flame front are subjected to such high pressures and temperatures that they do emit light. The mechanism by which this gas is excited is not known. As a result of the continual changes in pressure and temperature of the burned gases,

* There appears to be some confusion in the literature regarding the statement by Vaidya (reference 9) that these HCO bands occur "feebly in a Bunsen flame as noted by Rassweiler and Withrow, and with greater intensity in the flame of ether, as shown in a photograph by Emeléus." Kondratjew (reference 11) apparently interprets this statement as meaning that Vaidya believes the bands observed by Emeléus in the cold flames of ether are the same as the bands which Vaidya attributes to HCO. We believe that Vaidya in the quotation above, referred to the ordinary flame spectrum of ether and not to the cold flame spectrum. As pointed out by Kondratjew, the cold flame spectra of ether, hexane, acetaldehyde etc., observed by Emeléus (reference 12), are undoubtedly due to formaldehyde. To date we have not observed the formaldehyde emission spectrum either in a Bunsen burner flame or in the engine flames.

the composition of the gases behind the flame fronts in the engine probably changes continually in order to maintain equilibrium conditions. It is possible that these equilibrium or composition changes may be intimately connected with the excitation of the carbon dioxide molecules after the passage of the flame front.

The thickness of the flame front cannot be deduced accurately from any experiments performed to date. In the central frame in Fig. 4, the maximum width of the luminous region, *A*, appears to be approximately three-quarters of an inch, whereas in the other two frames the projected flame front widths are as small as three-sixteenths of an inch. On account of the possible curvature of the flame fronts in the vertical plane and on account of the forward motion of the flame during the exposure of each frame, it is probable that the true thickness of the flame front is considerably less than the widths of the luminous zones shown on the flame pictures.

With the added idea that the gasoline and air react in the flame front liberating the energy of combustion in this region, the combustion process may now be interpreted a little more fully. Consider what happens to any small portion of the charge which at the time of ignition is located near the center of the combustion chamber. As the flame approaches, this unburned charge is compressed and forced away from the advancing flame. When the flame front reaches this portion of the charge, the sudden release of its energy of combustion quickly raises its temperature and causes this portion of charge to expand. As the flame moves on through the charge, the burned gas is again compressed and forced back toward the spark plug. These compression and expansion processes bring about temperature changes which may be studied by direct experimental methods.

Temperature Measurements by the Sodium Line Reversal Method

Temperatures of the inflamed sections of the charge have been measured by the sodium line reversal method in a special engine having windows on opposite sides of the combustion chamber as shown in Fig. 6.[14] Light from a tungsten filament was passed through the engine flames which during each measurement were colored by adding a trace of a sodium salt to the intake air. A stroboscopic shutter, synchronized with the engine, passed light during each explosion for only a short time interval at any desired crank angle. The sodium D line was observed superimposed on the continuous spectrum from the filament; the temperature of the filament was increased until the line changed from absorption to emission. At the reversal point the brightness temperature of the filament (at 5900A) was the temperature of the flame in the engine. Measurements were made along three lines: *A*, *B* and *C*, shown in Fig. 6.

Illustrative temperature data are given in Fig. 7. Soon after ignition, the temperature of the freshly burned gas was approximately 3700°F. Just after flame propagation was complete, the temperature of the first-burned gas near the spark plug had risen to 4200°F. This rise in temperature resulted from the compression of the burned gases by the expansion of the burning gases in the flame front.

Figure 7 also illustrates the interesting fact that, soon after the flame propagation was complete, the temperature of the freshly burned gas was some 450°F lower than the temperature of the gases near the spark plug. The explanation of this temperature gradient is as follows: As the gas near the point of ignition burns, it expands against a low pressure doing work and losing energy thereby. Subsequently, as the rest of the charge inflames, the first-burned gases

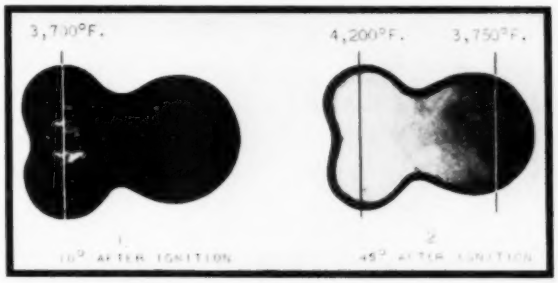

FIG. 7. Some line reversal temperatures observed in a gasoline engine.

are recompressed to approximately their original volume. Since the recompression occurs at a higher pressure than the previous expansion, the work done on the inflamed gas is greater

than the work which was done by the gas; hence, it gains energy at the expense of the gas in the rest of the chamber. Thus, the expansion and compression of the gases as the flame moves across the combustion chamber results in an unequal distribution throughout the chamber of the energy released by combustion; and, when flame propagation is complete the gases which burned first are hotter than the gases which burned last.

No effort has been made to use these measured temperatures for thermodynamic calculations for two reasons. First, each measured temperature represents some sort of average value along a line through the combustion chamber, as can be seen from Fig. 6; thus, neither the average temperature throughout the whole chamber nor the temperature at any given point in the chamber is directly deducible from these measurements. Second, the pressure measurements made simultaneously with the temperature measurements[14] have since been found to be unreliable.

Since the temperatures in the dark noninflamed portion of the charge are too low to excite the sodium D line, these temperatures cannot be measured by the line reversal method. But there is a real need for temperature measurements in these gases, and it is hoped that some suitable method can be developed for this purpose.

The Nature of Engine Knock

The main factor which is limiting the output as well as the thermal efficiency of present-day gasoline engines is the well-known engine knock. When a knocking explosion is photographed with the high speed camera, some of the frames of the resulting flame picture differ distinctly from those obtained when the engine is not knocking. In Fig. 8, frames 12 to 16 from the record of a nonknocking explosion reproduced in Fig. 2 are compared with corresponding frames from three knocking explosions. Except for a difference in the octane number of the fuel used, the knocking explosions presented in Fig. 8 were produced under the same engine conditions as the nonknocking explosion. Frames 12 at the left of this figure show that the flame has traveled about two-thirds of the distance across the combustion chamber in each of these explosions. The flame pictures show no significant differences in the types of inflammation in knocking and in nonknocking explosions either in frames 12 or in any of the frames recorded prior to frame 12; in other words, the first part of the flame propagation was not affected appreciably by the occurrence of engine knock. But, in frames 13, the differences between explosions 1 and 2 in Fig. 8 are very distinct. Spontaneously generated flames appeared ahead of the normal flame front in the knocking explosion. As a result of the simultaneous combustion along several flame fronts the rate of inflammation of the remainder of the charge was greatly increased. Thus in frame 14 of explosion 2, which was exposed 1/2250 second later than frame 13, the charge was practically all inflamed; only a small triangular dark patch in the lower right corner was still not ignited. Then in the next succeeding frame the consumption of the charge was complete. Not so in the nonknocking explosion, however. There the flame had a considerable portion of its course still to run.

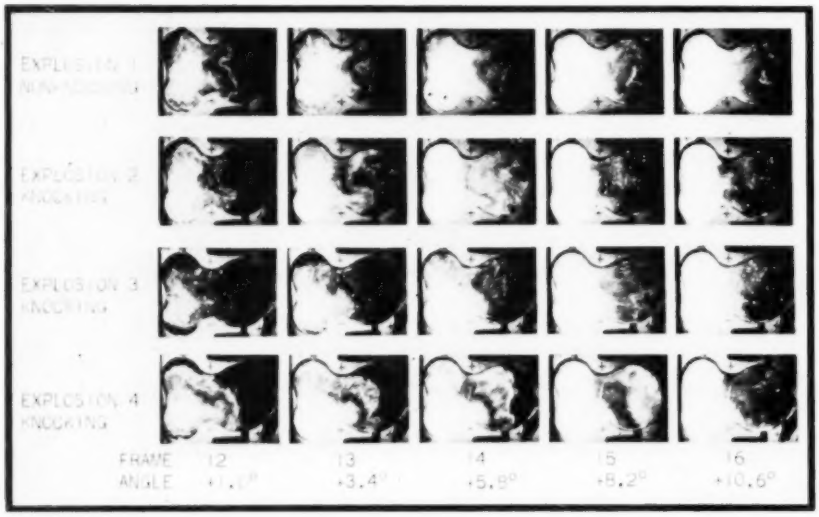

FIG. 8. Flame pictures comparing the inflammation of the last part of the charge in knocking and nonknocking explosions.

Comparison of the pictures in Fig. 8 shows that the knock differs from one explosion to another in the time and place at which the spontaneous inflammation appears as well as in the rate at which the last part of the charge is consumed by flame. Knocking explosions have been observed in which the time interval between the first indication of spontaneous inflammation and the completion of the burn was 2.4 crankshaft degrees or less; in other knocking explosions, time intervals of 7 or 8 crankshaft degrees have been observed.

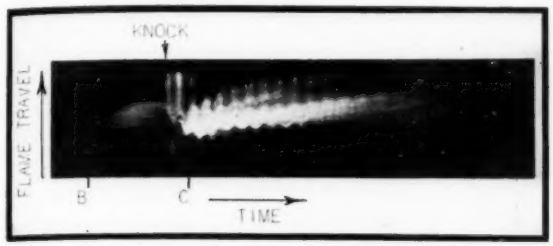

FIG. 9. Pressure waves detected in a knocking explosion by their effect on the luminosity of the burned gases.

As spontaneous inflammation sets in, the pressure development is accelerated by the increased rate of combustion and expansion of the part of the charge which burns at the time of knock. Evidence of the rapid expansion of this part of the charge at the time of knock is seen in Fig. 8 on the frames showing spontaneous ignition. The luminous streaks behind the flame fronts result from the movements of luminous spots toward the spark plug during the 2.2 crankshaft degree intervals in which each frame was exposed. The surge of gas induced by knock is frequently followed by violent vibrations of the gaseous charge. If knock is severe enough, these vibrations become visible under suitable means of observation, the most successful of which will now be described.

Time-Displacement Photographs Which Show Pressure Waves in the Inflamed Charge

Figure 9 is a time-displacement record of the flame motion in a single knocking explosion. In principle, this method of recording flame travel consists in permitting the flame to travel beneath a narrow window[15] which is imaged on a film moving at right angles to the direction of flame movement. The record so obtained shows the motion of the flame plotted against time. In Fig. 9, time is read from left to right and flame travel across the combustion chamber is read from bottom to top of the picture. The first part of the flame propagation is not clearly shown, but the motion of the flame just prior to knock is evident as well as the very rapid burning of the last part of the charge at the time of knock. Following knock a series of striae appear on the photograph. Careful examination of the photograph suggests that a pressure wave has been set up in the combustion chamber causing successive reilluminations of the charge.

That these luminous striae on the time-displacement photographs of knocking explosions are actually associated with pressure changes in the combustion space is shown by Fig. 10[16] where a suitable portion of a time-displacement photograph is compared with a pressure record of the same explosion. The time axes for the pressure record and the flame photograph are the same; thus the correspondence between the pressure variations in the former and the luminous striae in the latter is evident. This pressure record was obtained with a Dudell oscillograph which when undamped had a natural frequency of approximately 1500 cycles per second, and which was approximately 50 percent critically damped with oil; since the frequency of the

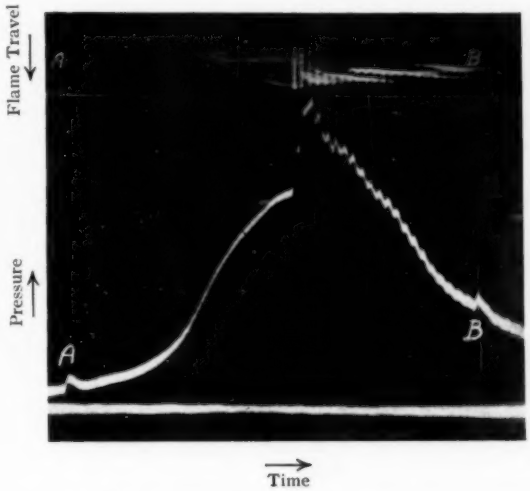

FIG. 10. The relationship between the frequencies of the pressure waves on a time-displacement record and the pressure variations shown on the pressure card of the same explosions.

pressure variations on the expansion side of the pressure card in Fig. 10 was approximately 3500 cycles per second, the magnitude of these variations cannot be determined directly from the pressure card. Frequency-response curves from this type of oscillograph element indicate that at 3500 cycles per second the deflections are only one-sixth to one-eighth of what would be expected with a high frequency oscillograph, thus it appears that the magnitudes of the pressure variations associated with the wave set up by the severe knock shown in Fig. 10 might amount to as much as 75 pounds per sq. in. (from condensation to rarefaction). This is the same order of magnitude as the values given by Boerlage and co-workers[17] who measured pressure variations of this type with a piezoelectric indicator and a cathode-ray oscillograph. Pressure variations of this magnitude are sufficient to produce forced vibrations in the engine parts and thus are probably responsible to a large degree for the sound of knock. In fact, experiments which lead to this conclusion have already been made independently by Wawrziniok[18] and by Draper.[19]

The pressure indicator used to obtain the record in Fig. 10 was located at the end of the combustion chamber opposite to the end in which knock occurred. This point is important for the following reason. The work of Draper[19] and of Boerlage and co-workers[17] has shown that under their experimental conditions the disturbance set up in the charge following knock is a standing wave and thus in some regions of the combustion chamber the pressure variations due to this wave will be much greater than in other regions. On the basis of the results of these other workers, it might be expected that in the engines used for obtaining the records in Figs. 9 and 10 the gas motion associated with the wave was a maximum near the center of the chamber. In Fig. 9 the apparent displacement of the gas from its equilibrium position due to the action of the wave near the center of the chamber soon after knock (just to the left of timing mark *c*) is approximately $\frac{1}{4}$ inch. The magnitude of this displacement is significant for two reasons: First, it permits the use of simple sound theory in estimating the pressure changes associated with the standing wave; and second, this disturbance provides a plausible explanation of the power loss associated with knock. Each of these points will now be considered.

Elting[20] gives the following relationship for determining from his time-displacement photographs of engine flames the magnitude of the pressure changes associated with the wave.

$$P - Po = \pi(\gamma/L)Pox,$$

where P is the maximum pressure in the condensation at the node,
P_o is the average pressure,
L is the length of the combustion chamber,
x is the maximum displacement of a particle at a loop from its equilibrium position,
γ is the ratio of the specific heats.

With the exception of γ and Po, all of the quantities in this relationship are known with a fair degree of accuracy for the record in Fig. 9. It is believed that Po was approximately 300 pounds per square inch shortly after knock and γ may be set equal to 1.25. L was 5 inches and x was 0.25 inch for the second transit of the wave in Fig. 9. Using these values it is found that the $P-Po$ was 59 lb. per sq. in. soon after knock or the pressure variation (condensation to rarefaction) was 108 lb. per square inch. This estimate agrees in order of magnitude with the estimate made above from the pressure card in Fig. 10.

In connection with the power loss associated with knock, it is well known that the rate of heat transfer from the combustion chamber to the jacket water is greatly increased by the occurrence of knock. Temperature measurements in the luminous gases during the expansion stroke under knocking and nonknocking conditions[14] are in agreement with this observation in that they show a greater rate of cooling of the

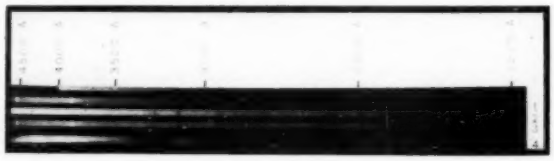

FIG. 11. Comparison of the absorption by charge in the knocking zone of an engine just prior to inflammation under knocking and nonknocking conditions. 1, Absorption by noninflamed charge—engine knocking; 2, absorption by noninflamed charge—engine not knocking; 3, source; 4, emission by inflamed charge.

charge under knocking conditions than under nonknocking conditions. These comparisons are made at comparable crank angles, and thus the increased rate of cooling cannot be accounted for by differences in the rate of expansion of the charge. Increased heat transfer from the gases to the walls might result from increased radiation or from increased convection and conduction. Experimental data are not yet complete enough to allow these losses to be evaluated quantitatively. However, an examination of the available information results in the attractive theory that the increased heat loss under knocking conditions results from a very simple physical phenomenon, namely, the stirring and scrubbing action of the violent gas movements induced by knock.

Absorption Spectra

Flame pictures of knocking and nonknocking explosions like those presented in Fig. 8 show that spontaneous inflammation is characteristic of the combustion process in the later phases of knocking explosions. Prior to the appearance of spontaneous inflammation, the flame pictures show no apparent differences between the combustion processes in knocking and in nonknocking explosions. But absorption spectra of the noninflamed portions of the charge have revealed distinct differences between knocking and nonknocking explosions even before the spontaneous inflammation sets in.[21–23] The equipment used for this study was the same as that shown in Fig. 6 except that an under-water spark between beryllium electrodes was sometimes substituted for the tungsten filament. Most of the absorption spectra were photographed at the end of the combustion chamber farthest from the point of ignition, that is, along the line of the optical system shown in Fig. 6.

Some typical absorption spectra are shown in Fig. 11. The upper two spectra were taken through the unburned portion of the charge just ahead of the flame fronts in the region where knock occurs when present. The third spectrum was taken with no absorbing material in the optical path. The spectra indicate that under nonknocking conditions no detectable amounts of reaction products having absorption bands

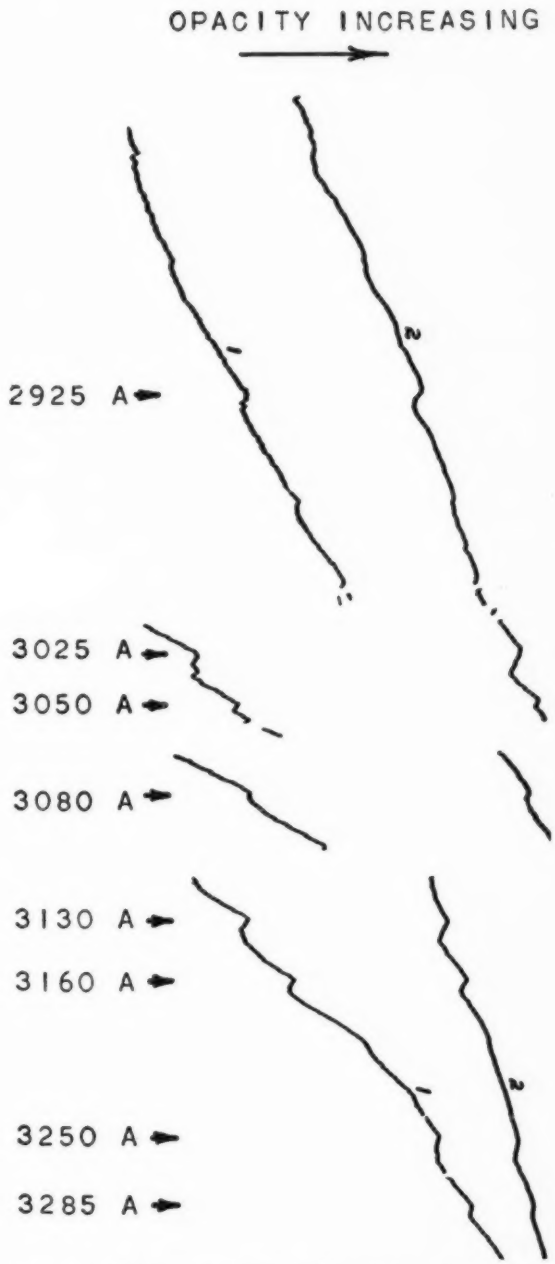

FIG. 12. Photometric records identifying formaldehyde in the noninflamed gases in the engine. Trace 1, noninflamed gases in engine just before knock; trace 2, formaldehyde outside the engine. Formaldehyde band heads are indicated by arrows.

in this spectral region were formed in the noninflamed charge. But spectrum 1, taken just prior to knock, shows definite absorption in the ultraviolet region from 3000A down to the lower limit of the spectra at approximately 2350A. Now the gasoline used for these experiments

was specially purified so that on entering the engine the fuel-air mixture was transparent in this spectral region. Thus, these spectra show definitely that under knocking conditions chemical reactions not observed under nonknocking conditions occur in the noninflamed charge ahead of the advancing flame. That formaldehyde is one of the products formed by these preflame reactions is shown by the appearance of characteristic formaldehyde bands in the absorption spectra. Microphotometer records identifying these bands are shown in Fig. 12.

It is of some interest to examine the possibility that some of the light emitted by the inflamed portions of the charge is absorbed by the noninflamed portion causing it to ignite in advance of the normal flame fronts or to knock. On this account an emission spectrum is reproduced together with the several absorption spectra in Fig. 11. This emission spectrum was exposed without using a stroboscopic shutter; consequently, it represents the combined emission from the flame fronts and from the burned gases behind the flame fronts in the engine. In order to register any faint bands that might be present, the spectrum was heavily exposed. The reproduction therefore shows very little structure, but the spectrum contains the CH, C_2 and CO_2 bands, shown in spectra 2 and 3 in Fig. 5, together with OH bands having heads at 2811A and 3064A. Now there are two important points to be noted in comparing the emission spectrum of the inflamed charge with the absorption spectra of the noninflamed charge. First, under nonknocking conditions, the gasoline-air mixtures used in these experiments were transparent throughout the entire spectral region where emission from the inflamed charge was observed. Second, absorption spectra of the noninflamed charge just prior to the beginning of knock show no strong absorption in the spectral region where light is emitted by the inflamed charge. On the basis of these observations, it would scarcely be expected that light from the flames in the spectral region shown in Fig. 11 would have a marked effect on the heating of the charge or on the acceleration of the dark reactions which lead to knock.

The deduction based on the comparison of emission and absorption spectra is supported by the following experimental observations. Light from a number of very intense sources, such as under-water sparks and carbon or mercury arcs, has been passed into the noninflamed charge when the engine was knocking and again when the engine was not knocking. The additional radiation produced no appreciable knock-inducing or knock-suppressing effects in any of these experiments. Direct experimental information of this sort has not yet been obtained in spectral regions outside the limits of transmission of fused quartz.

Bibliography

1. Rassweiler and Withrow, Ind. Eng. Chem. **28**, 672 (1936).
2. Withrow and Rassweiler, J. Soc. Aut. Eng. **39**, 297 (1936).
3. Rassweiler and Withrow, J. Soc. Aut. Eng. **42**, 185 (1938).
4. Withrow and Rassweiler, Ind. Eng. Chem. **23**, 769 (1931).
5. Rassweiler and Withrow, Ind. Eng. Chem. **24**, 528 (1932).
6. Weston, Proc. Roy. Soc. (London) **A109**, 176 (1925).
7. Kondratjew, Zeits. f. Physik **63**, 322 (1930).
8. Emeléus, J. Chem. Soc. **128**, 2948 (1926).
9. Vaidya, Proc. Roy. Soc. (London) **147**, 513 (1934).
10. Vaidya, "Memoirs," Ind. Inst. Science **2**, 352 (1935).
11. Kondratjew, Acta Physicochimica U.S.S.R. **4**, 556 (1936).
12. Emeléus, J. Chem. Soc. **131**, 1733 (1929).
13. Smithels and Ingle, Trans. Chem. Soc. **61**, 204 (1892).
14. Rassweiler and Withrow, J. Soc. Aut. Eng. **36**, 125 (1935).
15. Withrow and Boyd, Ind. Eng. Chem. **23**, 539 (1931).
16. Withrow and Rassweiler, The Automobile Engineer, **24**, 281 (1934).
17. Boerlage, Broeze, Van Driel and Peletier, Engineering, **143**, 254 (1937).
18. Wawrziniok, Automobiltechnische Zeits. **36**, 73 (1933); **36**, 136 (1933); N. A. C. A. Tech. Mem., No. 711 (1933).
19. Draper, N. A. C. A. Rep. No. 493 (1934) Inst. Aeronautical Sci. J., March (1938).
20. Elting, Appendix, N. A. C. A. Rep. No. 493 (1934).
21. Withrow and Rassweiler, Ind. Eng. Chem. **25**, 923 (1933)
22. Rassweiler and Withrow, Ind. Eng. Chem. **25**, 1359 (1933).
23. Withrow and Rassweiler, Ind. Eng. Chem. **27**, 872 (1935).

The Mobility Method of Computing the Vibration of Linear Mechanical and Acoustical Systems: Mechanical-Electrical Analogies*

BY F. A. FIRESTONE

Department of Physics, University of Michigan, Ann Arbor, Michigan

Introduction

THE well-established method for computing the vibrations produced in mechanical systems by impressed vibratory forces or by initial displacements or shocks, consists in writing down the differential equations applicable to the case, solving these equations, and determining the constants of integration by substituting the initial conditions. This procedure yields general equations for the motions of the different parts of the system and the slide rule can then be applied in computing the numerical values. While this method is applicable to a great variety of mechanical problems, differential equations is a fairly abstruse branch of mathematics, requiring continual practice for effective use, and the amount of time involved in solving moderately complicated problems is often prohibitive.

An alternative method of computing vibrations, which has been tried by some, is the method of electrical analogy, wherein one draws the electrical circuit which is analogous to the mechanical problem to be solved, then solves the analogous electrical problem, and finally converts the electrical answer back into mechanical terms. While there are a few meticulous souls who can arrive at correct answers by this method, most of those who have attempted it have become confused and have arrived at preposterous answers. I will show below that this blundering has not necessarily been due to lack of ability on the part of the computers, but is rather the result of imperfections in the mechanical-electrical analogy itself as taught in all the books dealing with this subject.

Furthermore, it can be shown that there is another analogy which is free of the imperfections of the old analogy, in fact, the new analogy is so close that it is no longer necessary to transfer the mechanical problem into electrical terms in order to arrive at the desired answer; the *methods* which the electrical engineer has developed for solving electrical circuit problems are taken over into mechanics and applied to the mechanical problem in purely mechanical terms. It is not necessary to make any reference to electricity.

The mobility method of computing vibration is the result of applying the electrical engineers' methods of computation to mechanical problems. The electrical engineer has developed the following distinctive tools:

1. A set of conventionalized symbols with which the essential characteristics of a circuit can be set forth in the form of a circuit diagram.

2. The concept of the potential difference *across* elements in the circuit as contrasted with the potential *of* points in the circuit relative to ground; the advantage here is that the relationship between the potential difference across an element and the current through it, depends only on the characteristics of the element itself and not on the characteristics of the rest of the system.

3. The use of complex numbers to represent simple harmonic voltages and currents, both the

* Paper presented at the Symposium on Physics in the Automotive Industry at Ann Arbor, Michigan, March 14 and 15, 1938.

magnitude and phase of these quantities being represented by the absolute value and angle of the complex numbers.

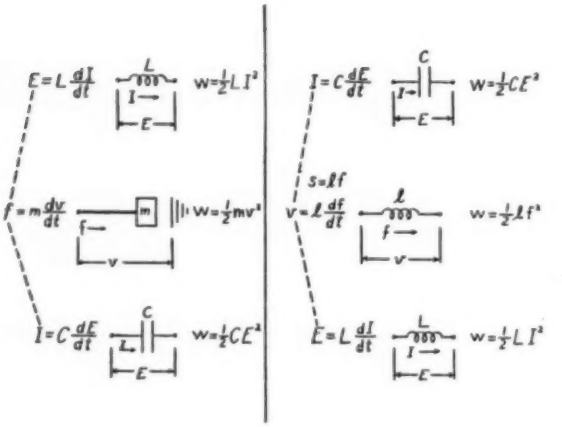

FIG. 1. The old and the new analogs of the mass and the spring.

4. The concept of the "impedance" of an element, which is defined as the complex ratio of the voltage across the element to the current through the element; rules are developed for computing the impedance of series or parallel combinations of elements and the current can then be found simply as the voltage divided by the impedance.

The mobility method provides a similar set of distinctive tools, of form suitable for application to mechanical vibration problems, as follows:

1. A set of conventionalized symbols with which the essential characteristics of a mechanical system can be set forth in the form of a schematic diagram.

2. The concept of the velocity *across* mechanical elements (velocity of one end of the element relative to the other end) as contrasted with the velocity *of* points in the system relative to ground; the advantage here is that the relationship between the velocity across an element and the force through it, depends only on the characteristics of the element itself and not on the characteristics of the rest of the system.

3. The use of complex numbers to represent simple harmonic velocities and forces, both the magnitude and phase of these quantities being represented by the absolute value and angle of the complex numbers.

4. The concept of the "mobility" of an element (ease of motion), which is defined as the complex ratio of the velocity across an element to the force through the element; simple rules are developed for computing the mobility of series or parallel combinations of elements and the force can then be found simply as the velocity divided by the mobility, or the velocity can be found as the force multiplied by the mobility.

Thus by the mobility method we can compute the velocity across each element in the system and the velocity of each point in the system, due to the action of an impressed vibratory force or velocity. Not only can the forced vibration be computed, but the natural frequencies of the free vibration of systems having but small damping, can be found. While the method is most easily applied to those systems in which the vibrations of all parts are parallel to a single line, it can be easily extended to cover many more complicated cases. Torsional vibrations may be computed as easily as linear vibrations. The presence of friction or damping adds no appreciable complication as long as it is of the type in which the force is proportional to the velocity.

Imperfections of the Old Mechanical-Electrical Analogy

Before explaining the mobility method of vibration computation, let us point out the imperfections of the old mechanical-electrical analogy, and outline the new analogy, since it is from this new analogy that the mobility method has sprung.

The left central part of Fig. 1 shows a mass whose velocity v is measured relative to the fixed point designated at the right; this may be considered either as the velocity *of* the mass or the velocity *across* the mass. If a force f of compression or tension is applied through the rod at the left of the mass, there will be a change in the velocity across the mass which can be computed from $f=mdv/dt$. The old analogy says that the inductance shown above the mass plays the same role in the electrical circuit as the mass does in the mechanical system, because an equation of similar form holds for the inductance namely, $E=LdI/dt$. Furthermore the

energy stored in the mass is $\frac{1}{2}mv^2$ and the energy stored in the inductance is $\frac{1}{2}LI^2$. Likewise at the right center of Fig. 1 is shown a spring of compliance l (compliance, stretching produced by unit force, reciprocal of the stiffness) across which there is a velocity v and through which there is a force f of compression or tension. The old analogy says that the condenser shown above the spring is analogous to the spring because the velocity across the spring is $v=ldf/dt$ while an equation of similar form holds for the condenser namely, $I=CdE/dt$. Furthermore, the energy stored in the spring is $\frac{1}{2}lf^2$ while the energy stored in the condenser is $\frac{1}{2}CE^2$. A similar analogy holds between mechanical resistors and electrical resistors.

In explaining this old analogy, the books do not usually go into as much detail as we did in the above paragraph in showing figures which outline in detail the nature of the quantities which are analogous. The analogy looks very pretty as long as one merely points out that the mechanical quantities are related by equations of the same form as the equations which relate the electrical quantities. However, when one notes that velocity *across* mechanical elements is in these equations analogous to current *through* the electrical elements, while force *through* is analogous to voltage *across*, the fundamental imperfection of this analogy is obvious. This results further in mechanical elements in series being represented in the analogous circuit by electrical elements in parallel, and *vice versa*. As an example of this left-handed relationship, see the mechanical system of the central part of Fig. 2 and its old analogous electrical circuit at the top of that figure. Most of the blunders which have been made by those who tried to use the old analogy in computing vibrations, can be ascribed to this inverse relationship of series and parallel, and of through and across.

Fortunately, there is another analogy, detailed in the lower part of Fig. 1, which is free from these imperfections. Here the condenser is put analogous to the mass, and the inductance analogous to the spring. Not only is the formal similarity of the equations complete as before, but velocity *across* is analogous to voltage *across*, and force *through* is analogous to current *through*. This results in mechanical elements in series being represented by electrical elements in series; similarly for elements in parallel. The analogous electrical circuit is therefore of a form very similar to the mechanical system itself, as illustrated by the new analogous electrical circuit at the bottom of Fig. 2 which represents the mechanical system in the center of the figure. We could now work out the analogous electrical problem and transfer our answer into mechanical terms, but with the analogy as close as is shown, we ask ourselves what advantage is to be gained

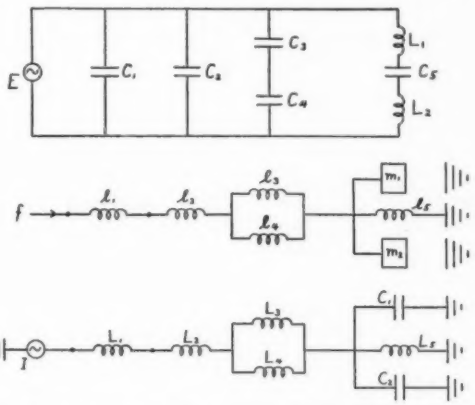

FIG. 2. A mechanical system (center) with its old analogous electrical circuit above and its new analogous electrical circuit below.

through working with the capital letters in the electrical circuit when we could as well work with the small letters in the mechanical system itself, while carrying out the computation in the same manner. The mobility method of computation is the final result of this investigation and consists in applying the new analogy merely in the development of the method of computation; in making computations by the mobility method, no reference is made to the analogy or to electrical systems.

In order that the equations may have an instructive and familiar appearance to those who know their electrical circuit theory we will change the letter symbols for force, velocity, and mass, from the usual f, v, and m to i, e, and c as shown below.

	USUAL SYMBOL	SYMBOL USED HERE
force	f	i
velocity	v	e
mass	m	c

Obviously the meaning of equations is not changed by a change in the letters which repre-

sent the quantities appearing in the equations, so anyone may feel free to use the usual letter symbols if the equations appeal to him more in

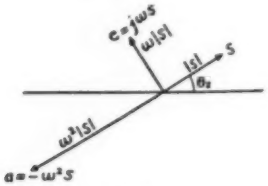

FIG. 2a. The relationship between the vectors representing displacement, velocity, and acceleration, in simple harmonic motion.

that form. (i and e above do not represent current and voltage; they represent force and velocity.)*

The Mobility Method of Vibration Computation **

For our purposes we may consider mechanical systems as being constructed of only three kinds of elements: springs, mechanical resistors, and masses. These correspond to the three fundamental mechanical properties of matter in bulk: elasticity, viscosity, and mass. A spring has a *displacement* across it proportional to the force through it (Hooke's law); a mechanical resistor has a *velocity* across it proportional to the force through it; and a mass has an *acceleration* across it proportional to the force through it (definition of force). The displacement produced across a spring by unit force through it is a constant of its structure called the *compliance l* of the spring and is measured in cm/dyne or inches/pound; the velocity produced across a mechanical resistor by unit force through it is called the *responsiveness r* of the resistor and is measured in kines/dyne (1 kine equals 1 cm/sec.) or inches/sec./pound; the acceleration produced across a mass by unit force acting on it is called the *mass* of the mass and is measured in grams or pounds/g ($g = 386$ inches/sec.^{2}). The mechanical resistor may be visualized as a pair of massless concentric tubes having a viscous oil in the space between the tubes so that the velocity across the combination (velocity of one tube relative to the other) is proportional to the force through the combination; substances like oil, rubber, felt, and deadening materials generally, have to a considerable extent the properties of a mechanical resistance, in addition to their elastic or mass properties. While any actual spring has some mass, and every mass has some elasticity, and every actual mechanical resistor has some mass, for purposes of analysis of mechanical systems we consider our mechanical elements as being "pure" and we take into account any important additional properties of any structure by adding elements to the schematic diagram. Regardless of the actual structure of our elements, we will represent them in our schematic diagrams by the symbols shown in the figures which follow; these same symbols will be used whether the vibration is linear or torsional.

If a simple harmonic force is sent through our mechanical elements, it will produce a simple harmonic displacement across the spring, a simple harmonic velocity across the resistor, and a simple harmonic acceleration across the the mass, in fact, if we confine our attention to the oscillating components of the motion we may say that each of these elements will have a simple harmonic displacement, velocity, and acceleration across it. Representing the vibratory motion as the real part of a vector rotating in the complex plane (as is common in electrical circuit theory)† we have the following relationships between the displacement, velocity, and acceleration, across any element:

	Instantaneous Value	Amplitude	Units c.g.s.	Units English
Displacement	$s_i = se^{j\omega t}$	s	cm	inches
Velocity	$e_i = ds_i/dt = ee^{j\omega t}$	$e = j\omega s$	kines	inches/sec.
Acceleration	$a_i = d^2s_i/dt^2 = ae^{j\omega t}$	$a = j\omega e = -\omega^2 s$	kines/sec.	inches/sec.^{2}
Force	$i_i = ie^{j\omega t}$	i	dynes	pounds

* For a further discussion of the relative advantages of the old and new analogies, see F. A. Firestone, "A New Analogy Between Mechanical and Electrical Systems," J. Acous. Soc. Am. **4**, 249–267 (1933). This paper was anticipated by a paper appearing in Germany in 1932 pointing out the new analogy, and which was called to my attention by its author in 1933; Walter Hahnle, "Die Darstellung Elektromechanischer Gebilde durch rein elektrische Schaltbilder," Wiss. Veröff. a. d. Siemens-Konzern, Vol. XI, No. 1 (Julius Springer, Berlin, 1932). A recent paper dealing exclusively with the old analogy is Myron Pawley, "The Design of a Mechanical Analogy for the General Linear Electrical Network with Lumped Parameters," J. Frank. Inst., **223**, 179–198 (1937).

** Anyone particularly interested in this subject will find a more detailed discussion in a mimeographed booklet of about 150 pages which the author has prepared for his students. This can be obtained from the author after July 1938 at a cost not to exceed $1.00.

† If the reader is not familiar with the use of complex numbers in representing vibrations, he can easily pick up the necessary knowledge by reading the first four pages of Appendix B of K. S. Johnson's book, *Transmission Circuits*

Here the angular frequency $\omega=2\pi f$ where f is the frequency of the vibration in cycles per second. $j=(-1)^{\frac{1}{2}}$. The displacement amplitude s is a complex constant whose norm or absolute value $|s|$ represents the actual displacement amplitude across the element (maximum displacement in the vibration) and whose angle θ_s represents the epoch angle of the displacement (portion of the cycle of motion in which the displacement started when $t=0$). The velocity amplitude e and the acceleration amplitude a are complex constants whose absolute values and angles are the actual amplitudes and epoch angles of these quantities. The relationships expressed in the above amplitude equations are set forth in Fig. 2a. The acceleration leads the velocity by 90° and the velocity leads the displacement by 90°. The multiplication of each of these vectors by $\epsilon^{j\omega t}$ causes the set of vectors to rotate with angular speed ω radians/sec. and the real part of each vector, or its projection on the horizontal real axis, is the instantaneous acceleration, velocity, and displacement, respectively. If any one of the three quantities s, e, or a is known, the other two can be found immediately from the equations at the right above. We will find it most convenient to compute e first, even though we may be primarily interested in finding s or a.

The mobility z of an element (or group of elements) is by definition the ratio of the velocity amplitude across the element to the force amplitude through the element;

$$z\equiv e/i \text{ kines/dyne or inches/sec./pound.}$$

The mobility is a complex number, its absolute value $|z|$ being the ease of motion, the amount of velocity produced by unit force, and its angle θ_z being the angle by which the velocity leads

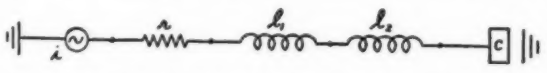

FIG. 3. A series mechanical system. The mobility across a number of elements in series is the sum of their separate mobilities; $z=z_1+z_2+z_3+$.

the force. The mobility depends only on the structure of the element and on the frequency of the impressed force or velocity, and is independent of the amount of force or velocity which is impressed since these are proportional to each other. For convenience, we may give names to the real and imaginary parts of the mobility, calling them the *responsiveness* r and *excitability* x, respectively. Thus

$$\text{mobility}=\text{responsiveness}+j\ \text{excitability};$$
$$z=r+jx.$$

If a system has some responsiveness in its mobility it absorbs mechanical energy and turns it into heat or waves or some other form of

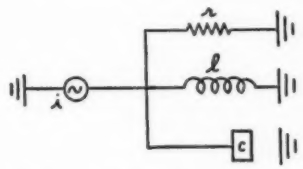

FIG. 4. A parallel mechanical system; $z=1/(1/z_1+1/z_2+1/z_3+)$.

energy, that is, it really *responds* to the vibration; while if the mobility of a system is a pure excitability, energy oscillates in and out of the system but no energy is permanently extracted from the source, that is, the system merely gets *excited*.

The mobility of each kind of element can be easily computed from a knowledge of the fundamental constant of the element and the frequency of the impressed vibration. If an oscillating force of amplitude i is sent through a spring of compliance l, the displacement amplitude across the spring will be $s=li$ (from the definition of compliance). The velocity amplitude across the spring will therefore be $e=j\omega s=j\omega li$. The mobility of a spring is therefore

$$z=e/i=j\omega li/i=j\omega l$$

and is a pure excitability proportional to the frequency ω. On the other hand, if an oscillating force of amplitude i is sent through a mechanical resistor of responsiveness r, it will produce a velocity across the resistor $e=ri$ (from the definition of the responsiveness of a resistor). The mobility of a resistor is therefore.

$$z=e/i=ri/i=r$$

and is a pure responsiveness independent of the frequency. If an oscillating force of amplitude i is impressed on a mass c, it will produce an

for Telephonic Communication (Van Nostrand); or consulting the instruction book accompanying the Keuffel and Esser log log vector slide rule.

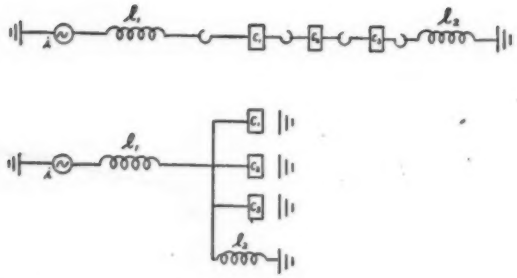

FIG. 5. How to make a blunder in analyzing a mechanical system: the three masses shown in the upper diagram are in parallel since one terminal of each is the ground and their movable terminals are connected together; the two hooks on opposite sides of each mass are not two terminals, they are the same terminal. The schematic diagram of the structure at the top is shown in the lower part of the figure.

acceleration across the mass of amplitude $a=i/c$ (from the definition of force, otherwise known as Newton's laws of motion). The velocity amplitude across the mass will therefore be $e=a/j\omega=i/j\omega c$ and the mobility will be

$$z=e/i=1/j\omega c=-j/\omega c,$$

a pure negative excitability inversely proportional to the frequency. Summarizing, the mobility of each of our three mechanical elements is simply:

ELEMENT	MOBILITY	C.G.S.	ENGLISH
Spring	$z=j\omega l$	kines/dyne	inches/sec./pound
Resistor	$z=r$	"	"
Mass	$z=-j/\omega c$	"	"

In the above equations the units are as follows:

		C.G.S.	ENGLISH
Spring	has compliance	of l cm/dyne	or inches/pound
Resistor	has responsiveness	of r kines/dyne	or inches/sec./pound
Mass	has mass	of c grams	or pound sec.^{2}/inch (or w/g)

Elements are said to be connected in series when their terminals are connected end to end (with not more than two terminals to any junction point) as shown in Fig. 3. Elements are connected in parallel when their terminals are connected to two common junction points as shown in Fig. 4. If there is any question as to whether in any specific example the elements are connected in series or in parallel, one should note that functionally a series connection results in the same force acting through all the elements, while the velocity across the combination is the sum of the velocities across the individual elements; a parallel connection results in the same velocity across all the elements while the force through the combination is the sum of the forces through the individual elements. The mobility of a series combination of elements is therefore

$$z=e/i=(e_1+e_2+e_3+)/i=z_1+z_2+z_3+,$$

and is simply the sum of the mobilities of the individual elements. The mobility of a parallel combination of elements is

$$z=\frac{e}{i}=\frac{e}{i_1+i_2+i_3+}=\frac{1}{1/z_1+1/z_2+1/z_3+}$$

and is the reciprocal of the sum of the reciprocals of the mobilities of the individual elements. It should be remembered that one terminal of every mass is the fixed point relative to which the velocity of the mass is measured, otherwise one may look at Fig. 5 and conclude erroneously that the masses shown there are in series because they are hooked end to end; however, the two hooks on each mass are not the two terminals of the mass, they are the same terminal, there is no relative velocity between them, they move together, and the other terminal of each mass is the floor of the laboratory. The schematic diagram of these masses is shown in the lower part of Fig. 5, indicating that the masses are in parallel and that the force on the parallel combination of elements is the sum of the forces required by the individual elements. Since all masses have one terminal in common (the frame of reference), it is not possible to connect a number of them in series in any simple manner.

The mobility method of vibration computation consists in drawing the schematic diagram of the mechanical system and applying the simple formulas of the last two paragraphs. The system will usually be merely a series-parallel arrangement of elements, and with the aid of the above formulas we can easily compute the mobility of the combination through which the given oscillating force is applied. The velocity amplitude across this combination can then be found merely as $e=iz$. The details of such computations will be most quickly grasped by reference to the fairly complicated example shown in Fig. 6. Here a one-pound mass is supported by a vertical leaf spring of compliance 0.054 inches/pound. A 2-pound mass sits upon the 1-pound mass and is separated from it by a film of very viscous oil of responsiveness 0.1 inches/sec./pound so that the motion of the lower mass

transmits a force to the upper mass due to the viscosity. The 2-pound mass is connected to the frame of the machine through a spring of compliance 0.012 inches/pound and to a 3-pound mass through a spring of compliance 0.005 inches/pound. The 3-pound mass is supported by the frame of the machine through a film of very viscous oil of responsiveness 0.4 inches/sec./pound. A sinusoidal force of amplitude 10 pounds and frequency 15.91 cycles per second acts upon the 1 pound mass and reacts against the frame of the machine. We wish to find the velocity amplitude and displacement amplitude of each mass.

In drawing the schematic diagram of the system we identify the two terminals of each element of the system and connect together in the diagram those terminals which move together in the system. Those terminals which are stationary are connected to the ground symbol —||. Thus the force $i=10$ is shown at the left, acting between the ground and the movable terminal of the mass 1; the leaf spring is connected from this terminal to ground. The resistor representing the oil film is connected between the movable terminals of masses 1 and 2. We proceed similarly throughout the remainder of the system, remembering that one terminal of every mass is the ground, relative to which we measure the velocity of the mass. It is to be understood that regardless of the directions in which the vibrations might take place in any actual system, the vibrations in the schematic diagram are along a horizontal line, and the vertical lines in the diagram remain vertical throughout the vibration cycle. When the schematic diagram has been drawn the problem is already analyzed and we are as far along as we would have been if we had written down the differential equations of the system and had found their solutions, for we are now ready to start numerical computation.

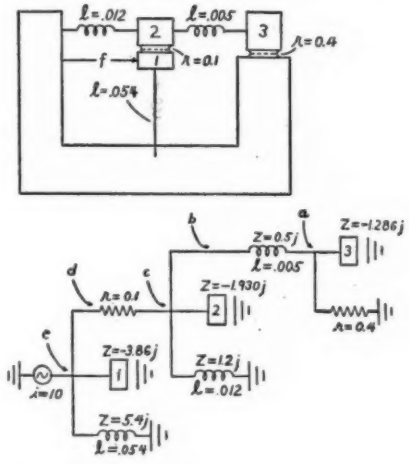

FIG. 6. A mechanical structure and its schematic diagram, a numerical problem solved by the mobility method in the text.

Using the formulas given above we first compute the mobility of each element at the impressed angular frequency $\omega=2\pi 15.91=100$ radians/sec. This has been done and the results are tabulated above the elements in the figure (remember that $c=w/g$), except for the resistors, whose mobilities equal their responsivenesses. The mobility of the point a looking toward the right, is the mobility of the parallel combination of mass 3 and the resistor;

$$z_a=\frac{1}{1/0.4+1/-1.286j}=\frac{1}{2.5+0.778j}$$

$$=\frac{2.5-0.778j}{2.5^2+0.778^2}=0.3640-0.1133j.$$

The mobility of the point b looking toward the right, is the mobility of the spring, in series with the mobility z_a;

$$z_b=0.5j+(0.3640-0.1133j)=0.3640+0.3867j.$$

The mobility of the point c looking toward the right, is the mobility of the parallel combination of z_b, the mass 2, and the spring;

$$z_c=\frac{1}{1/1.2j+1/-1.930j+1/(0.3640+0.3867j)}$$

$$=0.2864+0.3743j.$$

Similarly

$$z_d=0.1+(0.2864+0.3743j)=0.3864+0.3743j$$

and $$z_e=1\Big/\left(\frac{1}{5.4j}+\frac{1}{-3.86j}+\frac{1}{0.3864+0.3743j}\right)$$

$$=0.409+0.3737j.$$

Since the mobility of point e is by definition the velocity which unit force would produce at the point e, we can immediately find the velocity of

the point e due to the impressed force $i=10$ simply as

$$e_e=iz_e=10(0.409+0.3737j)=4.09+3.737j$$
$$=5.54\angle 42°.4 \text{ inches/sec.}$$

This means that the maximum velocity of mass 1 is 5.54 inches/sec. while its motion leads the impressed force by a phase angle of 42°.4. $(5.54=(4.09^2+3.737^2)^{\frac{1}{2}}.)$ The velocity of the point d is the same as the velocity of e, $e_d=e_e$, so the force through the point d is*

$$i_d=\frac{e_d}{z_d}=\frac{5.54\angle 42°.40}{0.3864+0.3743j}=\frac{5.54\angle 42.40}{0.538\angle 44.08}$$
$$=10.28\angle -1°.68 \text{ pounds.}$$

One should not be disturbed to find that the force through d is greater than the impressed force of 10 pounds, since it is the *vector* sum of the forces through the spring, the mass, and d, which equals the impressed force. The force through the point c equals the force through the point d, $i_c=i_d$, so the velocity of c

$$e_c=i_cz_c=10.28\angle -1.68(0.28648+0.3743j)$$
$$=4.845\angle 51.00 \text{ inches/sec.}$$

Thus the velocity amplitude of the mass 2 is 4.845 inches/sec. and leads the impressed force $i=10$ by 51°. Similarly, since $e_b=e_c$

$$i_b=\frac{e_b}{z_b}=\frac{4.845\angle 51.00}{0.3640+0.3867j}=9.10\angle 4°.23 \text{ pounds,}$$

and since $i_a=i_b$

$$e_a=i_az_a=9.1\angle 04.23(0.3640-0.1133j)$$
$$=3.465\angle -13.08 \text{ inches/sec.}$$

Thus the velocity amplitude of mass 3 is 3.465 inches/sec. and lags the impressed force $i=10$ by 13°.08. The displacement amplitudes of the masses can be found by dividing their velocity amplitudes by $100j$ since $s=e/j\omega$. We summarize our answers as follows:

Velocity Amplitudes	Displacement Amplitudes
$e_1=e_e=5.54\ \angle\ 42.40$ inches/sec.	$s_1=0.0554\ \angle -47.60$ inches
$e_2=e_c=4.845\ \angle\ 51.00$ inches/sec.	$s_2=0.04845\ \angle -39.00$ inches
$e_3=e_a=3.465\ \angle -13.08$ inches/sec.	$s_3=0.03465\ \angle -103.08$ inches.

If the frequency of the impressed force were to be changed, the mobilities of the individual elements would be changed and the computation would have to be repeated from the first, in order to find the new velocities and displacements of the masses.

Reviewing the method applied above, the mobility at the driving point has been computed by the application of the series and parallel formulas, and the velocity of the driving point is found from $e=iz$. The force applied to the next junction point is found from $i=e/z$, and the velocity of that point from $e=iz$. By continuing this process, all force and velocity amplitudes can be found in any system which consists of a series-parallel connection of elements.

It can be shown quite simply that the average power dissipated in a mobility $z=|z|\angle\theta_z=r+jx$ when a simple harmonic force i is sent through it or a simple harmonic velocity e is impressed across it, can be computed from any of the following expressions:

$$p_{Av}=\frac{|e||i|}{2}\cos\theta_z=\frac{|e|^2}{2|z|}\cos\theta_z=\frac{|e|^2}{2r}\cos^2\theta_z,$$
$$p_{Av}=\frac{|i|^2}{2}r=\bar{i}^2r \text{ ergs/sec. or inch pounds/sec.}$$

The factor of 2 in the denominator of these equations becomes unity if we use the effective value of e and i, namely $\bar{e}$ and $\bar{\imath}$, which for simple harmonic motion are equal to $\bar{e}=0.707|e|$ and $\bar{\imath}=0.707|i|$. In the above example, the average power delivered by the force $i=10$ to the point e on which it acts, is

$$p_{Av}=\frac{|i|^2}{2}r_e=\frac{10^2}{2}0.409=20.45 \text{ inch pounds/sec.}$$

The average power dissipated by the resistor under mass 3 is

$$p_{Av}=\frac{|e_a|^2}{2r}=\frac{3.465^2}{2\times 0.4}=15.00 \text{ inch pounds/sec.}$$

The remainder of the power supplied by the source, namely 5.45 inch pounds/sec., must be dissipated by the other resistor since the springs and masses do not dissipate power; this value checks approximately with that which we obtain by direct computation;

$$\frac{|i|^2}{2}r=\frac{10.28^2}{2}0.1=5.28 \text{ inch pounds/sec.}$$

* In carrying out computations of this sort in which the complex numbers are changed from rectangular form to polar form, or *vice versa*, the log log vector slide rule is very convenient as it permits this operation to be performed with a single setting of the rule.

This is one method of checking the accuracy of the entire calculation.

Force and Velocity Laws

Some mechanical systems do not consist simply of a series-parallel arrangement of elements, for instance, if we add to the system discussed above, a spring connecting mass 1 directly to mass 3, the schematic diagram will look as shown in Fig. 7 and the mobility at the driving point cannot be computed merely from the series and parallel formulas. In order to find the forces and velocities in such a system we must use two general rules which we may call the

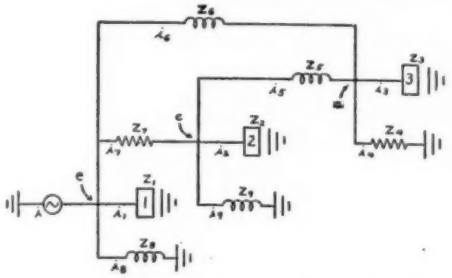

FIG. 7. A modification of the mechanical system shown in Fig. 6, which requires the application of the force and velocity laws for its solution.

force and velocity laws (Kirchhoff's laws in electricity):

Force law. The sum of all the forces acting on any junction point is zero.

Velocity law. The sum of all the velocities across the structures included in any closed mechanical circuit is zero.

Since the junction point to which a number of terminals of elements may be connected is considered as being massless, no force is required to move it, so the vector sum of all the force amplitudes acting on the junction must be zero. Forces through elements lying on the left of the junction may be taken with the signs given, and those on the right with their signs changed. (The force through an element is considered positive when it is a compressional force.) Since in going around a closed mechanical circuit we return to the starting point, or go from a grounded point to another grounded point, the sum of all the velocity differences across the structures included in the circuit must be zero. When writing down such a velocity equation, we progress around the circuit in a clockwise direction and write the velocity across each element passed through in the positive direction (to the right) with the sign given, and write each passed through in the negative direction, with its sign changed. (Velocity across an element is considered positive when the element is growing shorter; displacement is positive when the element is shorter than its normal length.) In applying the force and velocity laws we designate each of the unknown forces through series of elements by a letter, and then write down the equations indicated by the laws. This will yield a sufficient number of equations for determining the unknown forces. When the forces are known, velocities can be found at once from $e=iz$.

As an example, let us write down the force and velocity equations for the system of Fig. 7. At the junctions a, c, and e, respectively, we find the following complex equations:

$$\begin{aligned} i_5+i_6-i_3-i_4&=0,\\ i_7-i_5-i_2-i_9&=0,\\ i\ -i_6-i_7-i_1-i_8&=0. \end{aligned}$$

We now write down velocity laws around various closed circuits as follows:

$$\begin{aligned} i_3z_3-i_4z_4&=0,\\ i_2z_2-i_9z_9&=0,\\ i_1z_1-i_8z_8&=0,\\ i_6z_6-i_5z_5-i_7z_7&=0,\\ -i_1z_1+i_7z_7+i_2z_2&=0,\\ -i_2z_2+i_5z_5+i_3z_3&=0. \end{aligned}$$

Since at any frequency the z's in the above equations are known from the constants of the elements, we have 9 simultaneous equations which can be solved (perhaps by determinants) for the 9 unknown forces, or as many of them as we wish to know. The velocity of mass 1 is then $e_1=i_1z_1$; similarly for the other masses.

While this method will work for any system whose schematic diagram can be drawn, the series-parallel method is simpler when it is applicable.

Other General Laws

There are a number of other dynamical laws which are well known in electrical circuit theory but which can be advantageously applied to the mechanical systems as represented in our schematic diagrams. These laws will merely be stated here in mechanical terms without proof.

Thevenin's theorem. While we often think of a force vibrator as being capable of impressing a certain constant amplitude of oscillating force regardless of the mobility of the mechanical system on which it acts, there is a limit to the velocity with which any practical force producing device can move its terminals even when it is not connected to anything, so it cannot send as much force through a system of high mobility as through one of low mobility. Likewise, a practical velocity producing vibrator is limited as regards the force amplitude which it can send through systems of even very low mobility, so it cannot produce as much velocity across a system of low mobility as across one of high mobility. The *internal mobility* of a vibrator is defined as the velocity amplitude which it can produce between its own terminals when not connected to anything, divided by the force amplitude which it can produce through an immovable object;

$$z_s = \frac{e \text{ free}}{i \text{ blocked}}.$$

The velocity form of Thevenin's theorem states that any vibrator is equivalent to an ideal velocity vibrator of velocity amplitude equal to *e free*, in series with its internal mobility z_s, and the force sent through any system of mobility z to which this vibrator might be connected is (see Fig. 8)

$$i = \frac{e \text{ free}}{z_s + z}.$$

The velocity produced across the system can be found as $e = iz$. The force form of Thevenin's theorem states that any vibrator is equivalent to an ideal force vibrator of force amplitude

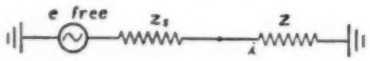

FIG. 8. According to the velocity form of Thevenin's theorem, any complicated vibrator is equivalent to an ideal velocity vibrator of velocity amplitude equal to e free, in series with the internal mobility of the vibrator $z_s = e$ free/i blocked. The force i sent through a load of mobility z connected to the actual vibrator is $i = e$ free/$(z_s + z)$.

equal to *i blocked*, in parallel with its internal mobility z_s, and the velocity produced across any system of mobility z to which this vibrator might be connected is (see Fig. 9)

$$e = \frac{i \text{ blocked}}{1/z_s + 1/z}.$$

Even a complicated portion of a system may be considered as the vibrator and its internal mobility determined by observing or computing its *e* free and *i* blocked; the effect of this portion of the system on the balance of the system can be computed from either of the formulas given above. Such a procedure would be advantageous when one wished to compute the vibration which a given portion of the system would produce in a number of different driven systems; the entire system would not have to be recomputed for each trial, only the changed driven systems.

The reciprocity theorem. If a force of high internal mobility is connected between terminals AB of a mechanical system and produces a certain velocity between terminals CD, it will produce that same velocity, both in magnitude and phase, between terminals AB if connected between terminals CD. Or, if a velocity of low internal mobility is impressed in series with an arm X in a mechanical system and produces a certain force through an arm Y, it will produce that same force through X if connected in series with Y. These are the two forms of the reciprocity theorem and permit one to immediately compute the vibration which will be transmitted in one direction through a mechanical system

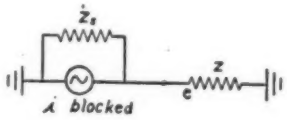

FIG. 9. According to the force form of Thevenin's theorem, any complicated vibrator is equivalent to an ideal force vibrator of force amplitude equal to i blocked, in parallel with the internal mobility z_s. The velocity e across a load of mobility z connected to the actual vibrator is $e = i$ blocked/$(1/z_s + 1/z)$.

by a given force or velocity when he knows how much is transmitted in the other direction. This theorem is true for vibrations of any wave form, and for both the transients and the forced vibration.

The principle of superposition. If a number of vibratory forces and/or velocities act simultaneously in various parts of a mechanical system, the instantaneous forces and velocities produced in the different parts of the system are simply the sum of the instantaneous forces and velocities which the separate vibrators would

produce when acting alone. If the frequencies of all the vibrators are the same, the resultant force or velocity amplitude at any point is simply the vector sum of the force and velocity amplitudes produced by the vibrators when acting alone. In computing the vibration produced by one of the vibrators acting alone, the internal mobilities of the other vibrators must remain connected in the system even though these vibrators are not introducing any energy into the system.

Compensation theorem. If a system is modified by making a change Δz in the mobility of one of its branches, the force increment thereby pro-

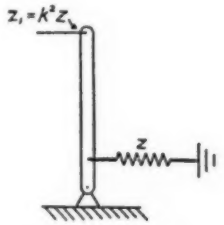

FIG. 10. A lever of ratio k, changes the mobility by a factor k^2.

duced through any arm in the system is equal to the force that would be produced through that arm by a compensating velocity acting in series with the *modified* branch, whose value is $-i\Delta z$, where i is the original force through the modified branch.

Mobility matching with levers or gears. If we have given a vibrator of internal mobility $z_s = r_s + jx_s$, we can extract maximum power from this vibrator by connecting it to a load whose mobility is the conjugate complex of z_s, namely to $z = r_s - jx_s$. If the angle of the mobility of the load is fixed while only the absolute value of the mobility of the load is subject to choice, maximum power will be delivered by the vibrator to the load when the absolute value of the load mobility equals the absolute value of the internal mobility of the vibrator; when $|z| = |z_s|$. As shown in Fig. 10 a massless lever whose arms have lengths of ratio k : 1, increases the velocity by a factor k and decreases the force by a factor k, so the mobility looking toward the lever is k^2 times the mobility of the load to which the lever is connected; $z_1 = k^2 z$. Thus a massless lever or gear can be used to connect the vibrator to the load, thereby changing the absolute value of the load mobility without changing its angle and bringing about a mobility match which will cause maximum power to be delivered by the vibrator to the load; further increase of power

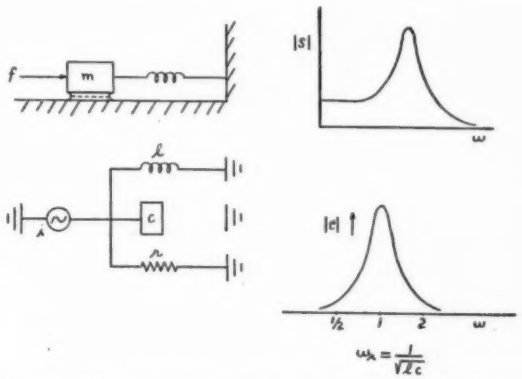

FIG. 11. The elementary problem of the forced vibration of the parallel mechanical system of one degree of freedom, the first problem discussed by most books on vibration (and unfortunately always considered as analogous to a *series* electrical circuit).

can be brought about only by resonating the system by the addition of a suitable excitability.

Examples

The first problem dealt with by most books is the simple system shown in Fig. 11 wherein a mass connected to a fixed point through a spring and supported on a fixed surface by an oil film, is acted on by a vibrating force. The schematic diagram shows the elements in parallel since one terminal of each is the fixed point, and their other terminals are fastened together. Since this is a parallel system we can at once write down the velocity across the system, or the velocity of the mass, as

$$e = iz = \frac{i}{1/r + 1/(-j/\omega c) + 1/j\omega l} = \frac{i}{1/r + j(\omega c - 1/\omega l)}$$

and the displacement amplitude

$$s = e/j\omega.$$

If $|e|$ and $|s|$ are plotted against the frequency of the impressed force they yield the familiar resonance curves of the form shown in the figure; the velocity resonance curve is symmetrical when plotted against a logarithmic frequency scale. The actual velocity amplitude is maximum

when $\omega c = 1/\omega l$ giving $\omega_r = 1/(lc)^{\frac{1}{2}}$. An example of this kind of a system is not easy to find on an automobile.

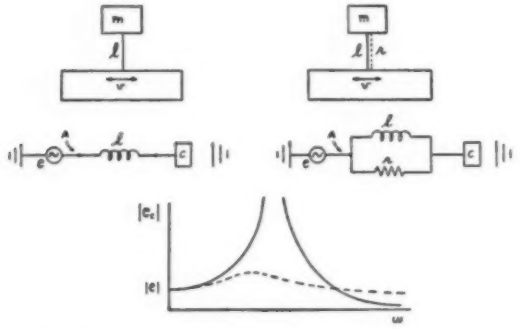

FIG. 12. A simple mechanical system, both without and with resistance, subjected to an impressed vibration.

A more common type of system is shown at the left of Fig. 12. A massive base which is vibrating with a given velocity, supports a leaf spring which carries a mass on its outer end. This might represent some accessory which is fastened to the motor by an elastic bracket, or the knob on the end of the shift lever, or a radio amplifier which we wish to protect from vibration by an elastic suspension, or the vibrating element of a tuned vibration microphone such as is screwed to a gear test stand in order to indicate the amount of gear note, or very crudely the center of a door panel which receives vibration from the door frame. Since the velocities of the base and the mass are measured relative to ground, one terminal of the velocity vibrator and of the mass is shown as the ground in the schematic diagram, while the spring has its terminals connected to the movable terminals of these elements. The mobility at the point A is the mobility of the spring and mass in series, and the force through the combination is

$$i = \frac{e}{z_A} = \frac{e}{j\omega l - j/\omega c}$$

and the velocity of the mass is

$$e_c = iz_c = i\left(\frac{-j}{\omega c}\right) = \frac{e}{1-\omega^2/\omega_r^2} \quad \text{where } \omega_r = 1/(lc)^{\frac{1}{2}}.$$

If the actual velocity amplitude across the mass is plotted against frequency of the impressed velocity, the solid curve shown in the figure is obtained; this indicates that below the resonant frequency the sprung mass vibrates with a greater velocity than the source of vibration, while considerably above resonance the sprung mass has a very low velocity. At resonance the sprung mass has a very high velocity and the system reacts on the vibrator with a large force. If now we add a resistor in parallel with the spring by making the spring out of rubber or adding a damping material to the door panel, we get the system shown at the right of Fig. 12. Here again

$$i = \frac{e}{z_a} = e \Big/ \left(\frac{1}{1/r + 1/j\omega l} - \frac{j}{\omega c}\right)$$

and

$$e_c = i(-j/\omega c).$$

This yields the dotted curve shown in the figure which indicates that the addition of the damping has materially reduced the velocity of the sprung mass in the neighborhood of the resonance frequency, but at higher frequencies the damping has increased the velocity above what it was with a purely elastic spring. (At the higher frequencies, however, a door panel would vibrate in more complicated modes so this analysis would no longer apply to it.)

The mobility method of computation is not limited to linear vibrations but is equally applicable to torsional vibrations if the units are properly chosen. The same symbols can be used in the schematic diagram, but with the understanding that the vibrations in the elements are torsional. e is the angular velocity across an element in radians/sec. i is the torque through an element in dyne cm or pound inches. z is the torsional mobility in rad./sec./dyne cm or rad./sec./pound inch. l is the torsional compliance in rad./dyne cm or rad./pound inch. r is the torsional responsiveness in the same units as mobility. c is the moment of inertia in gram cm^2 or pound inches^2/g (or pound inch sec.^{2}). An example is shown in Fig. 13 which represents a six cylinder crank shaft with flywheel. Each crank and connecting rod has been replaced by its equivalent disk as explained in the books on such matters and we wish to compute the oscillation of each crank and the flywheel due to a certain sinusoidal component of the torque

applied to the first crank. The schematic diagram is as shown in the figure. As in our first example discussed on p. 379 we start with the mobility of c_7 and compute the mobilities at successive junction points until we obtain the mobility at the driving point at the first crank. We then compute the forces through the springs and the velocities of the other cranks and flywheel. In this example, the computation will be simpler than in our first example because all of the mobilities are pure imaginary instead of complex, there being no resistors in the system. The vibration of the flywheel due to the vibratory torques supplied at all the cranks can be found by applying the principle of superposition mentioned above.

Suppose further that we wished to find the natural frequencies of this crank shaft. At any natural frequency, any mass can be maintained in vibration with a finite velocity without maintaining any vibrating force on the mass. At a natural frequency, the mobility of any vibrating mass and the system to which it is connected, is infinite. Therefore, we can locate the natural frequencies by computing the mobility of any point in the system at a number of different frequencies and noting which frequency makes the mobility infinite. This is not as difficult as might at first sight appear since the mobility changes sign on passing through infinity, so at least one natural frequency lies between any two frequencies of computation if the mobilities at these frequencies are of different sign. There will be as many natural frequencies as there are

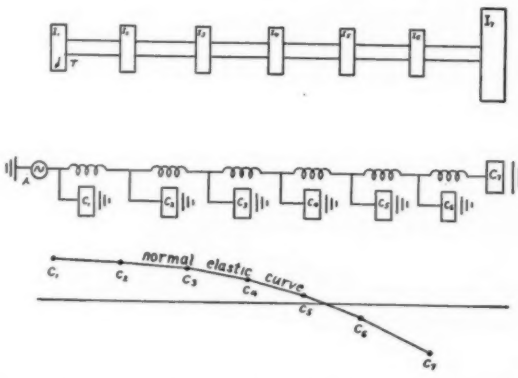

FIG. 13. The torsional vibrations of a crank shaft may be analyzed by the mobility method; not only can the forced vibration be found but the natural frequencies and normal modes of vibration can be computed.

active degrees of freedom of the system, six in this example. When a natural frequency has been found, the normal mode of vibration can be computed merely by applying a vibratory velocity of this frequency to one point in the system and computing the velocities of the other points. In this example the lowest natural frequency results in a normal elastic curve somewhat as shown in the lower part of the figure, the first five cranks swinging against the last crank and the flywheel.

Acoustical Mobility

The mobility method is also applicable to the computation of the performance of certain types of enclosed acoustical systems, such as intake silencers. Just as the vibration of mechanical systems is expressed in terms of the force through elements and the velocity across them, a simple harmonic sound traveling along the inside of a tube is described at any cross section of the tube by giving its *sound pressure* and its *volume velocity*. The sound pressure is the variation of the pressure at the cross section of the tube above and below the normal atmospheric pressure, and the maximum value of this variation is called the *sound pressure amplitude* I measured in dynes/cm^2. The volume velocity is the rate at which air is flowing through the cross section due to the sound and the maximum value of this oscillating quantity is called the *volume velocity amplitude* E measured in cm^3/sec.

The acoustical mobility Z of an area lying in the wave front, is defined as the volume velocity amplitude through the area divided by the sound pressure amplitude at the area;

$$Z \equiv E/I, \text{ cm}^5/\text{dyne sec.}$$

The acoustical mobility is the ease of motion of the air lying in the area, the amount of oscillatory volume velocity produced by unit sound pressure amplitude.

The acoustical mobility depends on the structure of the acoustical system lying beyond the area and on the frequency of the impressed sound pressure; it can be computed from simple formulas for a number of structures and combinations of structures. The formulas are simplified in form if the frequency enters them in the

form of a wave number k (the number of waves in 2π cm) which is defined as $k \equiv \omega/c$ where c is the speed of propagation of sound in the medium in cm/sec. Another constant of the medium which enters the equations is called the specific acoustic responsiveness of the medium and is defined as $R_s \equiv 1/\rho_0 c$ where ρ_0 is the normal density of the medium in grams/cm³; for air $R_s \equiv 0.025$ cm³/dyne sec. under average conditions. The acoustical elements are necks, volumes, and acoustical resistors. In Fig. 14 a neck and a volume, whose linear dimensions must be small compared to the wave-length, are combined into a bottle shaped structure called a Helmholtz resonator. The acoustical mobility of the area which opens into the wall of the volume of L cm³ can be shown to be

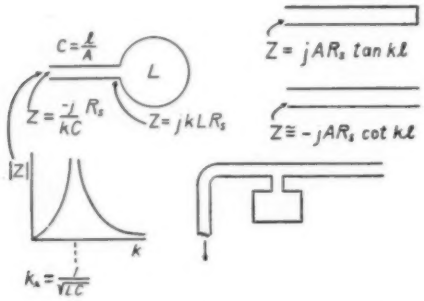

FIG. 14. The concept of acoustical mobility can be applied to the computation of the effectiveness of an intake silencer.

$$Z_L = jkL\ R_s.$$

The mobility of the area at one end of the neck, assuming that the other end opens into free space and calling the *slenderness* of the neck $C = l/A$ = length/area, in cm^{-1}, can be shown to be

$$Z_C = (-j\ kC)R_s.$$

The effective length of a neck is greater than its measured length by an end correction of approximately $\pi r/4$ at each end, where r is the radius of the neck in cm. If now the neck is connected to the volume to make the Helmholtz resonator, the air in the neck will move as a whole due to the sound pressure which might be applied at its outer end and the volume velocity E will be the same into the volume as into the neck, while the applied pressure will have to overcome the pressure built up in the volume and the pressure required to overcome the inertia of the air in the neck. The mobility of the combination, looking into the area at the outer end of the neck, is therefore

$$Z = \frac{1}{1/Z_L + 1/Z_C} = 1 \Big/ \left(\frac{1}{jkLR_s} + \frac{1}{-jR_s/kC} \right) = \frac{jkLR_s}{1 - k^2LC}.$$

This indicates a very high mobility or resonance when $k = 1/(LC)^{\frac{1}{2}}$ as shown in the graph of Fig. 14, at which frequency the air in the neck will move with maximum velocity and the sound pressure in the volume will be a considerable factor times the sound pressure impressed at the outer end of the neck.

Simple formulas have also been derived for the mobility looking into the open end of a tube of constant cross-sectional area A cm² and length l cm (no restriction on l as regards its ratio to the wave-length). If the tube is closed at the distant end so as to give perfect reflection

$$Z = jAR_s \tan kl.$$

If the tube is open at the distant end but the diameter of the tube is small compared to the wave-length, there will be approximately perfect reflection at the open end though with change of phase in the sound pressure, and the mobility at the sending end will be approximately

$$Z \cong -jAR_s \cot kl.$$

With this much theory we can understand the principle of the intake silencer which is shown in its simplest form in Fig. 14. The air comes through the horizontal tube and flows in the direction of the arrow into the carburetor, the pulsations in this flow constituting the sound which we wish to keep from radiating from the open end of the tube. A Helmholtz resonator is arranged as a side branch and so proportioned that its resonance frequency lies in the midst of the frequencies to be attenuated. The mobility of the resonator is therefore much higher than the mobility of the tube at the right, and the pulsations flow in and out of the resonator rather than out of the tube. The resonator is effective over a comparatively wide range of frequencies since its mobility is considerably less than the mobility of the tube over a fairly

wide range. If the wave-length becomes twice the length of the tube at the right, the mobility of the tube becomes high and there is no silencing action. The principle of the silencer can also be described by saying that the presence of the high mobility resonator cuts down the sound pressure at that point in the system, so that a smaller sound pressure actuates the tube at the right. The behavior of this acoustical system cannot be computed in detail unless the internal mobility of the sending end of the system to the left of the resonator, is known either by computation or measurement. Double resonators are often used on silencers, utilizing a second Helmholtz working out of the volume of the first resonator. The acoustical mobility of this double resonator can be computed from these same principles if the dimensions of the resonators are small compared to the wave-length.

Methods of experimentally measuring acoustical mobility have been developed and can be used to supplement or replace computation in design problems. While much more can be written on this subject, the above outline should serve to indicate the usefulness of the concept of acoustical mobility, the acoustical counterpart of the mechanical mobility. The mechanical mobility z of an area A cm^2 whose acoustical mobility is Z, is

$$z = Z / A^2 \text{ kines/dyne.}$$

Acoustical mobility has the useful properties that it is unchanged at a change of cross section of a tube, and the acoustical mobility of the combination of a number of systems which enter a common junction point small compared to the wave-length, is the sum of their separate acoustical mobilities;

$$Z = Z_1 + Z_2 + Z_3 + .$$

In Conclusion

The mobility method has its limitations. It is not applicable to the detailed computation of the transient vibrations excited in systems by arbitrary impulses; it is limited to the computation of forced vibrations or free vibration in normal modes. It is not so easily applied to systems like diaphragms, door panels, or stretched strings, in which the mass and elasticity are distributed rather uniformly throughout the system; it is most convenient when the masses, springs, and resistors are concentrated. It is not strictly applicable to systems containing springs whose force is not proportional to the displacement, or resistors whose force is not proportional to the velocity; were it not for the shock abosrber being a resistor with force not proportional to the velocity, the mobility method would be very convenient for computing the vibrations of the car body when driving over a road of sinusoidal contour. Such an analysis of riding qualities would require one schematic diagram referring to the vertical motion of the center of mass of the body, and another diagram referring to the pitching motion of the body. One must be careful when applying the mobility method to systems in which the vibrations are not all in the same line.

However, the mobility method is particularly advantageous in computing the forced vibration of linear mechanical systems, a kind of problem very important in practice. Those who know their electrical circuit theory will have noticed that due to our choice of symbols, the equations and methods have become of the same form as those used in electricity, although no reference is made to electricity in the solving of the problems. This similarity is helpful in remembering the equations and methods, although a lack of knowledge of electricity need not be considered a handicap in applying the mobility method. Noting the analogy which exists between mechanics as set forth in the mobility method, and electrical circuit theory as set forth in a book like Shea's *Transmission Networks and Wave Filters*, we may translate the conclusions of that book into mechanical terms with the assurance that they apply to every mechanical system whose schematic diagram is of the same form as the circuit diagram given in the book.

Here and There

New Appointments

Professor George E. Uhlenbeck of the University of Utrecht and formerly of the University of Michigan will be at Columbia as visiting professor of theroetical physics for the winter session of 1938–1939. Professor Uhlenbeck will lecture on statistical mechanics and on quantum mechanics.

★

Harvard University announces that Assistant Professor K. T. Bainbridge has been promoted to an associate professorship.

★

Professor Lucy Wilson is to be acting dean of Wellesley College during 1938–39. She will continue part-time teaching in the physics department.

★

At the end of the current year Professor Eugene Wigner, professor of mathematical physics at the University of Wisconsin, is leaving to accept the Jones professorship of mathematical physics at Princeton University.

★

Mr. Seville Chapman, who will receive his degree from the University of California at Berkeley in June, has recently been appointed instructor of physics at the University of Kansas.

★

Dr. Robert N. Varney, of New York University, has been appointed assistant professor of physics at Washington University, St. Louis, Mo. Dr. Varney did his undergraduate and graduate work at the University of California. He has worked on ionization by positive ions, and on neutrons.

★

Professor Edwin F. Stimpson, since 1901 a member of the department of physics at the University of Kansas, is retiring at the end of the present academic year on account of ill health.

★

At Rice Institute Dr. L. M. Mott-Smith is leaving the physics department to devote his whole time to the Mott-Smith geophysical prospecting corporation. Dr. William E. Bennett of Toronto has been appointed instructor in physics. Dr. T. W. Bonner has been granted one year's leave of absence to study in the Cavendish Laboratory on a Guggenheim Fellowship.

John F. Lewis Prize

The John F. Lewis Prize of $300 and an illuminated diploma awarded "to the American citizen who shall announce at any general or special meeting of the American Philosophical Society and publish among its papers, some truth which the council of the society shall deem worthy of award" was given at its recent meeting to Professor Arthur J. Dempster, of the University of Chicago, in recognition of his work on mass spectroscopy and mass analysis of the chemical elements. The presentation of this prize was made at the annual dinner by Dr. Robert A. Millikan.

Science

★

Awards of the Lalor Foundation

The Board of Trustees of the Lalor Foundation has announced the selection of winners of five awards from the Lalor Foundation for research in chemistry for the academic year 1938–1939. These awards comprise three fellowship grants of $2500 each and two supplemental awards of $1250 each. The recipients of the awards are:

Dr. Leland J. Haworth, of the University of Wisconsin, to continue his work with Professor F. G. Keyes in the Research Laboratory of Physical Chemistry at the Massachusetts Institute of Technology, on the fundamental properties of materials at low temperatures.

Dr. R. S. Livingston, associate professor at the University of Minnesota, to spend a sabbatical year working with Professor Frank, the Johns Hopkins University, on the study of photosensitized chemical oxidations.

Dr. Lucy Pickett, assistant professor at Mount Holyoke College, to carry on studies of absorption spectra of pure hydrocarbons with Professor Henri at the University of Liège, in Belgium, and for work at Harvard University. Dr. Pickett has also been awarded a fellowship by the Committee for the Relief of Belgium.

Dr. Walter W. Pigman, of the University of Maryland, for a year's leave of absence from his position in the National Bureau of Standards in Washington, to work with Professor Helferich of Leipzig, on the chemical nature and constitution of enzymes.

Dr. John W. Stout, of the University of California, to continue his researches with Professor Giauque on the thermal and magnetic properties of various substances at the lowest temperatures available by adiabatic magnetic cooling.

International Congress for Applied Mechanics

The Fifth International Congress for Applied Mechanics will be held from September 12 to 16, 1938 at Cambridge, Massachusetts, at Harvard University and Massachusetts Institute of Technology. The Congress is a meeting of individuals interested in applied mechanics, and any such person is invited to become a member by registration and payment of the congress fee of $5.

The work of the Congress will be accomplished by means of technical sessions at which communications from members will be read and discussed. The field of applied mechanics will be divided into the following general heads:

I. Structures, Elasticity, Plasticity, Fatigue, Strength Theory, Crystal Structure
II. Hydro- and Aerodynamics, Gasdynamics, Hydraulics, Meteorology, Water Waves, Heat Transfer
III. Dynamics of Solids, Vibration and Sound, Friction and Lubrication, Wear and Seizure.

Members are invited to exhibit and demonstrate apparatus and models. Early notice should be given as to requirements of space, stands, lights, current, water, air, etc.

Members are invited to visit Washington on Monday, September 19 and spend the day at the National Bureau of Standards. They may then take the night boat to Old Point Comfort, Virginia and spend Tuesday at Langley Field Laboratories.

For further information inquiries should be addressed to: Fifth International Congress for Applied Mechanics, Massachusetts Institute of Technology, Cambridge, Massachusetts.

★

Summer Sessions

The University of Pittsburgh will have a special summer session on the Physics of Metals from July 5 to August 12. The following courses are to be offered:

JULY 6–AUGUST 12

Introductory Theory of Metals. N. F. MOTT, University of Bristol

JULY 6–JULY 15

Electrical Conduction in Metals. JOHN BARDEEN, Harvard University

JULY 18–JULY 29

Atomic Arrangements in Solids. F. SEITZ, General Electric Laboratories, and F. BITTER, Massachusetts Institute of Technology

JULY 25–AUGUST 12

Order-Disorder Phenomena in Alloys. F. C. NIX, Bell Telephone Laboratories

JULY 6–AUGUST 12

Special Topics in the Physics of Solids. N. F. MOTT

Formal lectures will be held on the first four afternoons of the week, thus reserving Friday afternoons for special colloquia on topics of interest. The following program has been arranged:

Physical Tools of Use in Metallurgy, 4 P.M. Friday, July 8
H. R. NELSON, Battelle Memorial Institute, *Study of Surfaces by Electron Diffraction*
C. S. BARRETT, Carnegie Institute of Technology, *Use of X-Ray Diffraction*
KEIVEN BURNS, University of Pittsburgh, *Spectroscopy in Metals Industries*

Creep in Metals, 4 P.M. Friday, July 15
P. G. MCVETTY, Westinghouse Electric and Manufacturing Company
Second speaker to be announced.

Elastic Properties of Metals, 4 P.M. Friday, July 22
R. L. TEMPLIN, Aluminum Company of America
M. M. FROCHT, Carnegie Institute of Technology, *Photoelastic Method of Stress Analysis*

Internal Friction in Metals, 4 P.M. Friday, July 29
C. ZENER, College of the City of New York
Speaker from Jones and Laughlin Steel Corporation

Mechanism of Hardening, 4 P.M. Friday, August 5
R. F. MEHL, Carnegie Institute of Technology
M. F. MOTT, Visiting Professor, University of Pittsburgh

Fatigue in Metals, 4 P.M. Friday, August 12
H. F. MOORE, University of Illinois
D. J. MCADAM, National Bureau of Standards

For further details write to Professor E. Hutchisson at the University of Pittsburgh.

★

The Massachusetts Institute of Technology announces a special summer program on spectroscopy to be held in Cambridge from July 13 to July 23. During this period courses in practical spectroscopy will be offered and spectrographic conferences will be held. Spectroscopic research will be carried on from June 1 to August 1. The tentative program for the 1938 conference on spectroscopy and its applications is as follows:

MONDAY, July 18, at 9:30 A.M.: *Spectroscopic Analysis of Materials.*
H. R. KREIDER, American Medical Association Laboratory. **The Broad Scope of the Spectrograph as an Analytical Tool.**
R. A. SAWYER, University of Michigan. **Characteristics of Spectroscopic Light Sources.**
W. R. BRODE, Ohio State University. **Influence of Impurities on Line Strength in Quantitative Analysis.**
O. I. LEE, Lucius Pitkin, Inc. (with T. A. Wright). **On Identifying Minerals with the Aid of the Spectrograph.**
W. E. ALBERTSON, Massachusetts Institute of Technology. **Analysis of Materials by Fluorescence Methods.**
MONDAY, July 18, at 2 P.M.: *Spectroscopic Apparatus*
W. S. BAIRD, Baird Associates. **A Practical Grating Spectrograph for Industrial Use.**
G. H. DIEKE, Johns Hopkins University. **Characteristics of the Eagle Mounting of Concave Gratings.**
J. W. FORREST, Bausch & Lomb Optical Co. **An Improved Density Comparator.**
G. R. HARRISON, Massachusetts Institute of Technology. **A New High Speed Method of Absorption Spectrophotometry for the Range 10,000 to 2,000 A.**
TUESDAY, July 19, at 9:30 A.M.: *Applications of Absorption Spectrophotometry.*
FRITZ WEIGERT, Glasgow, Scotland. **Photochemistry of the Visible Spectrum.**
W. R. BRODE, Ohio State University. **The Relation Between the Color and Constitution of Azo Dyes.**
T. R. HOGNESS, University of Chicago. **Spectroscopic Studies on Enzyme Systems.**
R. L. MCFARLAN, United Drug Co. Laboratories. **Spectrographic Methods of Vitamin Determination.**
A. E. RUEHLE, Bell Telephone Laboratories. **Applications of Ultraviolet Absorption Spectra in Establishing the Structure of Vitamin B_1.**
TUESDAY, July 19, at 2 P.M.: *Spectroscopic Data and Technics.*
BRIAN O'BRIEN, University of Rochester. **The Application of Isodensity Contouring Methods to Spectrum Photometry.**
W. F. MEGGERS, National Bureau of Standards (with B. F. Scribner). **Bibliography of Spectrochemical Analysis.**
G. R. HARRISON, Massachusetts Institute of Technology. **New Tables of the 100,000 Principal Lines of the Chemical Elements between 10,000 and 2,000 A.**
W. F. MEGGERS, National Bureau of Standards. **Standard Wave-Lengths.**
TUESDAY EVENING: Informal Dinner and Discussion.
WEDNESDAY, July 20, at 9:30 A.M.: *Applications of Spectroscopy.*
B. F. SCRIBNER, National Bureau of Standards. **Spectrographic Detection of Rare Earths in Plants.**
B. C. BRUNSTETTER, U. S. Department of Agriculture (with A. T. Myers, H. L. Wilkins and M. A. Hein). **Simultaneous Quantitative Determination of Seven Elements in Grasses and Legumes.**
J. T. WALKER, Massachusetts State Police. **The Spectrograph as an Aid in Criminal Investigation.**
C. W. RANKIN, New York State Police Laboratory. **Applications of the Spectrograph to Criminal Investigation.**
FRITZ WEIGERT, Glasgow, Scotland. **A Simple Method of Testing Dispersion Filters.**
WEDNESDAY, July 20, at 2 P.M.: *General Spectroscopy and Discussion.*
O. R. WULF, U. S. Bureau of Chemistry and Soils (with E. H. Melvin). **Some Band Spectra in Emission at Ordinary Pressure and Temperature.**
J. S. CAMPBELL, University of Rochester. **Wave-Length Measurements of Lines with Structure.**

Further information may be obtained from Professor George R. Harrison, Massachusetts Institute of Technology.

A symposium on theoretical physics will be held at the University of Michigan from June 27 to August 20. It is designed to meet a variety of interests with considerable stress upon nuclear problems. The following courses have been arranged to date:

June 27–August 20
Relativity and Spin. H. A. KRAMERS, University of Leiden
Radiation Theory. H. A. KRAMERS
June 27–July 15
Selected Topics in Nuclear Physics. H. A. BETHE, Cornell University
Descriptive Theory of the Compound Nucleus, with Application to Yields of Nuclear Reactions. H. A. BETHE
Field Theory of Nuclear Forces. H. A. BETHE
June 29–June 30
Multiple Reflection of X-Rays in Crystals. P. P. EWALD, Cambridge University, England
How to Look at Crystal Structure Determinations. P. P. EWALD
July 11–August 5
Nuclear Physics. G. BREIT, University of Wisconsin
July 25–August 6
The Chemical Interpretation of Infra-Red and Raman Spectra. E. BRIGHT WILSON, JR., Harvard University
Interpretation of Molecular Spectra of Complex Molecules. E. BRIGHT WILSON, JR.
Molecular Spectra and Valence. E. BRIGHT WILSON, JR.
Molecular Spectra and Thermodynamics. E. BRIGHT WILSON, JR.
Internal Rotation in Organic Molecules. E. BRIGHT WILSON, JR.
August 1–August 12
Theory of the Solid State. FREDERICK SEITZ, General Electric Company

Special announcements of these sessions will be sent upon request to the department.

★

The Electrochemical Society

At the annual meeting of the Electrochemical Society held at Savannah, Georgia, the following officers were elected:

President, ROBERT L. BALDWIN of the National Carbon Co., Inc.
Vice Presidents, A. KENNETH GRAHAM of Philadelphia; LEON R. WESTBROOK of Cleveland; and S. SKOWRONSKI of Perth Amboy
Managers, R. B. MEARS, New Kensington, Pa.; H. E. HARING, Summit, New Jersey; L. C. JUDSON, New York City
Treasurer, ROBERT M. BURNS, Bell Telephone Laboratories, Inc.
Secretary, COLIN G. FINK, Columbia University.

At this meeting Mr. R. Spencer Soánes of Toronto, Canada, was awarded the society's *Prize to Young Authors*, for the paper published jointly by Mr. A. H. Heatley and Mr. Soanes entitled, "Potential Distribution in High Current Carbon Arcs in Air." Mr. Soanes is a research fellow with the Ontario Research Foundation, Toronto, Canada.

The Electrochemical Society has just awarded the tenth Weston Fellowship of $1000 to Dr. V. DeNora of Milan, Italy. Dr. DeNora will continue his research at Columbia University, investigating the codeposition of metals in the ionic and colloidal states, and the application of the Faraday.

★

Booklets Recently Received

General Radio Experimenter. Vol. 12, No. 11, April, 1938. 8 pp. This issue contains a description of a.c. operation for type 613-B beat-frequency oscillator, and of the behavior of type 505 condensers at high frequencies.

Shop and Laboratory. Vol. 2, No. 1, April, 1938. 12 pp. Some of the contents of this booklet are: (1) Mico Specimen Saw, (2) The 24-inch Measuring Engine, (3) Fiber Microtome, and (4) Mico Lab-Lite.

Cenco News Chats. Vol. 3, No. 18, April, 1938. 16 pp. This issue includes articles on aluminizing mirrors, "Electric Eye Extracts Information from Particles," and "Time's Valuable—Measure it Accurately."

Micromax. Catalog N-00B, 1938. 12 pp. Leeds and Northrup Co. of Philadelphia, Pa. This booklet describes various pneumatic temperature controls.

The Bakelite Corporation of New York City has issued a booklet describing another new product—Bakelite Polystyrene Molding Material.

Among Our Authors

Dr. Floyd K. Richtmyer is well known to all physicists. He is dean of the Graduate School at Cornell University. He received the Levy Medal from the Franklin Institute in 1929. He has been national president of Sigma Xi, of the American Association of Physics Teachers, of the Optical Society, and of the American Physical Society and is a member of the Board of Governors of the American Institute of Physics. He is also editor of the *Review of Scientific Instruments* and the *Journal of the Optical Society of America*.

Dr. Gerald M. Rassweiler graduated from Bucknell in 1924 with an A.B. degree. He received his M.S. and Ph.D. degrees from the University of Illinois in 1926 and 1928, respectively. During 1925, 1927 he was research physicist with the E. I. duPont de Nemours and Company. Since 1928 he has been research physicist with the General Motors Research Corporation.

Dr. F. Morgan received his B.S. in electrical engineering from Ohio State in 1927; his M.S. in physics from Purdue in 1932; and his Ph.D. from Ohio State in physics in 1936. He was an instructor at Purdue from 1927 until 1932; a graduate assistant at Ohio State from 1933 until 1936. In September, 1936, he accepted a position with the Gulf Research Laboratories.

Mr. Clifton G. Found received his B.A. from Toronto in 1914 and his M.A. from there in 1915. Since 1916 he has been research physicist with the General Electric Company at Schenectady. He has had much to do with the development of the new high efficiency sources of light.

Dr. Lloyd L. Withrow received his A.B. from Oberlin College in 1922, and his A.M. and Ph.D. degrees from the University of Wisconsin in 1923 and 1925, respec tively. From 1922 until 1926 he was an instructor of chemistry at Wisconsin. Since 1926 he has been connected with the General Motors Research Laboratory as a research chemist.

Dr. Selby M. Skinner received his B.S. degree from the University of Washington in 1929, and his Ph.D. in physics from California Institute of Technology in 1933. He has done research in atomic physics, and has been a research associate in a General Education Board project concerning the physical sciences. He is at present assistant professor of physical sciences in the college at the University of Chicago.

Dr. Herbert J. Reich was born at Staten Island, New York. He received the degrees of M.E. and Ph.D. from Cornell University in 1924 and 1928, respectively. From 1924 to 1925 he was an instructor of machine design at Cornell University. He was instructor of physics at that university until 1929. Later he accepted a position with the University of Illinois in the electrical engineering department where he is associate professor at present.

Dr. Morris Muskat received his A.B. and A.M. degrees from Ohio State University in 1926 and was a fellow at the California Institute of Technology from 1927–1929, taking his Ph.D. degree at that institute in 1929. From 1926 to 1927 he was an instructor in physics and chemistry at Bowling Green State Normal College, Ohio. Since 1929 he has been a theoretical physicist at the Gulf Research and Development Company, Pittsburgh, Pennsylvania. He is now in charge of the physics division in the Gulf laboratory.

Mr. Floyd A. Firestone received his B.S. from Case School of Applied Science in 1921. Since 1923 he has been assistant professor of physics at Michigan. He is the author of many papers in the field of acoustics.

Mr. Wallace A. Depp received his B.S. in electrical engineering from the University of Illinois in 1936. During the following summer he was in the student engineering course at the General Electric Company at Schenectady. He received his M.S. in electrical engineering also at the University of Illinois in 1937 under a Tau Beta Pi Fellowship. Since then he has been employed in the Vacuum Tube Development Department of the Bell Telephone Laboratories, Inc., in New York City.

Some of the New Books

The Advancing Front of Science. GEORGE W. GRAY. Pp. 364, No figs. 23×14 cm. Whittlesey House, McGraw-Hill Book Company, Inc., New York, 1937. Price $3.00.

This book presents up-to-date news of recent advances in physics, astrophysics, chemistry, biophysics, and psychology. The style is adapted to the abilities of intelligent laymen who have had at least a year of high-school physics or chemistry. Despite its elementary nature, the researches described are so recent, the reporting so reliable, and the writing so completely done that physicists and others with scientific training will read it with delight. Teachers of introductory science courses will profit by studying carefully the simple vocabulary of this work and by noting how the author leads the reader along a smooth, upward slope, cleverly avoiding the pitfalls and chasms that might cause disaster.

The first half of the book is devoted principally to physics and astrophysics. Among the topics treated are the ionized "ceilings" of the atmosphere, stellar motions, the new theories of the "red shift" of spectral lines, cosmic rays, proton-proton scattering, and acoustics. Then follow chapters on surface films, the mechanisms of cell growth, on man-made "thinking" machines, and on other phases of experimental psychology.

The author is a journalist whose earlier work, *New World Picture*, published last year won high commendation. In writing *The Advancing Front of Science* he interviewed more than seventy American leaders of research and visited their laboratories. Chapters of the finished manuscripts were checked by competent specialists in the several fields. Because of this technique and the carefulness of the author, the work is admirably free from important errors in physics. He has done a good job. May his tribe increase!

OSWALD BLACKWOOD
University of Pittsburgh

Magnetism. Lectures delivered before the Manchester and District Branch of the Institute of Physics on July 1 and 2, 1937. Pp. 102+vi, Figs. 47, 16×25 cm. The Institute of Physics, London, 1938. Price 4s. 6d. net.

This small book is the report of a conference on ferromagnetism, one of many similar conferences on physics in industry sponsored by the Institute of Physics with the object of bringing together scientific workers in industry and in the universities. It consists of six lectures, with a foreword by W. L. Bragg.

I. N. F. Mott, University of Bristol, *Magnetism and the Electron Theory of Metals* (13 pp.)
II. G. C. Richer, John Lysagts, Ltd., *Electrical Sheet Steel* (12 pp.)
III. C. Dannatt, Metropolitan-Vickers Electrical Co., *The Influence of the Properties of Available Magnetic Materials on Engineering Design* (8 pp.)
IV. E. C. Stoner, University of Leeds, *Magnetization Curves of Ferromagnetics* (25 pp.)
V. D. A. Oliver, Permanent Magnet Association, *Permanent Magnets* (18 pp.)
VI. A. J. Bradley, National Physical Laboratory, and A. Taylor, University of Manchester, *X-ray Studies on Permanent Magnets of Iron, Nickel and Aluminium* (12 pp.)

It is apparent from the titles that the lectures cover a wide range of interest within the field of ferromagnetism. They will appeal to those interested in the production and use of electrical sheet steel and permanent magnets and also to those interested in the atomic structure of magnetic materials and the explanation of the great differences in properties of materials having different compositions and heat-treatments. For example, the first lecture is concerned with spinning electrons, domains, Heisenberg "overlap" forces, the distribution of electrons among the various shells of the atom and the effect on this distribution of alloying. On the other hand, the fifth lecture describes the magnetic properties of materials commercially available for use in permanent magnets; after a discussion of methods of testing and of evaluating the properties of these materials, the author gives a history of the older materials, then in some detail the development, properties and present uses of the large number of valuable materials which have been invented during the last four or five years.

Of the other lectures the one by Stoner will be of interest to and understood by anyone at all concerned with ferromagnetism. The lectures by Richer and Dannatt point out to those engaged in research the limitations of the present commercial high-permeability materials and the properties which it would be desirable to have in them. The last lecture, by Bradley and Taylor, is a report of recent research of their own on the constitution of the unusually interesting three-component system Fe-Ni-Al.

The book can be recommended wholeheartedly to those occasionally or seriously interested in ferromagnetism. The foreword is of special interest to those concerned with the position of physics in industry.

R. M. BOZORTH
Bell Telephone Laboratories, Inc.

Contributed Original Research

Studies in Lubrication

I. The Theory of the Thick Film Lubrication of a Complete Journal Bearing of Finite Length

M. Muskat and F. Morgan
Gulf Research & Development Company, Pittsburgh, Pennsylvania
(Received February 23, 1938)

A successive approximation theory is developed for the hydrodynamics of journal bearing systems of finite length, the expansion parameter being the journal eccentricity. This is applied through the second approximation to full journal bearings of lengths exceeding the bearing perimeter. The existence of the lubricant source and associated end leakage is explicitly taken into account, it being assumed in the actual analysis that the source is set 90° in advance of the maximum film thickness. It is found that contrary to prevailing opinion, based on the infinitely long bearing theory, the friction coefficients and eccentricities for the systems are not uniquely determined by the "Sommerfeld variable"—$(r^2/c^2)(\mu N/P)$, where r = journal radius, c = radial clearance, μ = lubricant viscosity, N = journal speed in r.p.s., P = bearing load per unit projected bearing area. It depends also on the leakage flux or source strength. For the position of source assumed in the analysis the friction coefficients and eccentricities increase with increasing source strengths. Further, the load carrying capacities of the finite length bearings are shown to be considerably less than for the infinitely long bearings, and decrease with increasing source strength if the source is placed in the low pressure part of the film. Finally, the theory shows how the consideration of the source of the lubricant permits a resolution of the difficulties with respect to the negative film pressures predicted by the infinitely long bearing theory. The numerical calculations show that the third and higher approximations may be neglected for eccentricity ratios not exceeding 0.4. General formulas are also developed for the asymptotic behavior of the friction coefficients on both the journal and bearing at very low eccentricities or large values of the Sommerfeld variable. These apply to bearings of all lengths and to partial as well as full journal bearings.

Introduction

In 1886 Osborne Reynolds wrote[1] at the beginning of his classic paper on lubrication: "The subject [of lubrication] is of such fundamental importance in practical mechanics, and the opportunities for observation are so frequent, that it may well be a matter of surprise that any general laws should have for so long escaped detection." In spite of that discouraging situation Reynolds would have undoubtedly predicted that fifty-two years later the subject would be so thoroughly explored and investigated as to leave nothing more to do except to extend the decimal places used in representing the results of experimental data or theoretical calculations. Yet if he had, he would now be judged as having been overly optimistic. It is indeed true that the volume of literature published on lubrication is quite commensurate with the great importance of the subject. Unfortunately, however, the establishment of basic facts and principles of interpretation has not kept pace with the rapid accumulation of the printed pages, and there is still much to be learned. The development of the present status of the situation may be summarized as follows:

The original experiments which really gave rise to the hydrodynamic theory of lubrication were performed by Petroff[2] and Tower.[3] The

[1] O. Reynolds, Phil. Trans. Roy. Soc. **177**, 157 (1886).

[2] M. Petroff, Eng. J. St. Petersburg, Nos. 1, 2, 3, 4 (1883).

[3] B. Tower, Proc. Inst. Mech. Eng. **34**, 632–659 (1883). No pretense is being made here for completeness in

former explained his experiments quite simply by assuming that the lubricant in the journal bearing behaved like a thin film of viscous liquid of uniform thickness. On the other hand, Reynolds assumed that the film obeys the laws of classical hydrodynamics, the load being carried by pressure created in the converging portion of the film between the nonconcentric journal and bearing, the existence of such an eccentricity having been demonstrated by Tower. The analytical work of Reynolds, but with essentially the same physical approximations which take cognizance of the fact that the film thickness is very small compared to the other dimensions of physical interest, was put on a more firm basis in the classical paper of Sommerfeld[4] of 1904, and independently nine years later by Harrison.[5]

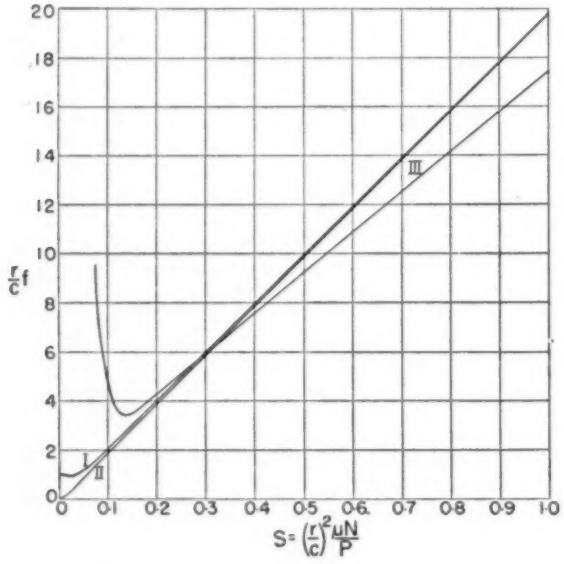

FIG. 1. Theoretical and experimental friction coefficient curves for full journal bearings. I: Sommerfeld curve for the friction on journal of an infinitely long journal bearing. II: Harrison curve for the friction on the bearing of an infinitely long journal bearing. III: Trend of typical published experimental data on full journal bearings. r=journal radius; c=radial clearance; μ=lubricant viscosity; N=journal speed in r.p.s.; P=bearing load per unit projected bearing area.

In these papers the integration of the Reynolds equations was carried through in closed form for journal bearings of infinite length including, in the case of Sommerfeld's work, both the complete journal bearing problem and the partial bearing of 180° arc. Sommerfeld's essential result lay in the calculation of the coefficient of friction as a function of the speed of rotation of the journal, N, the viscosity of the lubricant, μ, the load per unit projected area supported by the bearing, P, and the dimensions of the system represented by the journal radius, r, and radial clearance between the journal and bearing, c. The graphical representation of this result is indicated by curve I in Fig. 1, this particular form of plotting having been first published by M. D. Hersey.[6] Harrison made the additional contribution of explicitly pointing out that the coefficient of friction due to the frictional force on the bearing is less than that on the journal and gave the explicit formulas for each. That for the friction on the bearing is represented graphically by curve II of Fig. 1. Harrison also made calculations referring to air as a lubricant, in which the compressibility of the air was taken into account, so as to provide an explanation for Kingsbury's[7] experimental data on air lubricated journal bearings.

A similar type of complete hydrodynamic solution to the problem of lubrication was given for the case of rectangular plane surfaces of finite dimensions by Michell.[8]

Aside from the early works just mentioned, relatively little has been done in really advancing the fundamentals of the hydrodynamic theory of lubrication. Very useful numerical calculations, based on the original formulas of Sommerfeld and Harrison, have been made by Howarth[9] and Karelitz,[10] among others, their results being published in graphical form covering wide ranges of conditions for the lubrication of journal bearing systems. Other related calculations have

references and in reviewing all the tremendous literature that has been published on lubrication. Such a task would require a volume in itself. Only a few of the important contributions will be referred to explicitly. A large selection of references, however, will be found in the book by M. D. Hersey, *Theory of Lubrication* (1936).

[4] A Sommerfeld, Zeits. f. Math. Physik **50**, 97 (1904).

[5] W. J. Harrison, Trans. Camb. Phil. Soc. **22**, 39 (1913).

[6] M. D. Hersey, J. Wash. Acad. Sci. **4**, 542 (1914).

[7] A. Kingsbury, J. Am. Soc. Naval Eng. **9**, 267 (1897).

[8] A. G. M. Michell, Zeits. f. Math. Physik **52**, 123 (1905).

[9] H. A. S. Howarth, Trans. A. S. M. E. **45**, 421 (1923); **46**, 809 (1924); **47**, 1073 (1925).

[10] G. B. Karelitz, Trans. A. S. M. E. **47**, 1101 (1925).

been made by Gümbel,[11] and treatments of the effects of viscosity variation under special conditions have been given by Boswall.[12] From the point of view of the strict classical hydrodynamics, the problem of the complete journal bearing or fluid film viscous motion in an eccentric annular ring has been treated with complete rigor, except for the neglect of the inertia terms, by Duffing[13] and Reissner,[14] although Sommerfeld had already given a quite satisfactory demonstration in his original paper that the Stokes-Navier hydrodynamics would give essentially the same results as the Reynolds formulas when account is taken of the extremely small thickness of the lubricating film.

For the problem of journal bearings of finite length no satisfactory solutions are available. The implication of the Sommerfeld theory for the infinitely long bearing that over half of its perimeter the pressures would be negative has led to much discussion and skepticism as to the validity of the classical hydrodynamics. The literature suggests an undercurrent of feeling that possibly the treatment of the bearing of finite length might avoid this physical difficulty, but no demonstration of this method of escape has been attempted. In fact, Gümbel[11] definitely assumes that the viscous film breaks off at the azimuth in the bearing where the Sommerfeld theory would predict negative pressures, the pressure in these regions of the bearing being taken as atmospheric, corresponding to an air film. A rather widely used engineering approximation for the finite length bearing consists in supposing that the pressures along the central perimeter of the bearing are proportional to those given by the Sommerfeld theory, but that these fall off in a parabolic manner to atmospheric values at the ends of the bearing. While such assumptions have been variously justified on the basis of direct experimental tests and even by comparing with electrolytic model solutions[15] of the hydrodynamic problem, they still must be considered as little more than working hypotheses. An attempt has indeed been made by Reissner[16] to give a rigorous hydrodynamic theory of the bearing of finite length. However, since no provision was made in this theory for a direct entry of the lubricant into the bearing, it clearly corresponds to a case where over parts of the ends of the bearing the lubricant is leaking out whereas over the other parts it is being sucked in. This hardly corresponds to the physical conditions obtaining in practical journal bearing systems with forced lubrication.

With regard to the experimental studies of the problem it is also interesting to recall the situation in Reynolds' time. Quoting Reynolds once more:[1]

> "Besides the general experience obtained, the friction of lubricated surfaces has been the subject of much experimental investigation by able and careful experimenters. But, although in many cases empirical laws have been propounded, these fail for the most part to agree with each other and with the more general experience."

Unfortunately the situation is still pretty much the same. Again, it is true that experimental studies on lubrication have been so numerous as to almost defy a comprehensive review in a limited space. The apparatus has varied so widely among the different experimenters, and in many cases has involved so many unknown factors, that the results represent but little more than the characteristics of the particular machine being tested. Perhaps the only result upon which there appears to be even partial agreement is that the coefficient of friction follows a trend indicated by curve III in Fig. 1, the essential features of this curve being the asymptotic linearity of the curve for large values of the abscissas, the development of a minimum as the abscissa variable decreases, and an ultimate sharp rise when very low speeds, low viscosity lubricants, or high loads are involved. In fact, this behavior has been so generally observed that the conditions of lubrication are now characterized by the position which the measured friction coefficient takes on this curve. In particular, when the data fall to the right of

[11] L. Gümbel, *Jahrbuch Schiffbautech. Ges.* Vol. 18 (1917), p. 236.
[12] R. O. Boswall, *The Theory of Film Lubrication* (1928).
[13] G. Duffing, Zeits. f. angew. Math. u. Mech. **4**, 296 (1924).
[14] H. Reissner, Zeits. f. angew. Math. u. Mech. **15**, 81 (1935).
[15] A. Kingsbury, Trans. Am. Soc. Mech. Eng. **53**, 59 (1931).
[16] H. Reissner, Zeits. f. angew. Math. u. Mech. **16**, 275 (1936).

the minimum, it has become customary to denote the condition of lubrication as "thick film" or "fluid film" lubrication. The former term is supposed to indicate that the bearing and journal are approximately concentric, so that the fluid film is relatively thick over the whole bearing surface, a picture which does have sound physical justification. The latter term is taken to denote the fact that the lubricant really acts as a viscous film, since the friction coefficient curve does have some semblance to that theoretically predicted by Sommerfeld, namely, curve I.

When the data fall to the left of the minimum, the lubrication conditions are generally termed "thin film" or "partial film" lubrication. Here the former suggests that the journal moves eccentrically in the bearing, giving rise at some points to small film thicknesses in contrast to the case of thick film lubrication. The "partial film" notation is supposed to signify that since the general behavior of the curve is so radically different from that predicted by the Sommerfeld theory the latter does not describe the correct conditions, and in particular that the film is broken in the region where the pressures according to the Sommerfeld theory would assume large negative values, or where contact occurs between the metal surfaces.

The type of curve indicated by curve III of Fig. 1 has been known for a long time, and little of a fundamental nature has been done to give it a really satisfactory physical explanation. In fact, subsequent work has led to even further complications. For example, doubt has been cast upon the significance of the Sommerfeld variable $-(r^2/c^2)(\mu N/P)$—even in the thick film region, it being claimed by some investigators that the effect of the load P is not correctly described by this variable. And in the thin film region an entirely new phenomenon has been injected into the problem. It is that while the Sommerfeld variable satisfactorily determines the friction coefficient for a particular lubricant, the viscosity, as included in that variable, does not completely describe the lubricant. The result is that while the Sommerfeld or hydrodynamic theory would indicate that curves I and II of Fig. 1 are *universal* for *all* lubricants, the experiments in question indicate that lubricants have another property in addition to viscosity which may lead to different values of the friction coefficient even though the viscosity of the lubricating film is the same and the complete Sommerfeld variable is kept fixed. This new property has been termed "oiliness," with the implication that a lubricant giving a lower coefficient of friction than another, even though the Sommerfeld variable is the same, is more "oily" than the second lubricant. As reluctant as one may be to accept the addition of such a new property to the previously known characteristics of liquids, it must be admitted that a spreading of the friction coefficient curve in the thin film region is a well established fact under such experimental conditions as have led to its discovery.

This last phenomenon, which obviously has tremendous practical as well as commercial implications, does, of course, merit much study. From a physical point of view it is still extremely doubtful if it reflects a new bulk property of the lubricants involved. It seems much more likely that it is the expression of a condition of lubrication which is beyond the scope of the ordinary hydrodynamic theory, and which becomes so prominent under the "thin film conditions" as to mask the role played by the viscous fluid lubrication. In particular, it seems certain that under such conditions a large part of the friction is due to partial metal to metal contact between the journal and bearing, and that the lubricant itself begins to exhibit its properties as a surface film of a few molecular layers in thickness in a more pronounced form than its property of viscosity in a macroscopic liquid phase.[17] Of course, much work that is extremely useful from a practical point of view has been done in the study of this type of lubrication. The high efficiency of present day automotive construction and industrial machine developments attests to the success of these efforts. A great deal of excellent work has also been done in the more academic phases of the study of friction between sliding surfaces both with and without lubricants.[18] However, from the hydrodynamic point

[17] For a more detailed discussion of the physical interpretation of this phase of the problem, cf. P. D. Foote, J. App. Phys. **8**, 19 (1937).

[18] Worthy of particular mention are the lifetime studies

of view the subject of thin film lubrication still remains one about which practically nothing definite and fundamental is known.

Because most lubrication difficulties such as the burning or freezing of bearings involve the so-called thin film condition, this phase of the subject is evidently of greatest practical interest. Its obvious complexity, however, suggests that an attack upon the simpler and thick film type of lubrication might be a useful preliminary step before entering upon the more difficult thin film problem. That is, the thick film region might be used for the purpose of "calibrating" the technique of experimentation, and after this has been established one might slide down gradually along the friction coefficient curve so as to approach the thin film condition from a region that is already understood. This is essentially the point of view upon which has been based a program of study undertaken by the authors, and the first results of which are reported here.

In addition to the argument that the thick film region might provide a means for calibrating and controlling the method of attack upon the thin film lubrication problem, there is value in this procedure because the thick film type of lubrication is in itself not a closed and completed subject. For as was pointed out above, there is no universal agreement that the Sommerfeld theory for this region is really valid. Mention has been made of the uncertainty as to whether or not the effect of load upon the friction coefficient is properly expressed by the Sommerfeld variable. And of even greater interest is the fact that the asymptotic behavior of the friction coefficient curve for large values of the Sommerfeld variable, as indicated in curve III of Fig. 1, really does not fit the Sommerfeld theory. For the latter predicts that the asymptotic line should pass through the origin, whereas the published data almost universally give lines with a positive intercept on the friction coefficient axis. Moreover, little quantitative information is available as to the degree to which the observed friction coefficients agree numerically with the Sommerfeld theory predictions. Obviously, therefore, before the thick film region can be used as a calibrating guide for studies in the thin film region, the thick film type of lubrication must itself be subjected to considerably more investigation.

There are, of course, two phases to the study of the type proposed here, namely, the theoretical and experimental. The need for the latter arises from the fact that in most of the experiments thus far performed insufficient control has been applied in the determination of the important physical elements entering the problem. The greatest uncertainty has lain in a satisfactory knowledge of the true viscosity of the film within the journal bearings, which in turn involves an accurate determination of the film temperature. Insufficient attention has also been given in certain cases to the character of the metal surfaces as well as to the elimination of the various errors that may be introduced in accurately measuring the frictional forces. A report on an experimental study in which an attempt has been made to fill these gaps will be presented in a forthcoming paper.

In this paper will be presented an attempt to develop a hydrodynamic theory for the thick film lubrication conditions of a full journal bearing of finite length. In its completeness it will not even be comparable to the solution given by Sommerfeld for the bearing of infinite length, as it will be an approximation method restricted largely to the asymptotic limit of thick film conditions, that is, where the eccentricities of the journal in the bearing are small. It therefore represents nothing more than a first step toward a complete solution of the problem. On the other hand, it is felt to be sufficiently general as to provide definite information as to the real implications of the hydrodynamic theory of lubrication. In particular, it will provide the answer to the asymptotic behavior of the friction coefficient curve for finite bearings which has not been available heretofore. Obviously without such information one can never really tell whether the experimental data do or do not fit the theory, for it is not obvious that the asymptotic Sommerfeld behavior should also be followed by journal bearings of finite length.

---

of Sir W. Hardy on sliding friction, the work of R. Bulkley (Nat. Bur. Stand. J. Research **6**, 89 (1931)) on the viscous flow through extremely fine capillaries, and the beautiful experiments of F. B. Bowden (Proc. Roy. Soc. (1933–1937)) and collaborators on sliding friction phenomena.

Moreover the fluid source or point of entry of the lubricant, and hence its leakage from the ends of the bearings, will be explicitly taken into account. In this manner the essential difficulties of the negative pressures encountered in the Sommerfeld theory can be elucidated and therefore confidence restored in the fundamental validity of the hydrodynamic picture of lubrication. As will be shown in a later paper, the methods used here can also be applied to partial bearing problems, and thus has some degree of generality in spite of its inherent limitation as a successive approximation theory.

Analytical Theory

The analytical theory to be developed here will be explicitly based upon the Reynolds approximation. This is that the film thickness at every point between the journal and bearing is so small in comparison to the other dimensions of physical interest, in particular the journal radius r, that the viscous flow of the film may be approximated by that appropriate to a film between parallel plates. More explicitly, the contribution to the flow due to the pressure gradients is to be averaged over the thickness of the film in determining the pressure distribution in the film. Analytically these assumptions may be expressed by the relation that the vector velocity $\bar{v}$ in the film due to the pressure gradients is given by

$$\bar{v}=(h^2/12\mu)\nabla p, \tag{1}$$

where both $\bar{v}$ and the fluid pressure p are to be averaged over the film thickness, h, and μ is the bulk viscosity of the film. If U is the surface velocity of the journal, the dragging or pumping effect due to this rotation will clearly be $Uh/2$. Applying the equation of continuity to the film of lubricant, we then get at once:

$$\nabla\cdot\left(\frac{h^3}{12\mu}\nabla p\right)=\frac{U}{2r}\frac{\partial h}{\partial\theta}, \tag{2}$$

where θ is the azimuthal angle in the direction of rotation (cf. Fig. 2), and it is supposed that the journal and bearing have parallel axes, so that h varies only with θ.

Equation (2) is the fundamental Reynolds equation underlying the so-called hydrodynamic theory of the lubrication of journal bearings. Before, however, it can be used one must specify

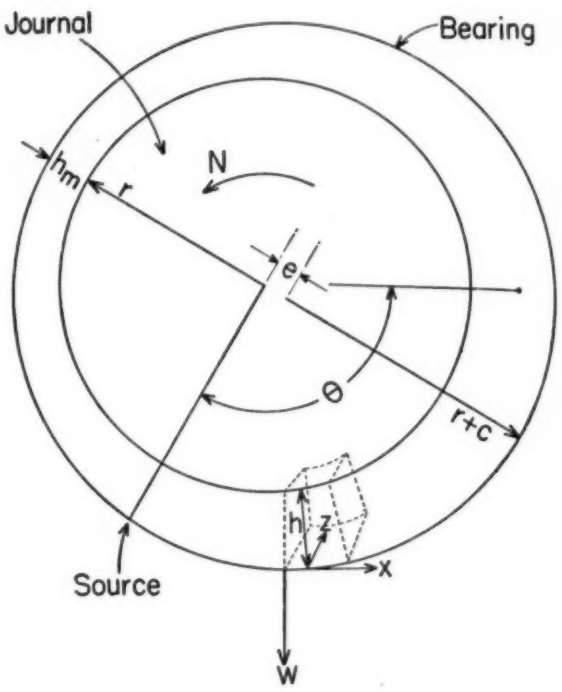

Fig. 2.

the particular geometrical and physical conditions appropriate to the specific lubrication system of interest. For the case of a practical journal bearing, where the film thickness or radial clearance between the cylindrical journal and bearing is very small compared to the journal radius, the film thickness h as a function of θ is given to a high degree of approximation by the equation

$$h=c+e\sin\theta, \tag{3}$$

where c is the radial clearance or difference between the radii of the bearing and journal, and e is the displacement between the axes of the journal and bearing (cf. Fig. 2). θ has been so chosen that $\theta=0$ is along the diameter where $h=c$.

Introducing now the notation

$$\eta=e/c; \qquad w=z/r; \qquad \beta=6\mu Ur/c^2, \tag{4}$$

where z is the coordinate along the journal bearing axis, and assuming that the viscosity μ is the same everywhere throughout the film,

Eq. (2) may be finally given the dimensionless[19] form

$$\frac{\partial}{\partial\theta}\left\{(1+\eta\sin\theta)^3\frac{\partial p}{\partial\theta}\right\}+(1+\eta\sin\theta)^3\frac{\partial^2 p}{\partial w^2}=\beta\eta\cos\theta. \quad (5)$$

Equation (5) may be considered as the generalized Reynolds equation governing the lubrication of journal bearings with small clearances. Upon dropping the second term on the left it reduces to that appropriate to the infinitely long bearing, which was solved by an approximation method by Reynolds and in closed form by Sommerfeld, the origin for θ in the latter work having been chosen at the point of maximum film thickness.

For the case of the infinitely long bearing Eq. (5) evidently becomes an ordinary differential equation, and the pressure distribution $p(\theta)$ can be derived immediately by quadratures. For the finite bearing, however, the equation is a second-order partial differential equation, and although the inhomogeneity can be removed by subtracting off the Sommerfeld solution from p, the solution of the homogeneous equation still presents great difficulties. Formal solutions can indeed be constructed by the method of separation of variables. However, the equations defining the functions of θ, while apparently belonging to the generalized Lamé equations, have parameters differing from those characterizing the standard Lamé solutions. While the derivation of the properties of these functions does not in itself offer insurmountable difficulties, their treatment in sufficient completeness to provide numerical solutions for the practical lubrication problem might well involve many months if not years of effort. For the present, therefore, this method of attack does not seem particularly promising.[20]

We are therefore forced to sacrifice elegance and mathematical neatness and attack the problem by approximation methods. The particular scheme to be developed here will be based upon the assumption that the eccentricity of the journal bearing η is small, and expand the solutions in powers of η. This will obviously limit the range of numerical validity of the solutions. However, it should give the asymptotic behavior of the system for smaller values of η, and hence large values of lubricant viscosity, journal speeds, or low values of bearing loads. As a satisfactory knowledge of the situation under even these restricted conditions is not now available, the present method should provide at least a start in the solution of the general problem. We therefore suppose formally that the pressure distribution $p(\theta, w)$ may be expanded[21] in the form

$$p(\theta, w)=\Sigma\eta^m p_m(\theta, w). \quad (6)$$

Putting this into Eq. (5), and equating the coefficients of like powers of η, we find the series of equations for p_m given by

$$\left.\begin{aligned}
&\nabla^2 p_0=0=\partial^2 p_0/\partial\theta^2+\partial^2 p_0/\partial w^2,\\
&\nabla^2 p_1=-3\cos\theta(\partial p_0/\partial\theta)+\beta\cos\theta,\\
&\nabla^2 p_2=-3\sin\theta\nabla^2 p_1-3\cos\theta(\partial p_1/\partial\theta)\\
&\qquad\qquad -6\sin\theta\cos\theta(\partial p_0/\partial\theta),\\
&\cdots\cdots\cdots\cdots\cdots\cdots\\
&\nabla^2 p_m=-3(\sin\theta\nabla^2 p_{m-1}+\cos\theta(\partial p_{m-1}/\partial\theta))\\
&\qquad -3\sin\theta(\sin\theta\nabla^2 p_{m-2}+2\cos\theta(\partial p_{m-2}/\partial\theta))\\
&\qquad -\sin^2\theta(\sin\theta\nabla^2 p_{m-3}+3\cos\theta(\partial p_{m-3}/\partial\theta)).
\end{aligned}\right\} \quad (7)$$

We thus see that formally the solution of Eq. (5) has been reduced to that of a series of equations of a known type, namely, the Poisson equations. Before attempting to solve them one must now define more explicitly the nature of the physical problem. Here we shall suppose that the bearing is a "full" journal bearing,

[19] Strictly speaking, one should divide through Eq. (5) by a unit pressure so as to make p and β also dimensionless. Since, however, we shall measure p in terms of atmospheres the unit pressure need not be introduced explicitly.

[20] It seems likely that these same arguments led both Sommerfeld and Michell to drop the problem. They both mention in their papers that they did not succeed in obtaining useful solutions for the finite bearing problem, and it is extremely doubtful if mere analytical complications would have discouraged either of them.

[21] Essentially the same type of expansion was made by Reynolds in the solution of the infinitely long bearing, although the expansions were actually carried out in the evaluation of the indefinite integrals giving $p(\theta)$. However, as Sommerfeld showed, these expansions were unnecessary for the infinite bearing as the integrals could be integrated in finite and closed form.

that is of 360° arc. Its dimensionless half-length will be taken as w_0. In order to simplify somewhat the present analysis it will be supposed that w_0 is of the order of or greater than π, which corresponds to a real bearing length of the order of or greater than the bearing perimeter.

It will also be supposed for convenience that the source of the lubricant of "strength" q, will be situated perpendicular to the diameter passing through the minimum and maximum film thicknesses (cf. Fig. 2). In a practical system the fluid source will most likely be placed in the bearing at a position fixed with respect to the vertical, so that its angle with the diameter passing through the minimum and maximum film thicknesses will vary with the speed, load, or fluid viscosity. This more general case, however, will be treated later, the simpler and somewhat artificial case chosen here sufficing nevertheless to indicate the general features of the solution. On the other hand, it is to be emphasized that this fluid source is a very important element of the problem. For without it the leakage of lubricant from the ends of the bearing would quickly deplete the lubricant, and with it the load carrying power of the film.

In addition to the above specifications for the solution one must require that the pressure distribution function $p(\theta\, w)$ reduces to the atmospheric value at the ends of the bearing $w=\pm w_0$, and that, together with $\partial p/\partial\theta$ it reproduces itself as θ makes the circuit of 2π around the circumference of the bearing. Finally, since the origin and source will be set midway between ends of the bearing, the solutions will have to be even in w.

Proceeding now to the solutions of these equations we find for the zeroth approximation:

Zeroth approximation

$$p_0=1-q\log\frac{\cosh w-\cos\theta}{\cosh w_0}, \tag{8}$$

where the flux strength q may be expressed in terms of the actual inflow Q through the source, and hence leakage from the ends of the bearing, by

$$q=3\mu Q/\pi c^3. \tag{8a}$$

It will be noted that Eq. (8) is a solution of Laplace's equation, represents a source at (0, 0), is even in w, is periodic in θ, and that $\partial p_0/\partial\theta$ is periodic in θ. At the ends of the bearing, $w=\pm w_0$, p_0 is not strictly uniform. Its variations from the value 1 are of the order of e^{-w_0}. However, by our previous assumption that the bearing is relatively long, terms of this order will be dropped throughout the present analysis. A higher degree of constancy of p_0 and the subsequent solutions at $w=\pm w_0$ could be readily obtained by adding on image terms of the true source, or by expanding p_0 and correcting for the terms that do not vanish at $w=\pm w_0$, and a strict uniformity could be achieved by adding on a Fourier series solution of Laplace's equation which would exactly cancel off the variations in p_0 and the subsequent solutions at $w=\pm w_0$. However, such correction terms need not be introduced unless one is explicitly considering bearings of relatively short length.

Although as already mentioned, the source term in Eq. (8) really represents a fundamental element of the solution of the bearing of finite length in contrast to that of infinite length, it must be introduced only in the case of the full journal bearing. For partial bearings the end leakage may be supplied by the excess of lubricant dragged into the bearing at its leading edge over that driven out at its trailing edge. The analysis for this case will also be reserved for a later paper.

First approximation

Combining Eq. (8) with the second of Eqs. (7), we see that the first-order pressure p_1 must satisfy the equation

$$\nabla^2 p_1=\beta\cos\theta+\frac{3q\sin\theta\cos\theta}{\cosh w-\cos\theta}. \tag{9}$$

Its solution may be shown to be

$$p_1=\beta\cos\theta\left(\frac{\cosh w}{\cosh w_0}-1\right)+3q\left[\sin\theta+\sin\frac{\theta}{2}\cosh\frac{w}{2}\log\frac{\cosh(w/2)-\cos(\theta/2)}{\cosh(w/2)+\cos(\theta/2)}\right]. \tag{10}$$

It will be easily verified that p_1 is free of singularities, is even in w, periodic in θ, and that $\partial p_1/\partial\theta$ is also periodic in θ. Since p_0 already reduces to the value 1 at $w=\pm w_0$, to the order of e^{-w_0}, p_1 has been adjusted so that it equals 0 at $w=\pm w_0$, to the order of e^{-w_0}.

It may be noted that whereas the effect of the source enters already into the zeroth approximation, the effect due to the rotation of the journal, represented by the term β, enters first in the first approximation.

Second approximation

Putting now the above values of p_0 and p_1 into the third of Eqs. (7), one finds a rather lengthy equation for p_2, namely,

$$\left.\begin{aligned}\nabla^2 p_2 = -3\beta \sin 2\theta\left(1-\frac{\cosh w}{2\cosh w_0}\right)-\frac{9}{2}q\cos\theta-9q\cos^2\theta-\frac{3q\cos\theta(3/2+\sin^2\theta-3/2\cosh w\cos\theta)}{\cosh w-\cos\theta}\\ -\frac{9}{2}q\cos\theta\cos\frac{\theta}{2}\cosh\frac{w}{2}\log\frac{\cosh(w/2)-\cos(\theta/2)}{\cosh(w/2)+\cos(\theta/2)}.\end{aligned}\right\}\tag{11}$$

It may be verified that a formal solution of this equation is given by

$$\left.\begin{aligned}p_{20}=\frac{\beta}{2}\sin 2\theta\left(\frac{3}{2}-\frac{\cosh w}{\cosh w_0}\right)+\frac{9}{4}q\cos\theta+\frac{3}{2}q\cos 2\theta-\frac{3}{4}qw\sinh w\cos\theta\\ +\frac{3}{4}q(\cos\theta\cosh w-1)\log\frac{\cosh w-\cos\theta}{\cosh w_0}-\frac{9}{8}q\Big(2\sin\theta\sin\frac{\theta}{2}\cosh\frac{w}{2}\\ +w\cos\frac{\theta}{2}\sinh\frac{w}{2}\Big)\log\frac{\cosh(w/2)-\cos(\theta/2)}{\cosh(w/2)+\cos(\theta/2)}-\frac{9}{4}qw\sin\frac{\theta}{2}\cosh\frac{w}{2}\tan^{-1}\frac{\sinh(w/2)}{\sin(\theta/2)}\\ -\frac{9}{8}q\sinh\frac{w}{2}\cos\frac{\theta}{2}\int_0^w\log\frac{\cosh(v/2)-\cos(\theta/2)}{\cosh(v/2)+\cos(\theta/2)}dv.\end{aligned}\right\}\tag{12}$$

This solution has the same values at $\theta=0$ and 2π, and is even in w. It has no singularities in the region of physical interest. However, it does not vanish at $w=w_0$, nor does its first derivative with respect to θ repeat at $\theta=0$ and 2π. Now

$$\int_0^w\log\frac{\cosh(v/2)-\cos(\theta/2)}{\cosh(v/2)+\cos(\theta/2)}dv=\pi(\theta-\pi)+8\sum_0^\infty\frac{\cos(2n+1)(\theta/2)e^{-(2n+1)|w|/2}}{(2n+1)^2},\tag{13}$$

where the right side is to be preceded by a minus sign if $w<0$. It therefore follows that at $w=w_0$, p_{20} has the value

$$\left.\begin{aligned}p_{20}=\frac{\beta}{4}\sin 2\theta-\frac{3}{2}q+\frac{9}{4}qw_0-\frac{3}{4}qw_0\sinh w_0\cos\theta-\frac{9}{8}\pi qw_0\cosh\frac{w_0}{2}\sin\frac{\theta}{2}\\ -\frac{9}{8}\pi q(\theta-\pi)\sinh\frac{w_0}{2}\cos\frac{\theta}{2}+0(e^{-w_0}).\end{aligned}\right\}\tag{14}$$

This may be canceled to the order of e^{-w_0} by adding on the harmonic function:

$$p_{21}=-\frac{\beta}{4}\frac{\sin 2\theta\cosh 2w}{\cosh 2w_0}+\frac{3}{4}w_0 q\tanh w_0\cos\theta\cosh w+\frac{3}{2}q-\frac{9}{4}qw_0 \\ +\frac{9\pi q}{8}\tanh\frac{w_0}{2}\left\{(\theta-\pi)\cos\frac{\theta}{2}\cosh\frac{w}{2}+w\sin\frac{\theta}{2}\sinh\frac{w}{2}\right\}. \tag{15}$$

There is still left the adjustment of p_{20} so that its derivative with respect to θ will be continuous at $\theta=0$. Thus it is readily found that whereas at $\theta=2\pi$,

$$\frac{\partial p_{20}}{\partial\theta}+\frac{\partial p_{21}}{\partial\theta}=\frac{\beta}{2}\left(3-2\frac{\cosh w}{\cosh w_0}-\frac{\cosh 2w}{\cosh 2w_0}\right)+\frac{9}{8}\pi q e^{-|w/2|}\left(\left|\frac{w}{2}\right|-1\right),$$

at $\theta=0$,

$$\frac{\partial p_{20}}{\partial\theta}+\frac{\partial p_{21}}{\partial\theta}=\frac{\beta}{2}\left(3-2\frac{\cosh w}{\cosh w_0}-\frac{\cosh 2w}{\cosh 2w_0}\right)-\frac{9}{8}\pi q e^{-|w/2|}\left(\left|\frac{w}{2}\right|-1\right).$$

To cancel the terms proportional to q one may add the Fourier series harmonic function given by

$$p_{22}=\sum_{\text{odd}}A_n\cos\frac{m\pi w}{2w_0}\cosh\frac{m\pi}{2w_0}(\theta-\pi), \tag{16}$$

where

$$A_n=\frac{\partial q w_0\sin m\pi/2}{\pi(m^2+w_0^2/\pi^2)\sinh m\pi^2/2w_0}\left[e^{-w_0/2}\left(1-\frac{w_0}{2}\right)-\frac{2e^{-w_0/2}(w_0^2/\pi^2)}{m^2+w_0^2/\pi^2}+\frac{2mw_0\sin m\pi/2}{\pi(m^2+w_0^2/\pi^2)}\right].$$

The final solution for p_2 satisfying all the physical conditions of the problem is now given by

$$p_2=p_{20}+p_{21}+p_{22}. \tag{17}$$

One could proceed in a similar manner to find the higher approximation terms. While the procedure for determining these higher order terms is quite straightforward, it hardly seems warranted at present to undertake the work involved. We shall therefore content ourselves with such values of the eccentricity η that the terms beyond p_2 will not contribute appreciably to the solutions.

Load carrying power of the film

While the most satisfactory tests of the hydrodynamic theory would perhaps lie in a comparison of the theoretically predicted pressure distributions within the fluid film and those observed experimentally, it is far simpler and more direct to base the comparison upon the integrated properties of the system, such as the load carrying power of the film and the friction it exerts upon the moving surfaces. We shall therefore proceed to the study of these features of the problem, and in particular to the calculation of the friction coefficient curves of the type shown in Fig. 1 for the infinitely long bearing. As the analysis involved is nothing more than a routine application of the integral calculus, we shall simply state the results. Thus we find for the dimensionless load components that can be supported by the film lubricant[22] the following quantities:

$$\int_{-w_0}^{w_0}dw\int_0^{2\pi}p_0\sin\theta d\theta=0,\quad \int_{-w_0}^{w_0}dw\int_0^{2\pi}p_1\sin\theta d\theta=-\pi q[3-4e^{-w_0}+e^{-2w_0}], \\ \int_{-w_0}^{w_0}dw\int_0^{2\pi}p_2\sin\theta d\theta=0, \tag{18}$$

[22] Strictly speaking, there will be additional load components contributed by the surface tractions on the journal and bearing surfaces. However, as these will be of the order of c/r smaller than those due to the fluid pressures, they may be safely neglected in the discussion of practical journal bearing systems.

$$\left.\begin{aligned}
&\int_{-w_0}^{w_0} dw \int_0^{2\pi} p_0 \cos\theta d\theta = 4\pi q(1-e^{-w_0}), \quad \int_{-w_0}^{w_0} dw \int_0^{2\pi} p_1 \cos\theta d\theta = 2\pi\beta(\tanh w_0 - w_0), \\
&\int_{-w_0}^{w_0} dw \int_0^{2\pi} p_2 \cos\theta d\theta = -2\pi q + 2\pi q e^{-w_0/2}(4-3w_0) + 6\pi q e^{-w_0/2}(1-w_0/2)(2\tanh(w_0/2) - \tanh w_0) \\
&\qquad - \frac{288 q e^{-w_0/2} w_0^5}{\pi^5} \sum_{\text{odd}} \frac{1}{(m^2 + w_0^2/\pi^2)^2 (m^2 + 4w_0^2/\pi^2)} \\
&\qquad + \frac{288 q w_0^4}{\pi^4} \sum_{\text{odd}} \frac{m \sin m\pi/2}{(m^2 + w_0^2/\pi^2)^2 (m^2 + 4w_0^2/\pi^2)} + 0(e^{-w_0}).
\end{aligned}\right\} \quad (19)$$

To the order of η^3 and e^{-w_0} the resultant dimensionless load carrying components of the film are:

(a) The component parallel to the diameter through the maximum and minimum film thicknesses:

$$P_p = \int_{-w_0}^{w_0} dw \int_0^{2\pi} p \sin\theta d\theta = -3\pi q\eta. \quad (20)$$

(b) The component normal to the diameter through the minimum and maximum film thicknesses:

$$-P_n = \int_{-w_0}^{w_0} dw \int_0^{2\pi} p \cos\theta d\theta = 4\pi q - 2\pi\beta\eta(w_0 - \tanh w_0) + \eta^2 q[-2\pi + 2\pi e^{-w_0/2}(4-3w_0) + A], \quad (21)$$

where A denotes the last three lines in Eq. (19) divided by q.

We now introduce the following dimensionless quantities:

$$S = \frac{r^2}{c^2}\frac{\mu N}{P}; \quad \bar{q} = \frac{q}{(P_p^2 + P_n^2)^{\frac{1}{2}}} = \frac{qr^2}{W}; \quad \bar{w} = w_0/\pi, \quad (22)$$

where N is the journal speed in r.p.s., P is the load per unit projected area, and W is the total load supported by the film. S is what has been previously termed the "Sommerfeld variable;" $\bar{q}$ is the dimensionless flux, which is proportional to the strength of the fluid source per unit load pressure, and $\bar{w}$ is the dimensionless length of the bearing which expresses the length in units of the bearing perimeter. Recalling the definition of β in Eq. (1), we find in terms of the above notation that: $\beta = 3S(P_p^2 + P_n^2)^{\frac{1}{2}}/\bar{w}$.

Applying now the physical requirement that the total load carrying power of the film is the load which it actually must support, that is,

$$W^2 = (P_p^2 + P_n^2)r^4, \quad (23)$$

and inserting for the right side the expressions given in Eqs. (20) and (21), we obtain on dividing through by W an equation in the dimensionless quantities $\bar{q}$, S, and $\bar{w}$ which, when solved for S, takes the form

$$S = \frac{(1-\eta^2\bar{q}^2(P_p/\eta q)^2)^{\frac{1}{2}} + 4\pi\bar{q} + \eta^2\bar{q}\{-2\pi + 2\pi e^{-\pi\bar{w}/2}(4-3\pi\bar{w}) + A\}}{6\pi\eta(\pi\bar{w} - \tanh\pi\bar{w})/\bar{w}} \quad (24)$$

Choosing the bearing length $\bar{w}$, the dimensionless leakage $\bar{q}$, and the eccentricity η, this relation gives the value of the Sommerfeld variable under which such conditions of flow can be obtained. Several curves of η *vs.* S calculated by this equation are given in Fig. 3. Before proceeding now to the ultimate calculation of the friction coefficient as a function of S, we shall digress and derive a general formula relating these quantities.

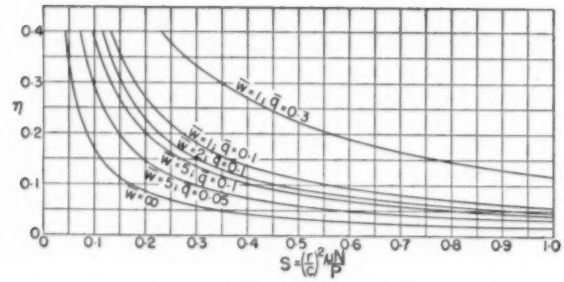

FIG. 3. Theoretical variation of journal eccentricity, η, with the Sommerfeld variable S. $\bar{w}$ = (bearing length)/(bearing perimeter). $\bar{q}$ = dimensionless source strength.

A General Formula for the Friction Coefficient in Journal Bearings

The connecting link between the frictional forces in a lubricating film and the surface speeds and pressure gradients lies in the well-established relations that the surface traction on the bearing along the direction θ is given by

$$\sigma_j = \mu U/h + (h/2r)(\partial p/\partial\theta), \tag{25}$$

while that on the bearing is

$$\sigma_b = \mu U/h - (h/2r)(\partial p/\partial\theta). \tag{26}$$

The general procedure used heretofore, since the time of Sommerfeld, in obtaining the frictional forces and ultimately the coefficient of friction has been to write out explicitly the values of the right sides of Eqs. (25) and (26), after finding the pressure distributions, and then integrating over the journal or bearing surfaces. Such a procedure thus involves additional integrations of the same type that is required for the determination of the load components. Moreover it gives no indication of the nature of the frictional forces until the pressure distributions have been explicitly determined.

If, however, the integrations of the second terms are carried out only formally, one obtains immediately general formulas for the friction forces and friction coefficient without the necessity for specifying in detail the complete solution for the pressure distributions. Thus for the case of the forces on the journal, we have for the total frictional force the value

$$F_j = r\int_0^L dz\int_\alpha^\gamma \sigma_j d\theta = r\mu U\int_0^L dz\int_\alpha^\gamma \frac{d\theta}{h} + \frac{1}{2}\int_0^L dz\int_\alpha^\gamma h\frac{\partial p}{\partial\theta}d\theta, \tag{27}$$

where the limits α to γ are used to indicate that this formula is valid for partial bearings of arc $\gamma-\alpha$ as well as for full journal bearings. As h is independent of z, the integration with respect to z of the first term simply gives L. In the case of the second term we integrate by parts, and note that if the bearing is a full journal bearing both h and p will return to the same value at the limits α, γ, which will then be zero and 2π, whereas for the case of the partial bearing p vanishes at both α and γ, since p represents the excess over atmospheric. In any case, therefore, the integrated term drops out, and recalling the definition of h in Eq. (3), one has

$$F_j = \frac{r\mu UL}{c}\int_\alpha^\gamma \frac{d\theta}{1+\eta\sin\theta} - \frac{c\eta}{2}\int_0^L dz\int_\alpha^\gamma p\cos\theta d\theta. \tag{28}$$

We now observe that the second integral, when multiplied by r, simply represents the negative of the total load component W_n normal to the diameter which passes through the minimum and maximum film thicknesses.

Now the coefficient of friction is defined as the ratio of the total frictional force to the total load. Denoting the friction coefficient by f, and the total load by W, and multiplying through both sides of Eq. (28) by r/c, we obtain

$$\frac{r}{c}f_j = \frac{\eta}{2}\frac{W_n}{W} + \frac{\mu r^2 UL}{c^2 W}\int_\alpha^\gamma \frac{d\theta}{1+\eta\sin\theta}. \tag{29}$$

Introducing finally the angle Φ between the resultant load and the normal to the diameter passing through the minimum and maximum film thicknesses, and the geometrical factor δ which depends upon the extent of the bearing arc and is defined by

$$W = rLP\delta, \tag{30}$$

where P is the load per unit projected area, and recalling the definition of the Sommerfeld variable S, the general formula is obtained that

$$\frac{r}{c}f_j = \frac{\eta}{2}\cos\Phi + \frac{2\pi S}{\delta}\int_\alpha^\gamma \frac{d\theta}{1+\eta\sin\theta}. \tag{31}$$

Similarly for the friction coefficient for the bearing,

$$\frac{r}{c}f_b=\frac{-\eta}{2}\cos\Phi+\frac{2\pi S}{\delta}\int_\alpha^\gamma\frac{d\theta}{1+\eta\sin\theta}. \quad (32)$$

These formulas do not, of course, permit an immediate calculation of the friction coefficients simply from a knowledge of the Sommerfeld variable S. However, they do suffice to bring out some very general properties of the friction coefficient. Thus, first, they are valid for bearings of finite length as well as those of infinite length. Secondly, they are valid both for partial as well as full journal bearings. Third, they give immediately by subtraction the general relation that

$$(r/c)(f_j-f_b)=\eta\cos\Phi, \quad (33)$$

which has heretofore been established generally only by physical arguments, and mathematically only for the infinitely long bearing.

Finally these relations give at once the asymptotic behavior for the friction coefficients under all conditions. For as S is increased the eccentricity η will approach zero, and the values of f_j and f_b will behave asymptotically according to the relations:

$$\frac{r}{c}f_j=\frac{r}{c}f_b=\frac{2\pi(\gamma-\alpha)S}{\delta}. \quad (34)$$

Again Eq. (34) holds for bearings of finite length as well as for infinitely long bearings. It states that for all types of journal bearings the friction coefficient *vs.* S curve will asymptotically approach a straight line passing through the origin and of a slope determined only by the length of the bearing arc but independent of the bearing length. In particular, for the full journal bearing where $\gamma-\alpha=2\pi$ and $\delta=2$, the slope of the asymptotic straight line is $2\pi^2$, as in the original Sommerfeld theory, while for general values of S and η:

$$\frac{r}{c}f_j=\frac{\eta}{2}\cos\Phi+\frac{2\pi^2 S}{(1-\eta^2)^{\frac{1}{2}}}. \quad (35)$$

For the partial bearing of 180° arc the asymptotic slope will be π^2. For other partial bearings the slope can be obtained by elementary geometrical reasoning.

The final friction calculations were made by means of Eq. (35), after having determined S as a function of η, $\bar{q}$ and $\bar{w}$ by means of Eq. (24). Typical results are shown graphically in Figs. 4 and 5.

Discussion

Before discussing in detail the results of the above developments, it is well to note explicitly that the journal bearing system under consideration corresponds to that shown in Fig. 2. Physically it represents either the case of a bearing floating on the journal with the lubricant inlet at the underside of the bearing, or, if one supposes it to be turned by 180°, it corresponds to a journal supported by the bearing with the lubricant inlet in the upper half of the bearing. As the former situation is that which has obtained in our first experimental studies of the problem, which will be reported in a following paper, we shall base our discussion upon it. Nothing, of course, is implied as to whether or not such a system is good or bad from the point of view of practical lubrication. Moreover the specific theoretical calculations reported here refer to the more artificial case where the lubricant inlet is always kept at 90° with respect to the journal diameter passing through the minimum and maximum film thicknesses. An attempt is being made to generalize this phase of the theory so as to permit a study of cases where the lubricant inlet position is kept fixed with respect to the vertical, and if successful it will be reported on later.

With the system of Fig. 2 in mind, one may begin the interpretation of the results. In particular, it is convenient to visualize the fluid dynamics of the system as follows: Thus the mere rotation of the journal in the bearing may be considered to have an effect even in the finite length bearing essentially equivalent to that in the infinitely long bearing of the Sommerfeld case. This effect is a resultant bearing-supporting pressure acting normal to the diameter passing through the minimum and maximum film thicknesses, and increasing in magnitude as the journal eccentricity increases. It is represented by the terms proportional to β in the pressure distributions of the above analysis, and in the

load component of Eq. (21). The effects of the lubricant source are essentially superposed on those of the journal rotation. These consist, first, of a force parallel to that due to the latter, but

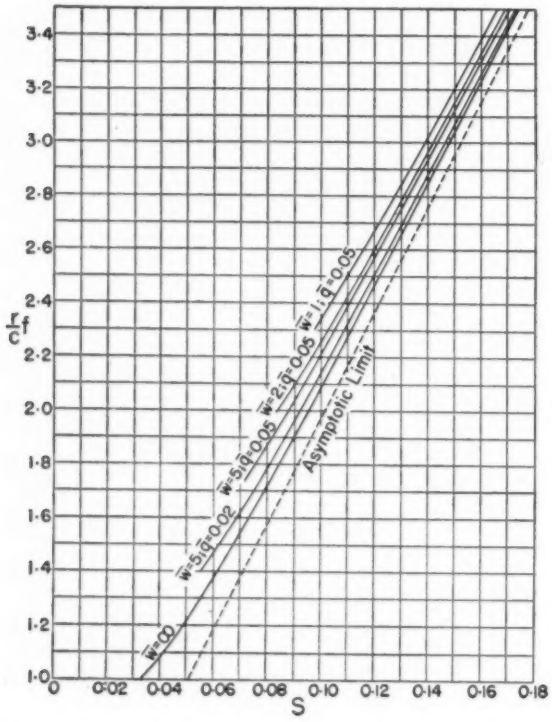

FIG. 4. Theoretical variation of friction coefficient on journal for low values of S. Notation as in Fig. 3.

oppositely directed so as to give a journal-supporting or bearing-depressing force, which corresponds to a concentric journal bearing system. Secondly, there is a force parallel to the diameter through the minimum and maximum film thicknesses, and which arises from the eccentricity of the journal in the bearing. The former is represented by the term $4\pi q$ in Eq. (21), and the latter by the value of P_p in Eq. (20). The existence of the second-order terms in Eq. (21) shows that this resolution is not rigorous, but as our theory anyway relates only to rather small eccentricities it will suffice for our present purposes.

With this picture in mind one can understand the qualitative features of the analytical results. Thus, in the case of Fig. 3, the fact that the bearings of finite length for a fixed value of S will have greater eccentricities than the infinitely long bearing follows from the necessity of counterbalancing the bearing depressing tendencies due to the source by greater bearing supporting effects of the rotation when the eccentricity is increased. Or conversely, a fixed eccentricity will correspond to a smaller resultant load carrying capacity of the film, and hence larger values of S in the case of the finite length bearing than for the infinitely long bearing. An immediate corollary of this explains why the curves for smaller $\bar{w}$ lie higher than those for larger $\bar{w}$, for the same $\bar{q}$, since in the shorter bearings the relative effects of the source should be higher than in the longer bearings. Likewise for a bearing of fixed length it is also natural from the above point of view that the higher source strength should lead to higher eccentricities than smaller source strengths, as the relative positions for the curves of fixed $\bar{w}$ and varying $\bar{q}$ directly verify.

The curves of Fig. 3 give a quantitative evaluation of another physical effect, namely, that on the relative load carrying capacities of finite and infinite journal bearings for given eccentricities, fixed speeds, and lubricants. For with the latter quantities kept constant, the load carrying capacities of the journal bearings are inversely proportional to the values of S in Fig. 3. Thus we find that for $\eta=0.2$ the load carrying capacity of a bearing with $\bar{w}=2$ and $\bar{q}=0.1$, is only 37 percent of that which an infinitely long bearing would have, and if the bearing length $\bar{w}=1$, with $\bar{q}=0.1$, the load carrying capacity is only 31 percent. Finally, if the value of $\bar{q}$ is tripled for the bearing length $\bar{w}=1$ the load carrying capacity is still further reduced to 15 percent. These effects are fundamentally due to the falling off of the pressure to atmospheric at the ends of the bearing when it is of finite length. However, there is superposed the effect of the source which accentuates this behavior by opposing the normal bearing supporting pressure distribution due to the journal rotation.[23]

With regard to the final values of the friction coefficient, it is now a simple matter to anticipate the results. For due to the higher eccentricities

[23] Of course, this opposing effect due to the fluid source depends on its assumed position in the lower half of the film. If the source were set in the upper or high pressure portion of the film, the normal component of the forces due to the source will *aid* the bearing-supporting forces resulting from the journal rotation.

that must be associated with a given value of S for the finite length bearing, it is to be expected that the friction forces and hence coefficient of friction will be higher than for the infinitely long bearing. Such is indeed the effect shown in Fig. 4, the relative positions of the curves corresponding to the associated values of η such as shown for analogous cases in Fig. 3. The general variation of the friction coefficient with η for fixed S will be seen from Eq. (35), from which it follows that the friction coefficient will increase as η increases, except possibly in the thin film region where the tendency of $\cos \Phi$ to decrease with increasing η might counterbalance the growth of the second term.

Although no great significance should be attached to the numerical values shown in Fig. 4 except for the specific cases for which they have been derived, they are of significance from a qualitative point of view. For they do show that even the hydrodynamic theory does not require that the friction coefficient be a function only of the Sommerfeld variable as has been generally supposed. On the contrary, it depends also upon the dimensionless lubricant flow $\bar{q}$, and even moderate values of $\bar{q}$ will change the friction coefficient by as much as 10 percent for the smaller values of S. While it is not inconceivable that for low values of S the effect of $\bar{q}$ may become of the same order or even exceed the straight rotational or Sommerfeld friction terms and thus lead to rather marked rises in the friction coefficient curve at very low values of S, these effects are not to be confused with the ordinary thin film phenomena and the previously mentioned oiliness property. Rather they are simply hydrodynamic effects resulting from the distortion of the flow of lubricant in the film due to the presence of the source and finiteness of the bearing length.

The order of magnitude of $\bar{q}$ in practical systems may be estimated by assuming specific values for the physical constants involved. Thus choosing $c=0.003$ cm, $r=3$ cm, $\mu=10$ centipoise, and $W=25$ kg, it is found that $\bar{q}=0.2$ corresponds to a rate of lubricant inflow or end leakage of 9.2 cc/min. In many bearings the actual rate of flow is considerably larger than this, but the loads supported by the bearings are also larger, so that the value of $\bar{q}$ may still remain of the order of 0.2.

The actual pressure required to force the quantity of lubricant q through the bearing is essentially given by

$$\Delta p = q \log (2 \cosh w_0/\rho^2) = q(w_0 - 2 \log \rho), \quad (36)$$

where ρ is the radius of the inlet opening in the bearing surface divided by the journal radius. Thus for the above case, if the bearing length is equal to the bearing perimeter and the source radius is 0.3 mm, the feed pressure required to give $\bar{q}=0.2$ or a leakage of 9.2 cc/min. will be 6.8 atmospheres.

As already indicated, the effects of $\bar{q}$ and of the finiteness of the length of the bearing decrease as S increases or as the journal and bearing become more concentric. This is shown more clearly by the curves of Fig. 5 in which the scale for S is extended to 1.0, and the friction factors are plotted both for the infinitely long bearing of $\bar{q}=0$ and the bearing with $\bar{w}=1$ and

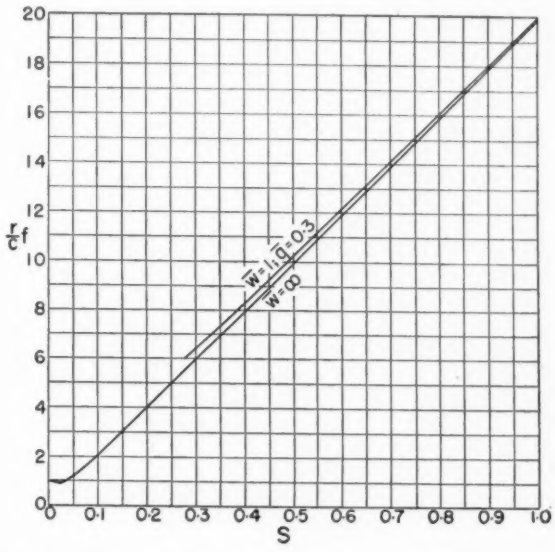

FIG. 5. Theoretical variation of friction coefficient on journal for larger values of S. Notation as in Fig. 3.

$\bar{q}=0.3$. It will be seen that by the time S reaches the value 1 the difference between the two curves becomes very small.

Returning to Fig. 4 it will be noted that the curves do not all extend to equally small values of S. There are two reasons for this. First, the seccessive approximation method used here does

not permit a study of the system for values of η that exceed 0.4, and as was seen in Fig. 3 the values of S giving such limiting values of η increase as $\bar{q}$ increases or $\bar{w}$ decreases. Secondly, the range of η is limited by the fact that the force component parallel to the diameter through the minimum and maximum film thicknesses which is induced by the journal eccentricity should never exceed the total load. This physical requirement is expressed mathematically by the appearance in Eq. (24) of the radical, which must always remain real. Recalling the value of P_p from Eq. (20) it follows that for a fixed $\bar{q}$ there is a maximum value of η which can be allowed. This effect also appears in the calculation of $\cos\Phi$ in Eq. (35), since the value of $\cos\Phi$ is simply the radical of Eq. (24), and uniformly decreases as η increases. Of course, this whole behavior arises from the fact that the source is assumed to lie always perpendicular to the diameter through the maximum and minimum film thicknesses. If this condition would be released the angle between the source and this diameter will change so as to limit the force components so as not to exceed the total load.

Another point of practical interest about the finite length bearing even for the special case treated here is that it indicates the solution to the long standing difficulty with the Sommerfeld theory of predicting negative pressures in the lubricating film. Thus according to the Sommerfeld theory the pressure distribution in the half below the diameter through the minimum and maximum film thicknesses in Fig. 2 is simply the negative reflection of that in the upper half. Even granting that a liquid could stand a certain degree of tension, the difficulty is not thereby removed, since the magnitude of the negative pressures according to the Sommerfeld theory will become arbitrarily large as the value of S decreases. In the theory developed here, however, it can be shown that these negative pressures which are induced by the rotation effect of the journal can be overcome by the pressure components due to the source of the lubricant. To avoid entering into a detailed study of the pressure distributions we shall simply focus our attention upon the pressure gradient at the ends of the bearing. Since the solutions have been deliberately adjusted to give atmospheric pressures at the ends, it is to be expected that if the pressure gradient is everywhere negative at the ends the pressure itself will exceed atmospheric everywhere in the interior. Moreover, the adjustment of the pressure gradients so as to be everywhere negative at the ends of the bearing will insure an outward flow of the lubricants all along the ends and thus exclude the possibility of a sucking of air into the film. This is perhaps of even greater significance from the point of view of avoiding a breakdown of the film than the mere question of the existence of negative pressures.

To show the nature of the situation as described by the above theory it will suffice to restrict ourselves to the first-order terms. To the order of e^{-w_0} it then follows that the axial gradient at the ends of the bearing is given by

$$\partial p/\partial w = -q+\beta\eta\cos\theta. \tag{37}$$

From this we see at once that in the lower half of the bearing the rotational effect tends to create positive pressure gradients, and hence would of itself induce the leakage of air into the film. The maximum effect will be at $\theta=0$. The condition for a resultant negative gradient at this azimuth will therefore become

$$-\bar{q}+3S\eta/\bar{w}<0, \tag{38}$$

after introducing the notation of Eq. (22).

Substituting the value of S as given by Eq. (24), and dropping the second-order terms, it is finally found that $\bar{q}$ must satisfy the relation

$$\bar{q}>\frac{1}{2\pi(\pi\bar{w}-\tanh\pi\bar{w}-2)}. \tag{39}$$

When $\bar{q}$ satisfies the inequality there will be no leakage of air into the bearing, whereas if it does not this tendency will not be overcome by the inflow of lubricant at the source. Eq. (39) is, of course, only an approximate relation from a numerical point of view. In particular, for the smaller values of $\bar{w}$ it will become unreliable and demand too high values of $\bar{q}$, because of the approximations made in the analysis with respect to $\bar{w}$, and the neglect of the terms of higher order in η. However, it does show that the source of lubricant definitely has a tendency to overcome the difficulties arising from the negative pressures

implied by the Sommerfeld theory and the associated gradients which would induce the sucking of air into the lubricating film. Here again the position of the lubricant inflow will be of importance. For if the source be placed in the high pressure part of the film its effectiveness in overcoming the Sommerfeld negative pressures will be very much diminished, even though such positions of the source will be more favorable from the point of view of reducing the friction coefficient.

The convergence of the approximation method used here may be most readily discussed from the point of view of the resultant load components. Since the second order terms in P_p automatically vanish, we shall consider only the P_n component. Here some elementary arithmetic considerations show that with respect to orders of magnitude, P_n may be approximated by the equation

$$-P_n/(P_n^2+P_p^2)^{\frac{1}{2}}=4\pi\bar{q}-50\eta S\pm 5\eta^2\bar{q}. \quad (40)$$

Recalling the relation between η and S as shown graphically in Fig. 3, it may then be verified that even for the maximum value $\eta=0.4$ used in this paper the ratio of the second order to the first order terms will be less than 0.04 for $\bar{q}$ not exceeding 0.1. For larger values of $\bar{q}$, the ratio will be larger. Yet unless $\bar{q}$ be made abnormally large, it is clear that the neglect of the third and higher order terms should lead to no great numerical errors in the deductions from the theory.

Finally, it should be noted that the theory developed here reduces in all cases to the Sommerfeld analysis, when the latter is expanded in powers of η, as $\bar{w}$ is made infinitely large and $\bar{q}$ is made vanishingly small. As should be expected, the transition to the infinitely long bearing problem can be made continuously from the finite bearing length case.

The authors are indebted to Mr. M. W. Meres of this laboratory for the numerical calculations reported in this paper, and to Dr. P. D. Foote, executive vice president of the Gulf Research & Development Company, for permission to publish it.

Film Lubrication of Finite Curved Surfaces*

SELBY M. SKINNER
University of Chicago, Chicago, Illinois
(Received March 10, 1938)

In treating film lubrication, Reynolds and Sommerfeld confined themselves to surfaces of infinite width, for mathematical reasons. Michell obtained the solution for a plane surface of finite width; the importance of this lies in the fact that leakage of lubricant through the lateral edges of a finite bearing reduces considerably the load supportable by the bearing. Solutions are obtained here for general cases of rectangular bearings with surfaces curved in both directions; for the Michell sector type of thrust bearing plate, in a case which allows consideration of the effect of the variation of film thickness with the radial distance from the center of rotation; and for the fitted finite journal bearing. General methods are exhibited suitable for handling other cases. In particular, the equations for the finite journal bearing in the general case are partially developed. Solutions for the journal bearing are shown to require laborious computation, so that an approximation to the film thickness is preferable; such an approximation, which can be handled relatively easily, is treated, and the solution obtained.

IN the course of a set of carefully planned and performed experiments reported in 1883,[1] Beauchamp Tower had drilled a hole for a lubricator in the brass of a journal bearing. To stop oil leakage, a temporary plug was placed in the hole. When the bearing was run again, pressure in the oil forced out the plug. Later work showed that pressures as great as double the mean load on the projected bearing surface were developed in the lubricant, and that integration of the measured lubricant pressures

* Presented in abstract (with the exception of Sections III and V) in Bull. Am. Phys. Soc. **12**, 7 (1937).
[1] Beauchamp Tower, Proc. Inst. Mech. Eng. (1883–5).

represented the total load on the bearing quite accurately.

Osborne Reynolds, examining these results, came to the conclusion that lubrication was a true hydrodynamic phenomenon. In his development of the hydrodynamic theory of lubrication,[2] he obtained Eq. (1)[3] for a thin lubricating layer between a moving and a fixed surface, whose radii of curvature are large compared with the thickness of the lubricating film.

$$\frac{\partial}{\partial x}\left(\frac{h^3}{6\mu}\frac{\partial p}{\partial x}\right)+\frac{\partial}{\partial y}\left(\frac{h^3}{6\mu}\frac{\partial p}{\partial y}\right)+\left(U\frac{\partial h}{\partial x}+V\frac{\partial h}{\partial y}\right)=0. \quad (1)$$

Here $p(x, y)$ is the pressure, $h(x, y)$ the thickness of the film, U, V, the speeds of the plate in the positive x and y direction, respectively, and μ the viscosity of the lubricant. A determination of the pressure distribution is the fundamental problem, since, when the pressure is known at all points, most of the quantities whose value is desired in practice may be computed; such quantities are: the total load which can be supported by the bearing, the center of pressure, the frictional resistance, the quantity of lubricant necessary, the shear stress on the lubricant, and, in a finite bearing, the quantity of lubricant escaping by way of the lateral edges.

Since the lubricant adheres to both surfaces, it is dragged into the space between them; if this is converging, more lubricant will be dragged in than will escape at the exit end until there is built up a pressure sufficient to prevent this; it is this pressure, acting upon the upper surface, which supports the load. With a converging film the metal surfaces do not touch, friction is greatly reduced, and wear of the bearing takes place more slowly. The thickness of the narrowest portion of the film must be great enough to allow small particles of impurities such as metal dust to pass through without touching the metal; therefore h will never be zero. Bearings of this type were used by Kingsbury and his coworkers in America in 1899.[4]

In 1904, Sommerfeld[5] made an important extension of Reynolds' results in several directions, particularly to journal bearings. Like Reynolds, he considered only cases in which the upper surface was of infinite width ($\partial p/\partial y=0$) thus gaining mathematical simplicity. First to consider a surface of finite width was Michell.[6] His investigations led to the independent invention of the type of bearing used by Kingsbury, and in view of his later work with certain applications of the bearing, one type is now called the Michell thrust bearing. Michell considered the plane bearing of finite width, in linear motion at a constant speed, defined by $h=cx$, $V=0$, and the boundary conditions, $p=0$ at $x=a$, b, and at $y=0$, π. His solution is discussed at length by Boswall[7] and rederived for an arbitrary width. Michell nowehere states that his is the only solvable case, but Boswall says,[8] "The exact mathematical solution of Reynolds' equation is, as shown by Michell, only possible if the viscosity is assumed constant and . . . the film thickness . . . a linear function of the variable." No exact treatment of this problem except when these two assumptions hold has appeared in the literature.[9] Rayleigh has considered the effects of departure from linearity for bearings of infinite width.[10]

A plane bearing is pivoted so as to be able to take up the angle to which it naturally adjusts itself. Sometimes the pivot is eliminated and the surface ground down to present a plane or curved wedge-shaped volume to the lubricant. The pivoted shoe does not need to be plane. In either case, the question arises, what is the effect of

---

[2] Osborne Reynolds, Phil. Trans. Roy. Soc. **177**, 157 (1886); also in *Collected Papers*.

[3] A slight correction in the last term on the right, made by Michell, has been included.

[4] A. Kingsbury, Trans. A. S. M. E. **17**, 96 (1895–6). J. Am. Soc. Nav. Eng. **9**, 267 (1897). For a comprehensive history of the entire subject of lubrication, M. D. Hersey, *Theory of Lubrication* (John Wiley & Sons, N. Y.), may be consulted.

[5] A. Sommerfeld, Zeits. f. Math. u. Phys. **50**, 97 (1904).

[6] A. G. M. Michell, Zeits. f. Math. u. Phys. **52**, 123 (1905).

[7] R. O. Boswall, *The Theory of Film Lubrication* (Longmans Green and Co., 1928), probably the most detailed existing treatment of "film" lubrication.

[8] Reference 7, p. 117. Similar statement, p. 111.

[9] Other treatments of the same case are: H. M. Martin, Engineering **100**, 101, 154, 196, 207 (1915); **109**, 233 (1920). Duffing, Zeits. f. angew. Math. u. Phys. **4**, 296 (1922). Kobayashi, Rep. 107, Aero. Res. Inst. Tokyo Imp. Univ. **8**, 385 (1934) (in Japanese).

[10] Rayleigh, Phil. Mag. **35**, 1 (1918). Also *Collected Papers*, Vol. 6, p. 523.

TABLE I.

$$\rho = \frac{\text{Width}}{\text{Length (in direction of motion)}}; \quad p_d = \frac{\text{Load}}{\text{Area}} \cdot \frac{K^2}{\mu U}; \quad h = Kx.$$

$\rho =$	∞ (a)	6(d)	5.2(c)	4(d)	π(c)	2(d)	1(b)	0.5(d)	0.33(b)	0.25(d)	0.10(b)	0(b)
$p_d =$	0.0506	.0458	.0442	.0433	.0404	.0353	.0213	.0089	.0046	.0028	.0004	0

From results of (a) Reynolds. (b) Michell. (c) Martin. (d) Approximate values by Duffing.

such curvature. More important than this is the fact that in cylindrical bearings of small angular length, the film thickness is so small that the conditions assumed here are fulfilled and the circular shaft may be considered resting on a film of lubricant whose thickness is:

$$h = cx^q = c(R\theta)^q \qquad \text{(A)}$$

where $q(\neq 1)$ is suitably chosen. The escape of lubricant which occurs at the lateral edges of bearings of finite width reduces greatly the supportable load; for example a comparison of results which have been computed for the plane bearing by various authors together with one which is easily computable from Michell's results yields Table I; p_d is the load supportable *per unit area* by the same bearing working under the same conditions of viscosity, speed, and *minimum and maximum film thickness* (max. h = twice min. h), but with varying width to length ratio. The first figure is the load supportable per unit area if the plate were part of an infinitely wide bearing (i.e., no leakage); the remainder refer to finite bearings.

In view of its many applications, therefore, a consideration of the effects of curvature in the three-dimensional case seems desirable. The method used may also be applied to cases other than rectangular curved plates; this will be done in two cases, namely the Michell thrust bearing sector plate, and the journal bearing. In both cases, certain solutions may be obtained which should be of value in practice.

General Considerations

Let us therefore examine Eq. (1). Consider first a plate moving parallel to one of its edges, and choose that direction for the x axis. Eq. (1) becomes

$$\frac{\partial}{\partial x}\left(\frac{h^3}{\mu}\frac{\partial p}{\partial x}\right) + \frac{\partial}{\partial y}\left(\frac{h^3}{\mu}\frac{\partial p}{\partial y}\right) = -6U\frac{\partial h}{\partial x}. \qquad (2)$$

Since the viscosity depends upon temperature and pressure, and frictional heat is produced in the lubricant, μ will depend upon x and y. The change of viscosity with temperature will depend upon the total amount of heat produced, and that carried away at each point in the film, and will probably most often be represented by an arbitrary function of x and y, such as one exponentially decreasing. The variation with pressure, which is often considered to be closely connected with the subject of "oiliness" may be easily handled. The increase of μ is usually of the general nature of an exponential function of the pressure. For example, Dow[11] presents values of μ for a wide range of pressures, for three temperatures, for each of three different lubricating oils; these data fit closely the general law

$$\mu = A + Be^{cp}.$$

Now in the derivation of (2), p has been assumed independent of z; under these conditions, if the function

$$\Phi = k - (1/cA)\log(B + Ae^{-cp}) \qquad \text{(2a)}$$

be considered, (2) becomes

$$\frac{\partial}{\partial x}\left(\frac{h^3}{6}\frac{\partial \Phi}{\partial x}\right) + \frac{\partial}{\partial y}\left(\frac{h^3}{6}\frac{\partial \Phi}{\partial y}\right) = -6U\frac{\partial h}{\partial x} \qquad \text{(2b)}$$

and the solution is the same as those given below, if p/μ be replaced by Φ. This will be considered further in the next article; here we merely notice that the effect in general is that, if with constant μ, the quantity p/μ would have the value K, then, if B is greater than, equal to, or

[11] R. B. Dow, J. App. Phys. **8**, 367 (1937).

less than 0, p will be less than, equal to or greater than KA and for small p, $p \sim K(B+A)$; the change,[12] while changing the calculated values, does not change significantly the trend of p. Accordingly in this paper, for convenience, μ will be taken to be constant, though the analysis is perfectly general in this regard, and the constancy is not required. A function Φ or one similar to Φ may be substituted in any of the formulas below, if the pressure change of viscosity is to be considered.

If the plates are parallel

$$\partial^2 p/\partial x^2 + \partial^2 p/dy^2 = 0$$

and the pressure can have neither an absolute maximum nor an absolute minimum within the film; everywhere under the plate, the pressure is that at the edges so that the plate is not supported. From Eq. (2) also, it is evident that a positive pressure will be built up in a film converging in the direction the lubricant is dragged by the lower surface.[13]

The boundary conditions that we consider require that the value of p be independent of y for certain definite values of x, and *vice versa*, so that a solution[14] of the form XY would be convenient. This is too much to expect, but any ordinary solution will be expressible as $\Sigma X_n Y_n$ where each product satisfies boundary conditions separately. Accordingly, we seek solutions of this type.

If the shape of the upper surface is such that

$$h = \xi(x)\eta(y) \tag{3a}$$

(ξ and η being in the physical case continuous and possessing continuous first derivatives) (2) may be written

$$\xi^{-3}(\xi^3 p_x)_x + \eta^{-3}(\eta^3 p_y)_y = -6\mu U \xi' \xi^{-3}\eta^{-2}; \tag{3}$$

subscripts denoting partial differentiation and primes total differentiation. Given two closed sets of orthogonal functions (satisfying the Sturm-Liouville equations below), $X_n(x)$, $Y_n(y)$, a solution may be found using either of the following procedures:

(*A*) $\xi^{-3}\xi'$ may be expanded as

$$\Sigma a_n X_n,^{15} \tag{4}$$

and p be set equal to

$$\Sigma X_n \cdot \theta_n(y),^{16} \tag{5}$$

with the result that

$$\sum_n \left[\xi^{-3}\frac{d}{dx}\left(\xi^3 \frac{dX_n}{dx}\right)\theta_n + \eta^{-3}\frac{d}{dy}\left(\eta^3 \frac{d\theta_n}{dy}\right)X_n + 6\mu U a_n \eta^{-2} X_n \right] = 0. \tag{6}$$

If the function X_n is such that the first term is $b_n X_n \theta_n$ for any n, it is merely necessary (since, the X_n, being orthogonal, are, of course, independent) to find solutions of

$$b_n\theta_n(y) + \eta^{-3}\frac{d}{dy}\left(\eta^3 \frac{d\theta_n}{dy}\right) = -6\mu U a_n \eta^{-2}. \tag{7}$$

Each of the latter will be the sum of a particular solution, and two independent solutions of the complementary equation, with constants adjusted to meet the boundary conditions. The functions X_n and θ_n both are solutions of a simple Sturm-Liouville equation, and by (5) yield the solution of (2).[17]

---

[12] When the effect of compressibility is taken into account, this does not hold. Moreover, temperature changes are still to be taken into account.

[13] For a maximum, $\partial p/\partial x = \partial p/\partial y = 0$, and $\partial^2 p/\partial x^2, \partial^2 p/\partial y^2 < 0$. The term on the right in (2) must therefore be negative.

[14] Physically it is obvious that a solution exists. This existence has been proved analytically for sufficiently restricted cases, i.e., of the type entering in the physical problem.

[15] Such expansion is justified if the function $\xi^{-3}\xi'$ is piecewise continuous with quadratically integrable first derivative, whether or not the function satisfies the boundary conditions. See, for example, Courant-Hilbert, *Methoden der Mathematischen Physik*, second edition, Vol. I, pp. 371–2. The representation is absolutely and uniformly convergent except at discontinuities where it converges in the mean and represents $\frac{1}{2}[f(x+0)+f(x-0)]$. This furnishes the justification, omitted by Michell, for his expansion of 1 as $\Sigma b_n \sin(ny)$.

[16] The validity of such expansions for p must be considered, since the series is to be differentiated term by term. It must be uniformly convergent, which in general requires proof. Proof is easily obtained in many simpler cases, among them those here developed, by considerations similar to those in Courant-Hilbert.

[17] Duffing (reference 9) has used what is equivalent to procedure *A*, to aid in a solution by approximation. He finds a particular solution, then expands the solution of the remaining homogeneous partial differential equation in a set of functions depending on x and y, respectively. The particular solution is then expanded in terms of the functions depending on x and added term by term to the latter solution. His particular solution is that for a plane bearing, but to approximate, in the next step, he neglects

(*B*) η^{-2} may be expanded as

$$\Sigma c_n Y_n(y) \tag{8a}$$

and p as

$$\Sigma F_n(x) \cdot Y_n, \tag{8b}$$

and the equation (3) becomes

$$\sum_n \left[\xi^{-3} \frac{d}{dx}\left(\xi^3 \frac{dF_n}{dx} \right) Y_n + \eta^{-3} \frac{d}{dy}\left(\eta^3 \frac{dY_n}{dy} \right) F_n \right. \\ \left. + 6\mu U c_n \xi^{-3} \xi' Y_n = 0, \right. \tag{9}$$

so that if

$$\eta^{-3} \frac{d}{dy}\left(\eta^3 \frac{dY_n}{dy} \right) = d_n Y_n, \tag{10}$$

then, due to the independence of the Y_n, it is merely necessary to find solutions of

$$\xi^{-3} \frac{d}{dx}\left(\xi^3 \frac{dF_n}{dx} \right) + d_n F_n = -6\mu U \frac{\xi'}{\xi^3} c_n \tag{11}$$

satisfying boundary conditions in x.

Thus, the expansions make possible a separation of variables, resulting in a homogeneous and a nonhomogeneous second-order differential equation, of the Sturm-Liouville type, involving a mutual parameter. There is no difficulty in fitting the solution of the nonhomogeneous equation to the boundary conditions, because of the presence of the particular solution. Any complete solution of the homogeneous equation may be made to satisfy one boundary condition by the choice of the proper ratio of the arbitrary constants. The requirement that it satisfy the second boundary condition provides an equation (in general, transcendental) for the determination of the parameter. In general, a denumerable infinity of values of this parameter are determined, which may be arranged in order of increasing magnitude. In the cases arising here, they are real. To each value of the parameter corresponds a function satisfying both the differential equation and the boundary conditions, which is therefore one of the required functions.[18] Michell's solution was the particular case $h = Ax$, and he used procedure (*B*), not recognizing the possibility of generalizing the method.

Considering, for the time being, a rectangular block, the chief problems concerning the effects of curvature which would seem to present themselves in practice are:

1. What effect would chamfer of the leading edge, or curvature of the surface in the direction of motion have upon the total load supported or upon the pressure distribution?

2. What effect would curvature or tilting in the direction perpendicular to the motion have upon the quantity of lubricant escaping along the lateral edges, and therefore upon the total load supported?[19]

Considerable information on each may be obtained by the use of a film-thickness function of the form (3a). If the function ξ is not linear, question 1 is being investigated, and if η is not a constant, question 2 is being investigated. From data obtained in both these cases, and in their combinations, a considerably more accurate picture of the behavior of such bearing surfaces should result.

Manifestly it is impossible to investigate all types of curvature. The exact solutions will be obtained here for several general types of surface. In a succeeding article, typical examples will be computed and the physical consequences discussed. Although the labor involved in any one computation is large, the solution may be applied with minor changes to each of three different cases, by the proper substitutions; these three are: the rectangular plate, the sector shaped plate in rotation (Michell thrust bearing), and the approximation (*A*) for the journal bearing, all of finite width.

---

a portion of the factor multiplying $\partial p/\partial x$, so that the expansion obtained for the homogeneous partial differential equation is that for a curved surface; to this is added the particular solution for the plane surface, and the solution used as an approximation to Michell's result.

[18] In many cases, the orthogonal functions have not been computed and tabulated, or functions have been determined for the d.e. but satisfying different boundary conditions. The labor connected with using these is usually greater than that involved in numerical solutions of the original problem, so it is desirable to confine the choice of h to those shapes whose solutions are expressed in terms of tabulated functions.

[19] A third question is the effect of variation in viscosity from point to point under the plate, upon, for example, the center of pressure. Consideration of this will be deferred.

I. Curvature Only in the Direction of Motion

The distinctive feature of such surfaces is that h is not a function of y, so that η may be taken as $\eta=1$. The method (B) is then obviously the more convenient, since (10) has the solution

$$Y_n=\sin(n\pi y/c), \quad (d_n=-n^2\pi^2/c^2) \tag{12}$$

satisfying the boundary conditions for a plate whose lateral edges are $y=0, c$. Eq. (8) then becomes

$$1=\frac{4}{\pi}\sum_n \frac{\sin[(2n+1)\pi y/c]}{2n+1} \tag{13}$$

as used by Michell, and the solution of (11) which satisfies the boundary conditions $F_n(a)=F_n(b)=0$ gives the exact solution

$$p=\Pi+\sum_n F_{2n+1}(x)\cdot\sin((2n+1)\pi y/c), \tag{14}$$

where Π is the atmospheric or bath pressure. No terms F_{2n} appear since the equation for this function is homogeneous and unless the parameter is a characteristic value for the equation (which will in general not be true) the function must be identically zero. Eq. (11) is a simple two-point boundary problem of the Sturm-Liouville type, and has a unique solution unless, again, the parameter has a characteristic value, in which case certain conditions must be fulfilled by the inhomogeneous term. This case does not arise here.

Let us consider as an example, the case previously mentioned, in which $h=\xi(x)=A(x+m)^q$ or with the same generality $\xi(x)=Ax^q$. Eq. (11) is then

$$F''_{2n+1}+(3q/x)F'_{2n+1}-(2n+1)^2\pi^2c^{-2}F_{2n+1} =-6\mu UA^{-2}\cdot(4q/\pi(2n+1))x^{-2q-1} \tag{16}$$

and letting

$$c^{-1}(2n+1)\pi x=s; \quad 3q=1-2m; \quad F_{2n+1}=s^mS;$$
$$C_{mn}=-8\mu UA^{-2}c^{(4m+1)/3}(1-2m) \times[(2n+1)\pi]^{-(4m+4)/3} \tag{16a}$$

we obtain

$$S''+(1/s)S'-(1+m^2/s^2)S=C_{mn}s^{(m-5)/3}, \tag{16b}$$

where now primes denote differentiation with respect to s. The expression on the left is Bessel's equation with imaginary argument. The solution is

$$S=A_1I_m(s)+B_1I_{-m}(s)+Q_m(s) \quad (m \text{ not an integer}) \tag{17}$$
$$=A_1I_m(s)+B_1K_m(s)+Q_m(s) \quad (m \text{ an integer}),$$

where Q is a particular solution of (16). Two particular solutions[20] are

$$Q_m=C_{mn}s^{(m+1)/3}\sum_{i=0}a_is^i$$
$$(1-2m)(1+4m)a_0=9; \quad a_1=0; \tag{18}$$
$$(3i+7-2m)(3i+7+4m)a_{i+2}=9a_i$$

useful for small values of x, and the asymptotic expansion

$$Q_m=C_{mn}s^{(m-5)/3}\sum_{i=0}b_is^{-i},$$
$$b_0=-1; \quad b_1=0; \tag{19}$$
$$9b_{i+2}=(3i-4m+5)(3i+2m+5)b_i$$

useful for large values of x. Boundary conditions, $F_{2n+1}=0$ at $x=a, b$, require that

$$A_1\Delta=Q(b)\phi(a)-Q(a)\phi(b),$$
$$B_1\Delta=Q(a)I_m(b)-Q(b)I_m(a), \tag{20}$$
$$\Delta=I_m(a)\phi(b)-I_m(b)\phi(a),$$

where $Q(a)$ stands for Q_m at $x=a$, etc. and $\phi=K_m$ or I_{-m} depending upon whether m is integral or not. A separate determination of A and B is required for each series expansion Q_m in (17). The complete solution for $h=Ax^q$, is then

$$p=\Pi+\sum_n\left[A_nI_{(1-3q)/2}\left(\frac{(2n+1)\pi x}{c}\right)+B_nK_{(1-3q)/2}\left(\frac{(2n+1)\pi x}{c}\right)+Q_{n,\,(1-3q)/2}\left(\frac{(2n+1)\pi x}{c}\right)\right]\sin\frac{(2n+1)\pi y}{c}, \tag{21}$$

[20] Other particular solutions may be found; general methods are available to obtain the solution including the particular solution (e.g. see E. L. Ince, *Ordinary Differential Equations* (Longmans, Green and Co.)), but these are convenient.

K being replaced by I if $(1-3q)/2$ is not integral. Both the series (18) or (19) and the solution (21) reduce to Michell's for $m=-1$, the case treated by him.

When $m=\frac{1}{2}$, $q=0$ so that $h=$const., $C_{mn}=0$, and therefore the term on the right in (16) vanishes. This is the situation already referred to, of a flat plate parallel to the lower surface. The particular solution is zero, and the boundary conditions require atmospheric pressure everywhere, again the known fact that such a plate cannot support a load by film pressure. For all $m\neq\frac{1}{2}$, the pressure at any point on the plate depends upon the speed, the shape of surface, and the viscosity of the lubricant. Computations now reduce to the calculation of the series and the use of standard tables.[21]

Again, if the shape of the lower surface of the plate is such that the film thickness is represented by the expression

$$h=h_0e^{kgx} \tag{22a}$$

and the edges of the plate are $x=0,\ a;\ y=0,\ c$; the use of procedure (A) gives the expansion below for the (gauge) pressure

$$\begin{aligned} Kp&=\exp(-\log x)\sum_n b_nb^{-2}\operatorname{sech}(bc)\sin(n\pi x/a)\\ &\quad\times\sinh(by)\sinh(b(c-y)),\\ b^2&=9g^2+(n^2\pi^2/4a^2),\\ b_n&=n\pi[1+(-1)^{n+1}\exp(-2ga)]/(4g^2a^2+n^2\pi^2)\\ &=\text{Fourier coeff. of }\exp(-2gx),\\ K&=h_0^2/24\mu Ug, \end{aligned} \tag{22b}$$

and the use of procedure (B) gives the alternative expansion

$$\begin{aligned} p&=6\mu Ugh_0^{-2}\exp(-6gx)\sum_n K_n\sin(n\pi y/c)\\ &\quad\times[\sinh(2b(a-x))+\exp(-2ag)\\ &\quad\times\sinh(2bx)-\exp(-2gx)\sinh 2ab], \end{aligned} \tag{22c}$$

$$4b^2c^2=36g^2c^2+n^2\pi^2;$$

$$K_n=(g^2-b^2)^{-1}a_n\operatorname{csch}(2ab);$$

$$a_{2n}=0;\quad a_{2n+1}=4/\pi(2n+1).$$

[21] If the procedure (A) had been used, the expression would have been

$$p-\Pi=\Sigma_n[I_n(b_n^{\frac{1}{2}}x)K_n(b_n^{\frac{1}{2}}a)-I_n(b_n^{\frac{1}{2}}a)K_n(b_n^{\frac{1}{2}}x)]\times[B_n\sin(b_n^{\frac{1}{2}}y+C_n)+6\mu Ua_nb_n^{-1}]$$

where b_n (real or complex) is determined by setting the quantity depending on x equal to zero for $x=b$, and then B_n and C_n chosen to satisfy boundary conditions for y. To do the latter, a_n must be determined from (4) using for X_n the quantity in braces in the expression for p. While this is perfectly possible, the labor involved is prohibitive.

The two solutions are different expansions of the same function, and will have the same value at any point, since the solution of this problem is known to be unique.

In both (21) and (22b) (and always, with constant viscosity) the dependence on viscosity and on speed is represented by a factor, the same for all terms, and may be taken out in front of the summation sign. The series need only be computed once for a given plate with a given minimum film thickness, and results for any viscosity of lubricant and any speed (for which the assumptions are not violated) are obtained by multiplication with the appropriate values of μ and U. With the film thickness (15) an increase of x and of y in the same ratio, merely multiplies the term on the right in (2) by a constant factor, so that geometrically similar plates with the appropriate minimum film thicknesses behave the same, if the proper change be made in the product of speed and viscosity.

II. Curvature both Normal to and in the Direction of Motion

First, we notice that no load can be supported, no matter what the curvature is normal to the direction of motion, if the lower surface of the block is everywhere parallel to the plane in the direction of motion.[22] This is again an illustration of the principle of the converging film. Physically, this principle indicates that if there is both convergence and divergence of the film, the shape and dimensions of the block must be such that the load-supporting effect of the convergence is greater than the counter-effect of any divergence; therefore the amount of divergence is limited by practical considerations. If maximum load support is the chief consideration, there should be no divergence under the block in the direction of motion; accordingly, both in this section and in

[22] Then $\xi'=0$ and $V=0$; therefore the term on the right in (2) vanishes.

the preceding one, practical problems would involve chiefly curves (so far as ξ is concerned) of the general type previously considered, that is monotonic, providing a decreasing thickness of film.

When we consider curvature normal to the direction of motion, however, the situation is much different. Here, physically, it is obvious that surfaces symmetrical with respect to the center line drawn in the direction of motion are most important. If the chief consideration is to shape the surface so as to decrease leakage of the lubricant along the lateral edges, little is gained by decreasing leakage at one edge if it is thereby increased at the other. Thus, while the method is equally applicable to nonsymmetrical cases, such as the investigation of the effect of tilting, only the symmetrical case will be worked out in detail by an example.

Let us take for the example the plane bearing considered by Michell ($\xi=Ax$), and give it a curvature (positive or negative) in the y direction. In order to stay within the range of tabulated functions, consider a curvature defined by $\eta=\sin^{\frac{1}{2}}(\alpha y+\beta)$ so that $h=Ax\sin^{\frac{1}{2}}(\alpha y+\beta)$ (23) Positive or negative curvature may be obtained by the proper choice of constants. In particular, the two centrally symmetric cases which would be useful are

$$h=Ax\cos^{\frac{1}{2}}(\alpha(y-c/2)) \quad \text{concave downward} \quad (24a)$$

$$=Ax\cosh^{\frac{1}{2}}(\alpha(y-c/2)) \quad \text{convex downward.} \quad (24b)$$

If the lubricant is not to escape, or its rate of leakage is to be diminished, the shape given by the first of Eqs. (24) would be the desirable one, intuitively, since a component of the reaction of the plate on the lubricant would be urging the latter toward the center of symmetry.

Letting

$$p=u[\sin(\alpha y+\beta)]^{-1};\quad u_x=(\partial u/\partial x)\text{ etc.};\quad F'=(dF/dx)\text{ etc.} \quad (25)$$

there results

$$x^{-3}(x^3u_x)_x+(u_{yy}+\alpha^2u)=6\mu UA^{-2}x^{-3}\sin^{-\frac{1}{2}}(\alpha y+\beta), \quad (26)$$

so that $u=\sum F_{2n+1}(x)\sin((2n+1)\pi y/c)$, (27)

$$F''_{2n+1}+(3/x)F'_{2n+1}-k_n^2F_{2n+1}=C_{2n+1}x^{-3}, \quad (28)$$

in which $k_n^2=-\alpha^2+(2n+1)^2(\pi^2c^{-2})$, (28a)

$$C_{2n+1}=12\mu UA^{-2}\pi^{-1}\int_0^{\pi}\sin^{-\frac{1}{2}}(\alpha ct/\pi+\beta)\times\sin(2n+1)t\cdot dt. \quad (28b)$$

Now in particular in (24a), h cannot be zero. $\therefore\ \alpha c<\pi$; $k_n^2>0$; so the expression for p for $h=Ax\cos^{\frac{1}{2}}(\alpha(y-c/2))$, is

$$p=[\cos(\alpha(y-c/2))]^{-1}\sum_n[A_1I_1(k_nx)+B_1I_1(k_nx)+Q_1(k_nx)]\sin((2n+1)\pi y/c), \quad (29)$$

in which A_1, B_1, and Q_1 are determined, with obvious modifications, by the formulas (17)–(20). The transformation (25) does not affect the validity of the solution, since the function "p/u" is bounded—h cannot be equal to zero.

Similarly solutions may be developed for combinations of any of the functions which have been used above, or any other curvatures which yield series of functions whose values have been tabulated. For example, the solution for

$$h=h_0e^{Ax}\sin^{\frac{1}{2}}(\alpha y+\beta) \quad (30)$$

is

$$p=K_0\exp(-6gx)[\sin(\alpha y+\beta)]^{-1}\sum_nK_n\times[\sinh(2b(a-x))+\exp(-2ag)\sinh(2bx)-\exp(-2gx)\sinh(2ab)]\sin((n\pi y)/c) \quad (31)$$

with $4b^2c^2=36g^2c^2+n^2\pi^2-\alpha^2c^2$ and appropriate changes in K_n; K_0.

III. Motion in an Arbitrary Direction with Respect to the Sides of the Plate

Let the plate be moving with a constant velocity W, the direction making an angle with the axis of x, whose cosine is K. Then the component velocities in the x and y directions are $U=KW$ and $V=(1-K^2)^{\frac{1}{2}}W$, so that (2) is

$$(h^3p_x)_x+(h^3p_y)_y=-6\mu KW(\partial h/\partial x)-6\mu W(1-K^2)^{\frac{1}{2}}(\partial h/\partial y). \quad (32)$$

As before, if there is no curvature or inclination

in one direction, the velocity in this direction has no effect on the pressure distribution. The lack of convergence or divergence in this direction means that there is no tendency to force lubricant into the space between the surfaces nor the reverse, as a result of the component motion in that direction. The problem then reduces itself to that discussed in I with the component velocity replacing the actual velocity in the equation.

If there is a curvature or inclination in each direction, each has its effect. Consider a plate inclined or curved in both the x and y directions so as to present a converging film to both components of the velocity. A pressure will be built up due to each, so that the actual load supported is that due to the sum of the lifting effects of each component. If a converging film exists in one direction and a diverging one in the other, the load which can be supported is reduced; (in the extreme case separation of the lubricant from the surface may occur). The center of pressure will in each instance be determined by both pressure effects.

Obviously, due to the linearity of the differential equation, and the boundary conditions, a solution may be made for the pressure distribution occasioned by each inclination or curvature separately, and the two be added together. The sum is a solution of the original problem. Thus, if

$$(h^3 f_x)_x+(h^3 f_y)_y=-6\mu K W h_x$$

and $$(h^3 g_x)_x+(h^3 g_y)_y=-6\mu(1-K^2)^{\frac{1}{2}} W h_y,$$

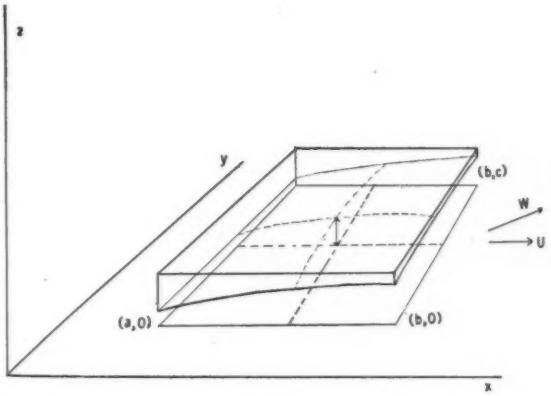

FIG. 1.

f and g each satisfying boundary conditions, where subscripts denote differentiation with respect to the variable, then $p=f+g$ satisfies (32). In actually carrying out the process, it is convenient to do both at the same time. Let $p=\sum X_n Y_n$, where either X_n or Y_n are a closed set of orthogonal functions satisfying the resulting Sturm-Liouville equation; if X_n is the set, then

$$-\xi'/\xi^3=\sum a_n X_n\,; \quad -1/\xi^2=\sum b_n X_n\,;$$

$$\eta^{-3}(\eta^3 Y_n')'+d_n Y_n=6\mu K W a_n \eta^{-2}$$

$$+6\mu(1-K^2)^{\frac{1}{2}} W b_n \eta^{-3}\eta',$$

in which primes denote differentiation. The procedure is identical with that used above.

IV. Sector-Shaped Surfaces in Rotation; the Michell Thrust Bearing

The boundary conditions so far discussed have been those for a square plate. If the plate be any other shape, the new boundary conditions usually increase the difficulty of the analytical solution. In certain cases the problem may be reformulated in new coordinates $u=u(x, y)$; $v=v(x, y)$ so that the boundary conditions again become those of the type that we have been considering, i.e. $p=0$ if $u=a$, b, or $v=c$, d; if the equation is separable for appropriate functions h, the same procedure may be used as before. One important particular case will be discussed here, namely that of the sector-shaped Michell thrust bearing plate. As usually constructed, the plate is shaped as in Fig. 2, the straight edges making an angle of some 30°–40° with each other. The plate is mounted so that it is movable about a radial line. When the shaft rotates about its axis, normal to the plane of the paper, this freedom of movement allows the plate to take up a position so that a converging film is presented to the lubricant. The pressure developed is then a thrust, so that an important use of this type of bearing is in marine work to take propeller thrust, and in vertically mounted turbo-generators. Such bearings are considerably more efficient than multi-collar bearings. They will take pressures over 100 times as great as the latter without seizing or requiring water-cooling, are self-adjusting, and save considerable space.

With the mounting used in such plates, the

film thickness when in operation is given by the expression

$$h=h_0+r\sin\theta, \tag{33}$$

where θ varies from about $-15°$ or $20°$ to about $+15°$ or $20°$, depending upon the plate. The only solution which has been made for this bearing is that of Boswall; he approximated the expression (33) by

$$h=k\theta \tag{33a}$$

The approximation $\sin\theta=\theta$ is clearly justified, in view of the small values of θ encountered. Since r, in a typical case, varies from $5''$ to $10''$, a consideration of its effect seems desirable. The h given below is a case for which a solution in relatively simple terms may be found.

$$h=Ar(\theta-b) \quad \text{or more simply} \quad h=Ar\theta. \tag{33b}$$

Table II gives a comparison of the actual film

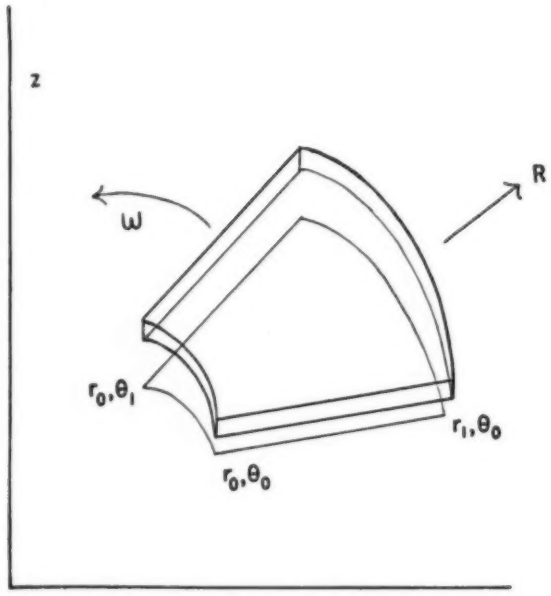

FIG. 2.

thickness as computed by the true formula, by this approximation, and by Boswall's approximation for a number of points within the film. Since inclusion of the term h_0 renders the solution considerably more difficult, this term is omitted. Even with this omission, the shape of an actual film is better approximated with the expression (33b) than with (33a).

The pressure equation may be derived as follows: The surface $z=h$ is moving with velocities

TABLE II.

r	θ	APPROX. $h-h_0=k_1\theta$	TRUE THICKNESS $h-h_0=kr\sin\theta$	APPROX. $h-h_0=k_2r\theta$
10	40°	$0.698k_1$	$6.428k$	$6.98k_2$
5	40°	$0.698k_1$	$3.214k$	$3.49k_2$
10	30°	$0.523k_1$	$5.000k$	$5.23k_2$
5	30°	$0.523k_1$	$2.500k$	$2.61k_2$
10	20°	$0.349k_1$	$3.420k$	$3.49k_2$
5	20°	$0.349k_1$	$1.710k$	$1.75k_2$
10	10°	$0.175k_1$	$1.736k$	$1.75k_2$
5	10°	$0.175k_1$	$0.868k$	$0.88k_2$

If k_1 and k_2 are each adjusted so that all 3 columns agree for one (r,θ), the expression $h-h_0=k_2r\theta$ represents the true film thickness much better than does $h-h_0=k_1\theta$.

ω and $\dot{R}$ in the θ and r directions. The quantity h is small compared with the dimensions of the block, and therefore $\partial p/\partial z$ is negligible. The surface $z=0$ is at rest. Consider an elementary portion of fluid between the planes $z=0$ and $z=h$. Since cylindrical coordinates are used, the element will be sector shaped. Let this be in motion with angular speed $\dot{\theta}$ and radial speed $\dot{r}$. The shearing stresses on a face normal to the z axis, acting in the directions of r and θ are

$$\mu(\partial\dot{r}/\partial z+\partial\dot{z}/\partial r)\,; \quad \mu(r\partial\dot{\theta}/\partial z+\partial\dot{z}/r\partial\theta). \tag{34}$$

Due to the dimensions of h, $\dot{z}$ is a small quantity of the first order, and its derivative in either direction may be neglected. The viscous drag on the element in the direction of increasing θ is the difference

$$[-\mu(r\partial\dot{\theta}/\partial z)r\delta r\delta\theta + \mu(r\partial\dot{\theta}/\partial z+r(\partial^2\dot{\theta}/\partial z^2)\delta z)r\delta r\delta\theta] \tag{34a}$$

and the pressures in the fluid on the faces $\delta z\delta r$ normal to θ are

$$p \quad \text{and} \quad -p-(\partial p/r\partial\theta)(r\delta\theta). \tag{34b}$$

The force equation for the element is then

$$[\mu r\partial^2\theta/\partial z^2-\partial p/r\partial\theta]r\delta r\delta\theta\delta z = \rho r\delta r\delta\theta\delta z(rd\dot{\theta}/dt) \tag{34c}$$

where ρ is the fluid density, and similarly

$$[\mu(\partial^2\dot{r}/\partial z^2)-\partial p/\partial r]r\delta r\delta\theta\delta z = \rho r\delta r\delta\theta\delta z(d\dot{r}/dt). \tag{34d}$$

The rates of increase of momentum on the right are small quantities compared to those on the

left and may be neglected, and since p is independent of z, and $\dot{\theta}=0$ at $z=0$, and $\dot{\theta}=\omega$ at $z=h$, etc.

$$\frac{\partial^2\dot{\theta}}{\partial z^2}=\frac{1}{\mu r^2}\frac{\partial p}{\partial\theta};\quad \frac{\partial^2\dot{r}}{\partial z^2}=\frac{1}{2\mu}\frac{\partial p}{\partial r};$$

$$\dot{\theta}=\frac{1}{2\mu r^2}\frac{\partial p}{\partial\theta}(z^2-hz)+\omega\frac{z}{h};$$

$$\dot{r}=\frac{1}{2\mu}\frac{\partial p}{\partial r}(z^2-hz)+\dot{R}\frac{z}{h}.$$

The total flow of lubricant across the face represented by δr is

$$\delta r\int_0^h r\dot{\theta}dz=(\delta r)\left[-\frac{h^3}{12\mu r}\frac{\partial p}{\partial\theta}+\omega\frac{rh}{2}\right]$$

and the total flow across the face defined by $r\delta\theta$ is

$$r(\delta\theta)\left[-\frac{h^3}{12\mu}\frac{\partial p}{\partial r}+\frac{\dot{R}h}{2}\right].$$

Therefore, the total flow into the element is

$$-\frac{1}{r}\frac{\partial}{\partial\theta}\left[\frac{h^3}{12\mu r}\frac{\partial p}{\partial\theta}-\frac{\omega rh}{2}\right]r\delta\theta\delta r$$
$$-\frac{\partial}{\partial r}\left[\frac{rh^3}{12\mu}\frac{\partial p}{\partial r}-\frac{\dot{R}rh}{2}\right]\delta\theta\delta r. \quad (35)$$

But the volume of the element is decreasing due to the movement of the upper plate at the rate

$$\omega[(hr\delta r\delta\theta)_{\theta+\delta\theta}-(hr\delta r\delta\theta)_\theta]$$
$$+\dot{R}[(hr\delta r\delta\theta)_{r+\delta r}-(hr\delta r\delta\theta)_r]$$
$$=\omega(\partial h/\partial\theta)r\delta r\delta\theta+\dot{R}\delta r\delta\theta(\partial/\partial r)(rh), \quad (35)$$

so that[23]

$$\frac{\partial}{\partial\theta}\left(\frac{h^3}{6\mu}\frac{\partial p}{\partial\theta}\right)+r\frac{\partial}{\partial r}\left(r\frac{h^3}{6\mu}\frac{\partial p}{\partial r}\right)=$$
$$-r^2\omega\frac{\partial h}{\partial\theta}-\dot{R}r\frac{\partial}{\partial r}(rh). \quad (36)$$

[23] This is not the equation obtained by transformation of coordinates; the latter errs in the second term on the right.

In the actual bearing, the motion is pure rotation so that $\dot{R}=0$, and by our assumptions $h=r\theta$. Substituting for h and making the transformation $r=r_0e^t$, $p=\exp(-3t/2)\cdot u$ so that $p=0$ at $t=0, d$; $r=r_0e^d$, (36) becomes

$$\theta^{-3}\frac{\partial}{\partial\theta}\left(\theta^3\frac{\partial u}{\partial\theta}\right)+\frac{\partial^2u}{\partial t^2}-\frac{9}{2}u=$$
$$-6\mu\omega\theta^{-3}\exp(3t/2), \quad (37)$$

so that if $$u=\sum_n X_n(\theta)\sin(n\pi t/d) \quad (38)$$

and, in the range 0, d,

$$\exp(3t/2)=\sum a_n\sin\frac{n\pi t}{d};$$

$$a_n=\frac{4n\pi[1+(-1)^{n+1}\exp(3d/2)]}{9d^2+4\pi^2n^2}$$

the function X_n satisfies the equation

$$\theta^{-3}\frac{d}{d\theta}\left(\theta^3\frac{dX_n}{d\theta}\right)-\left(\frac{n^2\pi^2}{d^2}+\frac{9}{2}\right)X_n=-6\mu\omega a_n\theta^{-3} \quad (39)$$

similar to Eq. (28). Therefore

$$X_n=\theta^{-1}[AI_1(b\theta)+BK_1(b\theta)+Q(b\theta)], \quad (40)$$

where $b^2=(n^2\pi^2/d^2)+9/2$

and $$p=\left(\frac{r}{r_0}\right)^{-\frac{1}{2}}\sum_n X_n\sin\left(\frac{n\pi}{d}\log(r/r_0)\right).$$

Similarly if h had been $Ar^j\theta^q$

$$\theta^{-3q}\left(\theta^{3q}\frac{\partial p}{\partial\theta}\right)_\theta+r^{1-3j}\left(r^{1+3j}\frac{\partial p}{\partial r}\right)_r=$$
$$-6\mu\omega A^{-2}qr^{2-2j}\theta^{-2q-1}$$

and if $r=r_0e^t$; $s=b\theta$; $b^2=((9/4)j^2+n^2\pi^2d^{-2})$;

$$3q=1-2m;\quad \exp\left(\frac{(4-j)t}{2}\right)=\sum a_n\sin\frac{n\pi t}{d};$$

$$p=\left(\frac{r}{r_0}\right)^{-3j/2}\sum_n s^mX_n(s)\sin\frac{n\pi t}{d};$$

$$X_n=AI_m(s)+BI_{-m}(s)+Q_m(s),$$

in which A, B, and Q are determined from Eq. (16a) with $C_{mn}=-6\mu\omega A^{-2}qa_nb^{-(4m+1)/3}$.

The similarity of this equation to that in (16a) shows that all partial computations which are made in that case may be used here with the corresponding change of variable. In particular, the case $h=r\theta$ makes use of the functions computed by Michell for the terms in x, and therefore with the appropriate values of $x=\log\ (r/r_0)$; $\theta=y$, the two are identical save for the factor $(r/r_0)^{-\frac{1}{2}}$.

V. The Journal Bearing

Many approximate solutions of the lubrication of the journal bearing have appeared. Exact solutions were given by Sommerfeld, Reynolds and others in the case of infinite width, and may be found discussed in Hersey[4] or Boswall.[7]

For the journal bearing, the pressure equation is obtained from (2) by letting $x=R\theta$, where R is constant. The film thickness is

$$h=mR(a+\cos\theta),$$

where $e=mR$ is the distance between the centers of the shaft and of the brass, and $r=aR$ is the difference in the radii. For details, Boswall may be consulted. Eq. (2) then becomes

$$(a+\cos\theta)^{-3}\frac{\partial}{\partial\theta}\left((a+\cos\theta)^3\frac{\partial p}{\partial\theta}\right)+R^2\frac{\partial^2 p}{\partial z^2}=-\frac{6\mu U}{m^2R}\frac{\sin\theta}{(a+\cos\theta)^3}, \quad (41)$$

so that if $1=\frac{4}{\pi}\sum\frac{\sin\ ((2n+1)\pi z/d)}{2n+1}$

and $p=\sum_n T_n(\theta)\sin\frac{(2n+1)\pi z}{d}$

$$(a+\cos\theta)^{-3}((a+\cos\theta)^3T_n')'-\frac{(2n+1)^2\pi^2}{d^2}R^2T_n=-\frac{6\mu U}{m^2R}\cdot\frac{4}{\pi(2n+1)}\cdot\frac{\sin\theta}{(a+\cos\theta)^3}. \quad (42)$$

This is an equation of the type considered by Hill,[24] with the added necessity of finding a particular solution. Since the procedure is well known, it will not be discussed further at present. An interesting result may be obtained by the substitution

$$\cos\theta=(x)^{\frac{1}{2}};\quad T_n(\theta)=X(x) \quad (43)$$

which yields the equation

$$x(1-x)X''+\left[\frac{3}{2}\frac{(x)^{\frac{1}{2}}(1-x)}{a+(x)^{\frac{1}{2}}}+\frac{1}{2}-x\right]X'-B^2X=A\frac{(1-x)^{\frac{1}{2}}}{(a+(x)^{\frac{1}{2}})^3}, \quad (44)$$

$$B=(2n+1)\pi Rd^{-1};\ A=-24\mu U[m^2\pi R(2n+1)]^{-1},$$

from which it is evident that for certain purposes somewhat more convenient particular procedures may be used.

The bedded brass

In particular, if the brass under consideration has been ground to the same curvature as the shaft, the case of the bedded brass, $r=0=a$, and (44) becomes

$$x(1-x)X''+(2-(5/2)x)X'-B^2X=Ax^{-\frac{1}{2}}(1-x)^{\frac{1}{2}}. \quad (45)$$

The complementary equation is the well-known hypergeometric equation. One solution is

$${}_nX_1=F(a,b;c;x)\quad\text{in which}\quad \begin{matrix}a+b=\frac{3}{2}\\ ab=B^2.\\ c=2\end{matrix} \quad (45a)$$

Since c is an integer, the second solution involves a logarithm; it is

$${}_nX_2={}_nX_1\log x+[(a-1)(b-1)x]^{-1}+\sum_{j=0}^{\infty}\left[\frac{a(a+1)\cdots(a+j-1)(b)(b+1)\cdots(b+j-1)}{j!(j+1)!}\times\left\{\sum_{i=0}^{j-1}\left(\frac{1}{a+i}+\frac{1}{b+i}-\frac{1}{i+1}-\frac{1}{i+2}\right)\right\}x^j\right]. \quad (45b)$$

The variable x is always $\leqq 1$, so that we need only find one particular solution. A convenient one convergent for $|x|<1$ is

[24] Acta Math. viii, 1886. See Whittaker and Watson, *Modern Analysis* (Cambridge University Press).

$$ {}_nX = A(\tfrac{1}{2} - B^2)^{-1}(1-x)^{\frac{1}{2}}x^{-\frac{3}{2}}\sum a_j x^j $$

$$ a_0 = 1\,; \qquad (45c) $$

$$ (j-\tfrac{1}{2})(j+\tfrac{1}{2})a_{j+1} = [(j+\tfrac{1}{2})(j-1)+B^2]a_j. $$

By making use of the properties of the hypergeometric function, and in particular of $F(\alpha, \beta; \alpha+\beta+\frac{1}{2}; x)$, certain interesting conclusions may be drawn. The solution will be discussed further.

The solution for the bedded brass is then

$$ p = \sum_n \sin \frac{(2n+1)\pi z}{d} [A_n X_1(\cos^2\theta) + B_n X_2(\cos^2\theta) + {}_nX(\cos^2\theta)], \qquad (46) $$

in which the constants are determined to fit conditions at the boundary. Computation is considerably more laborious than in the preceding cases, but use may be made of the asymptotic expressions for the hypergeometric functions with large parameters. The computational difficulty encountered in this case makes evident the greater difficulty which would be met in obtaining the numerical values of the solution of (41) or (44), and hence the desirability of using the approximation (*A*) or (22a) where possible.

Conclusion

The exact solution for an *arbitrary* film shape may not be obtained in a form useful for computation. It has been the purpose of this paper to call attention to the fact, that, the statements of Boswall and the apparent belief of many engineers notwithstanding, computable solutions to Reynolds' three-dimensional equation are possible in many cases, and to exhibit several such solutions which seem particularly useful for studies in bearing design and lubricants.

Dynamic Characteristics of Glow Discharge Tubes

Herbert J. Reich and Wallace A. Depp *
Department of Electrical Engineering, University of Illinois, Urbana, Illinois

(Received February 14, 1938)

This paper describes a method for determining the dynamic current voltage characteristic curves of glow discharge tubes. The technique differs from that previously used for the oscillographic study of glow tubes in that the manner in which the current varies with time is under control. This is accomplished by the use of a vacuum tube to limit the current passed by the glow tube. The rate at which the current rises and falls, the current amplitude, the frequency of repetition of the current cycle, and the interval between cycles can be varied at will by changing the wave form of the voltage applied to the grid of the control tube, and the grid bias of the control tube. A number of oscillograms obtained by this method are shown, and the form of the characteristics is explained on the basis of time taken for ionization and deionization of the gas.

THE study of the characteristics of glow discharges is important not only because of the practical value of glow discharge tubes, but also as a means of obtaining fundamental information regarding all forms of gaseous conduction. In particular, a thorough understanding of glow discharges is helpful in the study of arcs and the design of arc tubes, because the formation of an arc must often be preceded by glow discharge.

Static characteristic curves of glow discharge tubes are readily made, and the factors which determine the form of these curves have been satisfactorily explained.[1] These static curves do not, however, indicate the behavior of the tubes under dynamic operating conditions. Because of the time required for ionization and deionization to take place, the voltage under changing condi-

* Now with the Bell Telephone Laboratories.

[1] Darrow, *Electrical Phenomena in Gases*, Chapters IX and XII.

tions depends not only upon the current flowing at any instant, but also upon the current which has flowed previously and upon the rate of change of current. It is particularly difficult to determine by static means how the current and voltage vary immediately following ignition.[2] Any attempt to limit the current to values of the order of that prevailing at the instant of ignition invariably results in production of relaxation oscillations.

Some information regarding the dynamic behavior may be determined by making an oscillographic study of the relation between current and voltage when relaxation oscillations are taking place.[3] Typical characteristics obtained in this manner are shown in Fig. 1. The knowledge

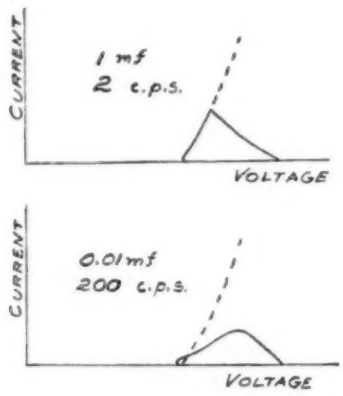

FIG. 1. Dynamic current voltage characteristics of glow tube used in relaxation oscillator.

which can be gained by this method is limited, however, because the manner in which the current and voltage vary with time during discharge is not under control, but is determined by the resistance, inductance, and capacitance of the circuit. Furthermore, the range through which the voltage varies is restricted.

CIRCUIT FOR THE DETERMINATION OF DYNAMIC CURRENT VOLTAGE CURVES

A more complete study of the dynamic behavior of glow discharge tubes can be made by means of the circuit shown in Fig. 2. The glow

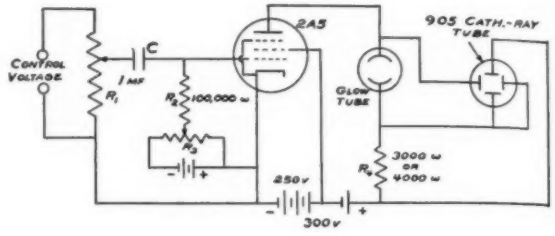

FIG. 2. Basic circuit for the oscillographic determination of dynamic characteristics of glow tubes.

tube, in series with a power pentode, is connected to a source of voltage considerably higher than the ignition voltage of the tube. The vacuum tube acts as a high resistance, the magnitude of which can be controlled as desired by means of voltage applied to the control grid. Thus the manner in which the current varies with time can be made to conform to any desired wave form. The voltage across the discharge tube is applied to one pair of deflecting plates of a cathode-ray oscillograph; the voltage developed across a resistance in series with the discharge tube is applied to the other pair. The image formed on the screen is a dynamic curve of tube current *vs.* tube voltage.

The complete circuit is shown schematically in Fig. 3. In obtaining most of the oscillograms

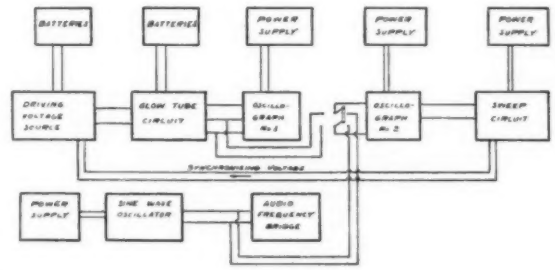

FIG. 3. Complete circuit for the oscillographic determination of dynamic characteristics of glow tubes.

shown in the paper the voltage applied to the grid of the control pentode was a sawtooth wave, obtained from a relaxation oscillator. By adjusting the amplitude, polarity, and frequency of this voltage, and the grid bias of the pentode, desired current wave forms were obtained. The frequency was determined by comparison with a sine wave oscillator. A separate cathode-ray oscillograph was used for adjusting and recording the wave form of the current.

[2] Ignition may be defined as the advent of a self-sustaining discharge, i.e., a discharge which will continue if the initial source of electrons and positive ions is removed. The ignition potential is the voltage at which ignition takes place.

[3] Slepian, *Conduction of Electricity in Gases*, pp. 78–109. R. Seeliger, Zeits. f. tech. Physik **15**, 329 (1934).

Oscillograms were first obtained by photographing the screen of the cathode-ray tube, but because of the large differences in brilliance between various portions of the image, this was not found to be entirely satisfactory. The records shown in the following figures are tracings made from the screen of a type 905 cathode-ray tube. Differences of brilliance, showing variations in the rate at which current and voltage change at different times in the cycle, are indicated in these tracings by the widths of the lines.

In preliminary experiments a number of different types of glow discharge tubes were used in order to determine whether the characteristic curves vary with the construction of the tube or with the type of gas. The characteristics of all the tubes tried were not found to differ greatly in their general aspects, and so further experiments were confined to an early form of type 874 voltage regulator tube containing argon, and to 2-watt G.E. neon-filled glow tubes. The construction of the electrodes of these two types of tubes is illustrated in Fig. 4. The 874 tube is an interesting

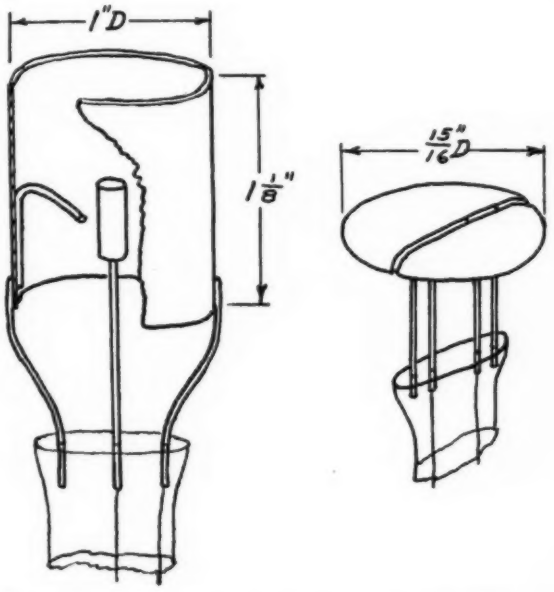

FIG. 4. Electrode structure of the two tubes the characteristics of which are shown in Figs. 5 to 9.

one for experimental purposes because of the great difference in area of the two electrodes. The area of the cylindrical outer electrode is sufficiently great so that the discharge was "normal," i.e., the cathode was only partially covered by glow, when the cylinder acted as cathode. When the rod acted as cathode, however, the discharge was "abnormal," i.e., the cathode was completely covered by glow, except at very small currents. The only resistance used in series with either tube was that of the control tube, and that of the resistance R_4 used to produce a voltage proportional to the current.

OSCILLOGRAMS

Four series of oscillograms, obtained with two tubes and two current wave forms at frequencies ranging from 60 to 8000 c.p.s. and constant current amplitude, are shown in Fig. 5. In these oscillograms the static characteristics are indiindicated by dashed lines. The static ignition potentials differ negligibly from the ignition potentials shown by the 60-cycle characteristics of the first and third columns. The form of the current wave is shown by the bottom oscillograms in each column. The 874 tube was connected so that the rod acted as cathode. Except at current too small to give appreciable deflection of the fluorescent spot, the discharge was "abnormal" in both tubes. Fig. 6 shows two sets of characteristics for the 874 tube obtained at constant frequency and different values of current amplitude.

In order to understand fully the portions of the characteristics immediately following ignition it is necessary to examine first the characteristic of Fig. 7, obtained when the current was started and stopped by means of a key, and limited only by a fixed resistance. Because voltage applied to the tube rises much more rapidly than the ionization can build up, the ignition potential greatly exceeds the static ignition potential. Because the external circuit contains only a fixed resistance, the decrease in tube voltage must be proportional to the increase of current. Between the point of ignition and the point on the static characteristic corresponding to the final current after the switch is closed, the dynamic characteristic is determined entirely by the external resistance, the slope being equal to the reciprocal of the external resistance. Similarly, when the resistance is replaced by a vacuum tube, the portion of the characteristic traced immediately after ignition takes place must be influenced by the characteristics of the control tube. The characteristic

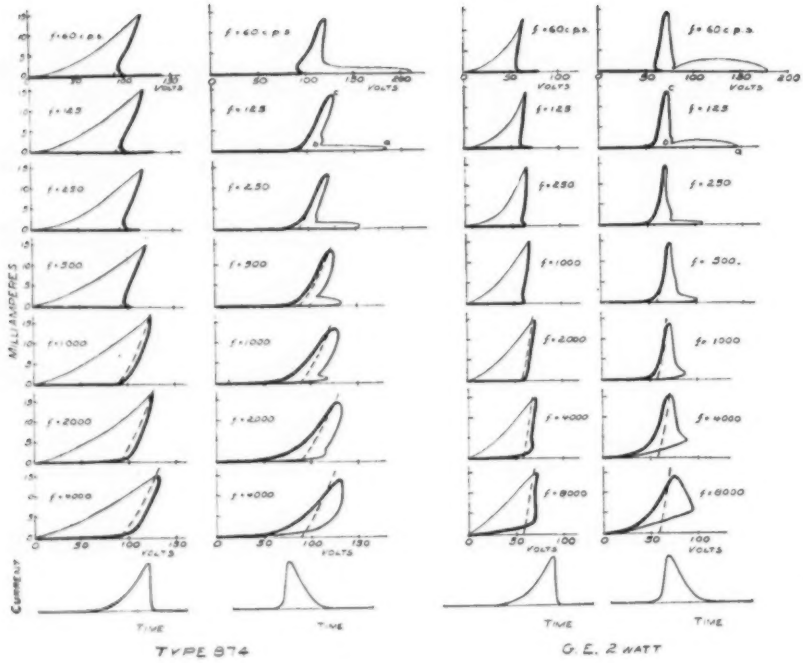

FIG. 5. Dynamic characteristics for two types of tubes; current amplitude constant, frequency and current wave form varied; rod of type 874 tube used as cathode.

curves of the 2A5 pentode, however, are of such form that at currents of the order of two milliamperes or less and voltages above 75 volts there is little change in plate current with plate voltage even for large changes of plate voltage. The change in tube current immediately following ignition is, therefore, determined almost entirely by the voltage applied to the grid of the control tube. When the frequency is low, and the control-grid voltage is increased gradually, as for the upper curves of columns 1 and 3 of Fig. 5, there is little change in control grid voltage during the time required for the tube to break down.[4] Hence, as soon as ignition takes place the tube voltage falls abruptly to a value determined by the glow tube. The voltage across the glow tube is subsequently determined practically entirely by the glow tube, since, at currents of 15 milliamperes or less, large changes of pentode plate voltage can take place at nearly constant current. The current is dependent upon the grid voltage of the control tube. The effect is similar to that which would be obtained by the use of a very high fixed resistor and a varying supply voltage, but the use of the pentode greatly reduces the required supply voltage, and makes possible variation of current in any desired manner.

When the voltage of the control tube is raised suddenly as in obtaining the oscillograms of columns 2 and 4, appreciable change of control grid voltage, and hence of current, takes place during the time the glow tube breaks down. This shows up clearly in portions *a–b* of the 125 cycle curves. (The writers have been unable to explain the rise and subsequent fall of current during breakdown observed in the 60-cycle and 125-cycle curves of column 4.) The portion *a–b* of the curves in columns 2 and 4, corresponding to breakdown, is very faint as seen on the screen, indicating that breakdown takes place very rapidly. The corresponding portion of the low-frequency characteristics of columns 1 and 3 would undoubtedly also be very faint, but is hidden by the portion of the characteristic traced while the voltage rises to the ignition value. The portion *b–c* is brighter than the portion *a–b*, but, since the current rises rapidly, is not so bright as the portion from *c* to the origin.

The most outstanding features of the characteristics of Fig. 5 and Fig. 6, and their probable explanations, are the following:

1. When the current rises abruptly, the ignition potential is considerably higher than the static ignition potential. This results from the time taken for ignition to take place. The voltage across the tube increases so rapidly that it exceeds the ignition potential before sufficient ionization can build up to result in a self-sustaining dis-

[4] Breakdown is the increase of current through the discharge without increase of voltage. The voltage at which breakdown takes place is called the breakdown voltage. Ignition is usually followed immediately by breakdown except in tubes in which the product of electrode spacing by gas pressure is very low. (See Slepian, *Conduction of Electricity in Gases*, pp. 97–101.)

charge. Another way of stating this is to say that the voltage required to cause the current to build up at the rate determined by the control tube exceeds the static ignition potential.

2. The ignition potential falls with increase of frequency of the current wave and with increase of current amplitude. If the current and frequency are made sufficiently high, the ignition voltage may be lower than the static extinction voltage. The reduction of ignition potential is undoubtedly explained by the presence of ions which have not had sufficient time to recombine or leave the interelectrode space. If the current is high, and little time intervenes between removal and reapplication of voltage, the ion density may be high enough to allow the formation of a self-sustaining discharge at voltages considerably lower than the static ignition voltage.

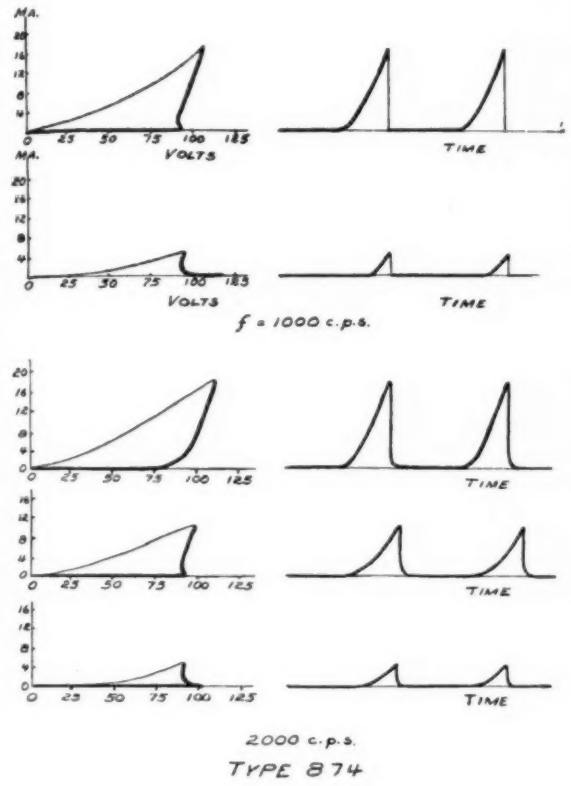

FIG. 6. Dynamic characteristics of type 874 tube with rod as cathode; frequency and current wave form constant, current amplitude varied.

3. When the current is decreased abruptly, it does not follow the static characteristic, but follows a slightly curved line to the origin. This is explained if it is assumed that the time required for deionization greatly exceeds the time taken for the current to fall to zero. The increase in tube resistance accompanying deionization is evidenced by the decrease in slope of the characteristic as the current falls.

4. When the current rises abruptly, or, in any case, when the frequency is high, the portion of the characteristic corresponding to increasing current lies to the right of the static characteristic. This is probably caused by the time taken for the ionization to build up beyond the value requisite to ignition. While the current is increasing, the value corresponding to a given voltage is lower than the current which would be obtained after the current has risen to the equilibrium (static) value for that voltage.

5. The characteristics obtained with gradually increasing current appear to indicate that if the current could be held constant after ignition at the value prevailing at the time of ignition, the voltage would fall abruptly to a value not greatly in excess of the static extinction potential.

Tilting of the characteristic away from the voltage axis, particularly noticeable in the 4000 and 8000 cycle oscillograms, is caused in part by capacitance of the glow tube electrodes and of the

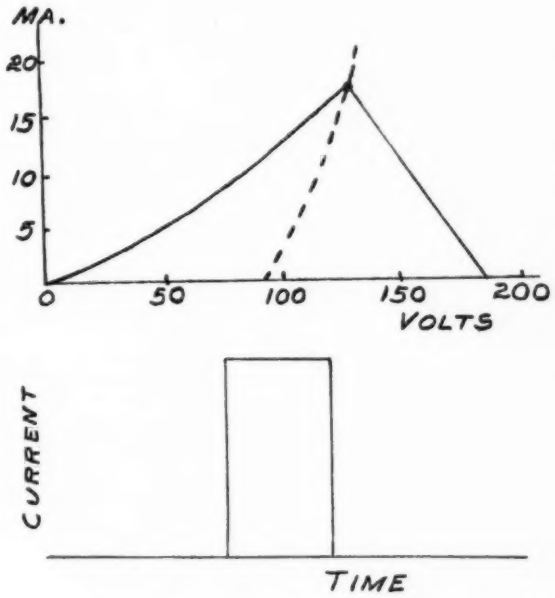

FIG. 7. Dynamic characteristic of type 874 tube with rod as cathode; current started and stopped by means of a key.

circuit. The effect of capacitance is the principle factor which prevents the application of this method to higher frequencies.

Figure 8(a) shows a characteristic obtained

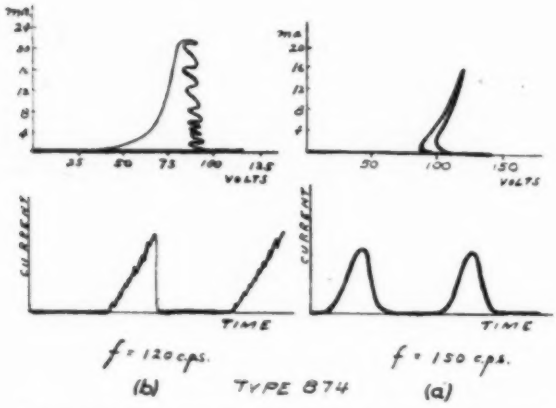

FIG. 8. (a) Dynamic characteristic of type 874 tube with rod as cathode; rates of rise and fall of current equal. (b) Dynamic characteristic of type 874 tube with cylinder as cathode.

when the current rises and falls at the same rate. The characteristic of Fig. 8(b), obtained with the 874 tube when the cylinder acts as cathode, is particularly interesting. The waves superimposed upon the rising portion of the characteristic result from some form of relaxation oscillation. It is not, however, the ordinary type of relaxation oscillation obtained when the current to the tube is limited to very small values by means of high series resistance. The oscillation appeared to be associated with movement of the glow over the surface of the cathode, but the light was insufficient to make it possible to determine this with the aid of a moving mirror. Fig. 9 shows characteristics obtained when the current is not reduced to zero.

CONCLUSION

The method which has been described gives considerable information concerning the dynamic behavior of glow discharges. The effects of time

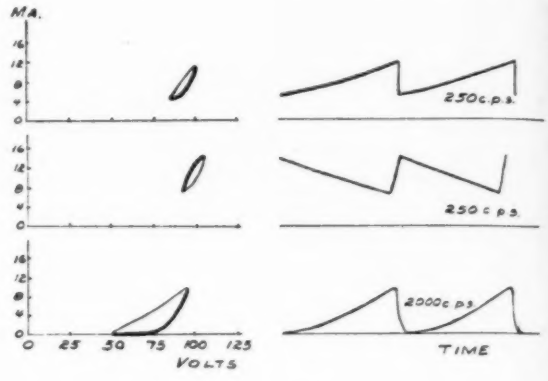

FIG. 9. Dynamic characteristics of type 874 tube with rod as cathode; current not reduced to zero.

taken for ignition, breakdown, and deionization are clearly shown. It is believed that it will be possible to apply this same method to a study of the ignition of arcs.

ACKNOWLEDGMENT

The authors wish to acknowledge their appreciation and indebtedness to the Tau Beta Pi honor society for a fellowship which made possible a portion of the work which forms the basis of this paper.[5] We are also grateful to Mr. Gilbert H. Fett, of this department, for helpful suggestions and assistance.

[5] The fellowship was granted to W. A. Depp for graduate study and research at this university during the school year 1936–37.